CHITOSAN-GELATINE COMPOSITE FILM WITH *Rhus chinensis* FRUIT EXTRACTS-LOADED SILVER NANOPARTICLES FOR FOOD PRESERVATION

By

LU LU TAUNG MAI

Thesis Submitted to the School of Graduate Studies, Universiti Putra Malaysia, in Fulfilment of the Requirements for the Degree of Doctor of Philosophy

June 2024

IPTPH 2024 4

Abstract of thesis presented to the Senate of Universiti Putra Malaysia in fulfilment of the requirement for the degree of Doctor of Philosophy

CHITOSAN-GELATIN COMPOSITE FILM WITH *Rhus chinensis* FRUIT EXTRACTS-LOADED SILVER NANOPARTICLES FOR FOOD PRESERVATION

By

LU LU TAUNG MAI

June 2024

Chairman : Professor Dato' H Ng Paik San, PhD
Institute : Tropical Forestry and Forest Products

Microbial contamination and the oxidation process contribute significantly to food spoilage. The use of synthetic preservatives in packaging raises concerns due to their toxicity. In contrast, phytochemicals derived from medicinal plants extracts are less toxic and have fewer side effects than their synthetic counterparts. Therefore, this study aims to fabricate bioactive composite films using chitosan/gelatin (CG) incorporated with plant extracts and silver nanoparticles (AgNPs) for enhanced biological activities and promote eco-efficient packaging. The study evaluates the effectiveness of bioactive compounds extracted from two types of medicinal plants, *Rhus chiensis* Mill fruit (RCM) and *Acacia concinna* (Willd.) DC pods (AC), using aqueous, 80% ethanol, and 80% methanol. From this study, RCM 80% ethanol extract exhibited optimal minimum bactericidal concentration (MBC) values for *E.coli* (1.563 mg/ml) and *S.aureus* (0.391 mg/ml). The antioxidant activities of RCM 80% ethanol revealed a total phenol content of 461.36 ± 13.26 mg GAE/g, IC_{50} values of 26.21 ± 0.09 µg/ml for ABTS radical scavenging, and 16.08 ± 0.06 µg/ml for DPPH radical scavenging. Gas chromatography-mass spectrometry (GCMS) identified the

phytochemical components as malic acid, pyrogallol, 2, 5-Furandione, 3-methyl, palmitic acid, and linoleic acid.

In the second stage, the optimal conditions for RCM 80% ethanol extract mediated synthesis of RCM-AgNPs was achieved at pH 7 and a temperature of 80 °C. UV-Vis spectroscopy confirmed RCM-AgNPs formation with a plasmon band around 430 nm. Dynamic light scattering (DLS) demonstrated the stability of the AgNPs with a zeta potential value of −25.56 ± 2.1 mV and Polydispersity Index (PDI) value of 0.5 ± 0.019. Transmission electron microscopy (TEM) analysis revealed spherical nanoparticles sized 7-30 nm. Meanwhile, the MBC values of RCM-AgNPs against *E.coli* and *S.aureus* were 39 µg/ml and 156 µg/ml, respectively. Cytotoxicity analysis using the 3T3 cell line indicated that RCM-AgNPs showed no toxic effects at concentrations up to 20 µg/ml. Subsequently, CG composite films were developed with varying ratios of RCM 80% ethanol extract and RCM-AgNPs using ultrasound treatment. Among the CG-RCM films, CG-RCM-4 (0.8%) exhibited the lowest value of water vapour permeability (WVP) of $2.76 \pm 0.45 \times 10^{-12}$ g $m^{-1}s^{-1}Pa^{-1}$ and the highest effectiveness activity against *S.aureus*. Addition of AgNPs enhanced the thickness without significantly affecting the WVP value and CG-RCM-AgNPs-4 (0.08%) had the highest inhabitation zone of *S.aureus* and *E.coli*. Over 14 days, the cumulative silver migration for CG-RCM-AgNPs-4 was 7 ± 0.2 µg/L, which is below the European Food Safety Authority's (EFSA) limit. Scanning electron microscopy (SEM) revealed a dense and compact structure of CG-RCM-4 and CG-RCM-AgNPs-4 composite films, even in the presence of particles agglomeration. Considering the physicochemical and biological properties of CG-RCM-4 and CG-RCM-AgNPs-4, these composite films can serve as antioxidant and antimicrobial active films.

Furthermore, chicken meat inhibited growth with these bioactive composite films demonstrated that CG-RCM-4 and CG-RCM-AgNPs-4 can improve chicken meat quality by minimising colour variation, slowing pH increment, and maintaining a total plate count below 7 log CFU/g at 4°C for 14 days when compared to the control CG film. Finally, these findings suggest RCM 80% ethanol extract and RCM-AgNPs as promising alternatives to chemical antioxidants and antibacterial agents in sustainable food packaging.

Keywords: Antimicrobial, Antioxidant, *Rhus chinensis* Mill. fruit, Composite film

SDG: 12: Responsible Consumption and Production, GOAL 13: Climate Action

Abstrak tesis yang dikemukakan kepada Senat Universiti Putra Malaysia sebagai memenuhi keperluan untuk ijazah Doktor Falsafah

FILEM KOMPOSIT KITOSAN-GELATIN DENGAN EKSTRAK BUAH *Rhus chinensis* DIMUATKAN NANOZARAH PERAK UNTUK PENGAWETAN MAKANAN

Oleh

LU LU TAUNG MAI

Jun 2024

Pengerusi : Professor Dato' H Ng Paik San, PhD
Institut : Perhutanan Tropika Dan Produk Hutan

Pencemaran mikrob dan proses pengoksidaan menyumbang kepada kerosakan makanan yang ketara. Penggunaan bahan pengawet sintetik dalam pembungkusan menimbulkan kebimbangan kerana ketoksikannya. Sebaliknya, fitokimia yang diperoleh daripada ekstrak tumbuhan ubatan adalah kurang toksik dan mempunyai kesan sampingan yang lebih sedikit berbanding dengan bahan sintetik. Oleh itu, kajian ini bertujuan untuk menghasilkan filem komposit bioaktif menggunakan kitosan/gelatin (CG) yang digabungkan dengan ekstrak tumbuhan dan zarah nano perak (AgNPs) untuk meningkatkan aktiviti biologi dan menggalakkan pembungkusan yang mesra alam. Kajian ini menilai keberkesanan sebation bioaktif daripada dua jenis tumbuhan ubatan iaitu buah *Rhus chinensis* Mill. (RCM) dan buah *Acacia concinna* (Willd.) DC (AC) yang diekstrak menggunakan air, 80% etanol, dan 80% metanol. Daripada kajian ini, ekstrak 80% etanol RCM menunjukkan nilai kepekatan bakteria minimum (MBC) yang optimum untuk *E. coli* (1.563 mg/ml) dan *S. aureus* (0.391 mg/ml). Aktiviti antioksidan ekstrak 80% etanol RCM menunjukkan jumlah kandungan fenol sebanyak 461.36 ± 13.26 mg GAE/g, nilai IC_{50} sebanyak 26.21 ±

0.09 μg/ml untuk penangkapan radikal ABTS, dan 16.08 ± 0.06 μg/ml untuk penangkapan radikal DPPH. Kromatografi gas-spektormetri jisim (GCMS) mengenal pasti komponen fitokimia sebagai asid malik, pirogalol, 2,5-furandion, 3-metil, asid palmitik, dan asid linolik.

Pada peringkat kedua, keadaan optimum untuk sintesis AgNPs-RCM yang dimediasi oleh ekstrak etanol 80% RCM dicapai pada pH10 dan suhu 80 °C. Spektroskopi ultra lembayung mengesahkan pembentukan AgNPs-RCM dengan jalur plasmon pada 430 nm. Penyerakan cahaya dinamik (DLS) menunjukkan kestabilan AgNPs dengan nilai potensi zeta −25.56 ± 2.1 mV dan indeks kepoliserakan (PDI) 0.5 ± 0. 019. Analisis mikroskopi elektron transmisi (TEM) menunjukkan zarah nano berbentuk sfera bersaiz 7-30 nm. Sementara itu, nilai MBC AgNPs- RCM terhadap *E.coli* dan *S. aureus* direkodkan pada 39 μg/ml dan 156 μg/ml. Analisis kesitotoksikan menggunakan garisan sel 3T3 menunjukkan bahawa AgNPs-RCM tidak memberikan kesan toksik sehingga kepekatan 20 μg/ml. Seterusnya, filem komposit CG telah disediakan dengan pelbagai nisbah ekstrak etanol 80% RCM dan AgNPs-RCM menggunakan rawatan ultrasonik. Antara semua filem CG-RCM, CG-RCM-4 (0.8%) menunjukkan nilai kebolehtelapan wap air (WVP) terendah iaitu $2.76 \pm 0.45 \times 10^{-12}$ $gm^{-1}s^{-1}Pa^{-1}$ dan mempamerkan keberkesanan tertinggi terhadap *S. aureus*. Penambahan AgNPs meningkatkan ketebalan tanpa memberi kesan besar terhadap nilai WVP dan CG-RCM-AgNPs-4 (0.08%) menunjukkan zon perencatan tertinggi bagi *S. aureus* dan *E. coli*. Penghijraan kumulatif perak untuk CG-RCMAgNPs-4 sepanjang 14 hari direkodkan pada 7 ± 0.2 μg/L berada di bawah had yang ditetapkan of Pihak Berkuasa Keselamatan Makanan Eropah (EFSA). Mikroskopi elektron pengimbasan (SEM) menunjukkan struktur padat dan mampat filem komposit

CG-RCM-4 dan CG-RCM-AgNPs-4 walaupun terdapat penggumpalan zarah. Berdasarkan sifat fizik-kimia dan biologi CG-RCM-4 dan CG-RCM-AgNPs-4, filem komposit ini boleh berfungsi sebagai filem aktif antioksidan dan antimikrob. Selain itu, pengunaan filem komposit bioaktif ini keatas daging ayam terbukti mampu meningkatkan kualiti daging dengan mengurangkan variasi warna, melambatkan peningkatan pH, dan mengekalkan jumlah kiraan plat dibawah 7 log CFU/g pada 4 °C selama 14 hari berbanding filem CG kawalan. Kesimpulannya, penemuan ini membuktikan ekstrak etanol 80% RCM dan RCM-AgNPs berpotensi sebagai ejen antioksidan dan antibakteria alternatif dalam pembungkusan makanan lestari.

Kata Kunci: Antimikrob. Antioksidan, Buah *Rhus chinensis* Mill., filem komposit

SDG: MATLAMAT 12: Penggunaan dan Pengeluaran Yang Bertanggunjawab,
MATLAMAT 13: Perubahan Iklim

ACKNOWLEDGEMENTS

To God be all the Glory. My deepest gratitude goes to the Almighty God under whose Mighty hands, I have received protection, grace, and the gift of life to see this day. All of my accomplishment during this study would not have been achieved without His blessing, unmerited favor and guidance through Jesus Christ.

My deepest heartfelt gratitude extends not only to my former supervisor, Dr Min Min Aung for her unwavering patience, supervision, guidance, dedication and love in guiding me to complete this study, but also to my current supervisor, Prof. Dato'Dr.H Ng Paik San for his continued support, advice, recommendations, encouragement and supervision. Additionally, I deeply appreciate the financial assistance that contributed to covering a portion of my costly tuition and provided extra support for my life off-campus. I would also like to extend my heartwarming thank you to the members of the supervisory committee: Dr. Ainun Zuriyati Mohamed @ Asa'ari and Dr. Ezyana Kamal Bahrin their valuable encouragement and support throughout this research.

I would like to extend my sincere appreciation to Assoc.Prof.Dr. Mass Jaffri Masarudin for granting me access to the microbiology laboratory. Furthermore, I am especially grateful to Prof. Hiroshi Uyama for his generous invitation to engage in a research attachment and for allowing me to characterize the samples at Uyama laboratory, Osaka University. I am also thankful to the staff at the Institute of Tropical Forestry and Forest Products (INTROP) for their assistances and patience during the experiments. Special recognition goes to the technical staff for their cooperation and support. Not to be forgotten, Assoc. Prof. Dr. Moe Thin Khin, Prof. Dr. Aung Win,

Prof. Dr. Ni Ni Aung, Prof. Dr. Than Than Nu, Prof. Dr. Hnaung Hnaung Win, Assoc.Prof.Yu-I Hsu, Mr. Tun Nile, and Dr. Marwah binti Rayung, who selflessly encouraged me to explore new directions in life and provided moral support.

I also take this chance to thank all my labmates, Dr. Kai ling, Dr. Nural, Kak Diyana, Hafiz, Hkawn Mai, ,Nwe Na Di, Redzuan, Illa, Wan, Norwahyuni, Zakiah, Samuel, Giselle, Hanusha, Azra, Shamani, Kak Izaida, Poh Yee, Mohammed Alamassi, Irma, Nisa, May Myat Noe, Madu, Lai Lai Win as well as hostel mates Kak Zida, Ekin, Nas for always being there for me whenever I needed any assistance, motivation, guidance and support.

Last but not least, I would also like to express my deepest gratitude and heartfelt thanks to my beloved parents, Mr. Mung Ra Magau and Mrs. Htu Bu Kale, for their special prayers, unwavering and continuous support, advice, and encouragement throughout this journey. I would not have reached this point without them. I am also grateful to my siblings, Ms Seng Ja Magau and Mr. Myo lat Aung Magau, for their constant support, prayers and presence in my life. Additionally, I extend my appreciation to my aunts, Roi Aung Kale, Ja Nan Jakashin, Roi Nu Kale, my late Uncle Sin Gi Nsoi, my cousins, and all other family members to their prayer, financial support, moral support, which played a significant role in helping me complete this study. I want to express my thanks to those whom I may have inadvertently omitted but who assisted me directly or indirectly in my studies.

I would not be where I am today without their valuable help and support. May God bless them abundantly and reward their kindness.

This thesis was submitted to the Senate of Universiti Putra Malaysia and has been accepted as fulfilment of the requirement for the degree of Doctor of Philosophy. The members of the Supervisory Committee were as follows:

H Ng Paik San, PhD
Professor
Faculty of Forestry and Environment
Universiti Putra Malaysia
(Chairman)

Ainun Zuriyati binti Mohamed @Asa'ari, PhD
Research Officer
Institute of Tropical Forestry and Forest Products
Universiti Putra Malaysia
(Member)

Ezyana bintin Kamal Bahrin, PhD
Senior Lecturer
Centre of Foundation Studies for Agricultural Science
Universiti Putra Malaysia
(Member)

_____
ZALILAH MOHD SHARIFF, PhD
Professor and Dean
School of Graduate Studies
Universiti Putra Malaysia

Date: 24 February 2025

TABLE OF CONTENTS

LIST OF TABLES

LIST OF FIGURES

LIST OF ABBREVIATIONS

3T3 cell line	Mouse-embryonic fibroblast cell
ABTS	2,2'-azino-bis (3-ethylbenzothiazoline-6-sulfonic acid) diammonium salt
AC	*Acacia concinna* (Willd.) DC.
ANOVA	One-way analysis of variance
AP	Active Packaging
ASTM	American Society for Testing and Materials
ATCC	American Type Culture Collection
BHA	Butylated hydroxyanisole
BHT	Butylated hydroxytoluence
CFU	Colony Forming Unit
DLS	Dynamic Light Scattering
DMSO	Dimethyl Sulfoxide
DPPH	2,2-diphenyl-1-picrylhydrazyl
EAB	Elongation at Break
EDX	Energy-Dispersive X-ray Spectroscopy
EFSA	European Food Safety Authority
FTIR	Fourier Transform Infrared Spectroscopy
GCMS	Gas Chromatography-Mass Spectroscopy
IC_{50}	Half maximal inhibitory concentration
ISOP	Intelligent or smart packaging
MBC	Minimum Bactericidal Concentration
MIC	Minimum Inhibitory Concentration
MC	Moisture Content

MTT	3-(4,5-dimethylthiazol-2-yl)-2,5-diphenyl tetrazolium	Bromide
PDI	Polydispersity Index	
RCM	*Rhus chinensis* Mill.	
SEM	Scanning Electron Microscopy	
SOGP	Sustainable or green packaging	
TEM	Transmission Electron Microscopy	
TGA	Thermogravimetric Analysis	
TPC	Total phenolic content	
TS	Tensile Strength	
WS	Water Solubility	
WVP	Water Vapor Permeability	
XRD	X-ray diffraction	

CHAPTER 1

INTRODUCTION

1.1 Background

The Food and Agricultural Organisation of the United Nations (FAO) estimates that global food waste amounts to approximately 1.6 billion tonnes of primary goods equivalents. This results in an annual emission of 3.3 billion tonnes of CO_2 into the atmosphere (Heymich et al., 2021). Mohammad Diah Wahari, the deputy chief executive officer of Solid Waste Management and Public Cleaning Company (SWCorp), highlights the alarming amount of food wasted by Malaysians. A staggering 16,688 tonnes of food are discarded daily, a quantity that could easily provide three meals a day for 12 million people (Bathmanathan et al., 2023). Microorganisms and oxidative processes that cause food spoilage contribute significantly to food loss and waste (Orlo et al., 2023; Wong et al., 2023).

The primary goal of modern food technology is to develop novel methods to reduce or eliminate microbial contamination in food. This is achieved through the use of food additives that prevent bacterial deterioration, as well as the development of active and eco-friendly food packaging. Previous researcher reported that synthetic preservatives like nitrates, benzoates, sulfite, sorbates, parabens, formaldehyde, BHT, BHA, and various others may lead to significant health risks such as hypersensitivity, allergic reactions, cancer, asthma, and neurological damage (Anand & Sati, 2013). Synthetic antimicrobial and antioxidant agents in packaging are controversial due to potential

negative consequences (Felter et al., 2021; Hauser et al., 2016), leading to increased interest in natural extracted from fruit, spices, vegetables, herbs, and cereals. These bioactive compounds derived from plants, including extracts and essential oils, have antimicrobial and antioxidant properties, making them a healthy and promising option for improving product safety and quality. Plant extracts with phenolic compounds disrupt the cell membranes of harmful microorganisms (Ong et al., 2021) and also provide antioxidant effects by preventing the oxidation of cell components (Alirezalu et al., 2020). Adding these bioactive compounds to food products can extend the shelf life and provide health benefits to consumers.

The deciduous tree *Rhus chinensis* Mill., also known as "Nutgall tree" or "Chinese sumac," is a member of the Anacardiaceae family and is widely cultivated in China, Japan, the north-eastern regions of India, and other Asian nations. Folk medicine practitioners in Asia have long employed *Rhus chinensis* Mill. It is known that several substances, including leaves, roots, stems, bark, fruit, and particularly the galls on *Rhus chinensis* Mill. leaves (Galla chinensis), have both curative and preventative properties (Djakpo & Yao, 2010). Nemkuk et al. demonstrated that *Rhus chinensis* Mill. fruit extract has effective antibacterial activity against *P. aeruginosa, E. coli, S. dysenteriae, S. aureus, S. dysenteriae,* and *S. dysenteriae* (Nemkul et al., 2021). *Acacia concinna* (Willd.) DC. Commonly referred to as Soap-Pod or shikakai, is a member of the Fabaceae plant family. This botanical species is cultivated in a range of Asian countries, including but not limited to India, Sri Lanka, Myanmar, and Thailand (Natarajan & Natarajan, 2009; Poomanee et al., 2015). To treat fevers brought on by malaria infections, its leaves are infused (Raja & Sivaraj, 2012). The pods are used to strengthen hair and combat dandruff (Patil, 2023). The methanol extract derived from

the bark of this plant exhibits antibacterial properties against gram-postive bacteria strains, including *Staphylococcus aureus*, *Streptococcus mutans*, *lactobacillus casei*, *lactobacillus acidophilus*, and *Bacillus megaterium*, as reported by Pazhamalai in 2019 (Pazhamalai, 2019). Thus, the extracts obtained from these plants are highly valued as a crucial source of bioactive compounds for creating food preservation agent and packaging with antimicrobial and antioxidant properties. The goal is to minimise food waste and combat food spoilage.

There has been significant focus on silver nanoparticles (AgNPs) due to their potent antibacterial properties. Furthermore, when compared to other metals, silver exhibits the least toxicity for mammalian cells. AgNPs have been the primary focus of recent studies on antibacterial nanocompounds in food packaging. The use of biocompatible, non-toxic, and environmentally benign biological processes for NP synthesis is crucial, especially in fields like medicine and the food sector. The synthesis of AgNPs through plants is a straightforward and cost-effective method that utilises plant extracts as valuable natural resources. This technique is considered to be environmentally friendly. The primary components of plant extracts include polysaccharides, polyphenols, alkaloids, aldehydes, proteins, and amino acids. These components can serve as stabilising and reducing agents (Kumar et al., 2021).

The researchers have initiated the investigation of bio-polymer-based packaging composite film due to environmental concerns such as non-biodegradability and non-recyclability. Gelatin, a water-soluble protein derived from collagen, has the potential to be used in food packaging, particularly due to its biodegradability, wide availability, and film-forming capabilities. However, despite its advantages, the practical use of

gelatin films in biodegradable food preservation is limited by issues like inconsistent mechanical strength and poor water resistance in high humidity conditions. There have been significant efforts made to address these drawbacks, and gelatin is composite with chitosan. Chitosan is a cationic biopolymer with natural biomass origin that is naturally biocompatible, biodegradable, antibacterial, and can form films. The functional groups of chitosan ($-NH_3^+$ and -OH) and gelatin ($-NH_2$, -OH, -COOH/-COO) form hydrogen bonds and electrostatic interactions when linked together using a suitable cross-linker. This interaction enhances their compatibility and chemistry. Notably, films made from a mixture of chitosan and gelatin (CG) exhibit superior mechanical and barrier properties in comparison to films made solely from their individual components (Lu et al., 2022; Shi et al., 2022) .

The goal of this study is to investigate the phytochemical and antimicrobial properties of extracts from *Rhus chinensis* Mill. fruit and *Acacia concinna* (Willd.) DC pods. The extract from the chosen medicinal plant is used to synthesise silver nanoparticles through plant-mediated processes. The plant extract and silver nanoparticles synthesised via plant-mediated were then used as bioactive agents in the development of chitosan-gelatin biopolymer-based bioactive composite films for food packaging applications, as well as antimicrobial and antioxidant agents for food preservation.

1.2 Problem statement

Although synthetic food additives have demonstrated antimicrobial and antioxidant properties, the majority of them pose risks to human health as they are harmful, non-renewable, hazardous, or dangerous. Therefore, it is strongly recommended,

particularly for consumers, to utilise natural and safe antibacterial and antioxidant substances (Avila-sosa et al., 2012; Hu et al., 2020). The plant extracts contain a high number of phenolic compounds, including phenolic acids and flavonoids. These compounds possess antibacterial properties against different microorganisms, along with antiviral, antioxidant, and anti-inflammatory effects (Abdollahzadeh et al., 2021). As a result, the AgNPs created through plant-mediated synthesis are more environmentally friendly. This is due to the presence of organic natural matter on their surfaces, which prevents oxidation and the formation of harmful Ag+ ions. Additionally, these nanoparticles are biocompatible and do not pose a risk to animal and plant tissues. Amooaghaie et al. demonstrated that silver nanoparticles produced through a green approach (using Nigella sativa leaf extract) were safer compared to a chemical method involving sodium borohydrate and sodium citrate (Amooaghaie et al., 2015). Additionally, coffee extract-mediated AgNPs may be a preferable choice for antimicrobial uses in food preservation because they have no adverse effects on human or mouse cells (Kumar et al., 2021).

Most traditional packaging materials are made from non-biodegradable substances like polypropylene (PP), polystyrene (PS), and poly (ethylene terephthalate) (PET), which are derived from petroleum. Not only have significant environmental concerns arisen as a result of this, but also 20-25% of the residential food waste worldwide (Sid et al., 2021) . As a result, different bio-based and biodegradable polymer matrices have been embraced as substitutes to produce packaging that is more environmentally friendly (Vieira et al., 2022). Gelatin, derived from collagen through partial hydrolysis (Felter et al., 2021; Hauser et al., 2016) and known as a water-soluble protein, has gained attention from researchers for its excellent film-forming properties, non-toxicity,

biodegradability, miscibility, edibility, and widespread availability, making it a promising choice for food packaging. However, despite its advantages, the practical use of gelatin films in biodegradable food preservation is limited by issues like inconsistent mechanical strength and poor water resistance in high humidity conditions. To address this issue, a technique involves combining chitosan, a cationic linear polysaccharide with beneficial properties such as non-toxicity, biodegradability, and food safety, with gelatin. Combining chitosan and gelatin creates a cohesive composite network through intermolecular hydrogen bonding between polymer chains, enhancing the film's physicochemical and mechanical properties. Plant-based products with antioxidant and antibacterial properties can be used instead of synthetic additives to improve chitosan-gelatin composite films, addressing food spoilage caused by microbial growth and oxidation. Plant-derived phytochemicals are safer and have fewer side effects than synthetic antioxidants and organic acid preservatives.

The development of active polymeric films combined with *Rhus chinensis* Mill. fruit extracts that can improve biological activity (i.e., antioxidant and antimicrobial) as well as the *Rhus chinensis* Mill. fruit extract mediated synthesis of silver nanoparticles is at the forefront of research. To the best of the author's knowledge, no studies have been conducted on the characterisation of *Rhus chinensis* Mill. fruit extract-mediated synthesis silver nanoparticles. The *Rhus chinensis* Mill. fruit extract and its synthesised silver nanoparticles are applied to reinforce biopolymer composite films and serve as bioactive agents for food preservations.

1.3 Justification of the study

In this current study, we are extracting and utilizing bioactive agents from two of the most popular edible traditional medicinal plants in Myitkyina, the northern part of Myanmar; *Acacia concinna* (willd.) DC, commonly known as shikakai, and *Rhus chiensis* Mill, known as Chinese sumac. Previous research has shown that *Acacia concinna* (Willd.) DC and *Rhus chinensis* Mill. have traditional medicinal uses, phytochemical constituents, pharmacological properties, and biological activities. Furthermore, these two types of medicinal plants are widely distributed not only in Myanmar but also throughout Asia, making them suitable for large-scale commercial extraction. These plants deserve further investigation because there is no published research on the use of their extracts in reinforcing biopolymer composite films or as bioactive agents for food preservation.

The effectiveness of extracting high-quality bioactive constituents with strong antimicrobial properties from plants relies on various factors, including sample pre-treatment (Krakowska-Sieprawska et al., 2022) , extraction techniques, and solvent selection (Chemat et al., 2019; Susanna et al., 2022). A selection of extraction solvents is offered, including distilled water, 80% ethanol and 80% methanol, known for their high yield efficiency and eco-friendly properties, making them ideal environmentally sustainable options (Chemat et al., 2019; Gacem et al., 2019).Traditional methods like maceration, percolation, and Soxhlet extraction are common but inefficient and time-consuming (Pai et al., 2022).Supercritical fluid extraction (SFE) using a nontoxic solvating agent like CO_2 has gained interest but is costlier. The ideal extraction methods for the food industry combines high efficiency with low operating and

maintains costs (Shinde & Mahadik, 2019). Recently, there has been a shift towards green extraction methods, which emphasise environmentally friendly solvent techniques that minimise resource consumption and improve yields. Ultrasonic-assisted extraction (UAE) is highlighted for its role in achieving green chemistry principles. UAE efficiently extracts bioactive components from plants, reducing extraction time and enhancing extract quality and yield. This method allows for complete extraction with higher purity in minutes and high reproducibility, aligning with sustainable practices by significantly reducing the use of organic solvents (Shen et al., 2023).

Silver nanoparticles (AgNPs) are extensively researched for their potent bactericidal properties against various microorganisms, including bacteria, yeasts, fungi, and viruses. Notably, AgNPs exhibit low volatility and stability at high temperature, allowing integration into matrices through methods like coating, absorption, or direct incorporation (Carbone et al., 2016). Silver, compared to other metals, shows the least toxicity to animal cells (Simbine et al., 2019). Previous studies indicated that AgNPs synthesised using coffee extract (Rónavári et al., 2017) and black chickpea peel extract (Kothandaraman et al., 2023) exhibit non-cytotoxic effects on normal cells. This suggests that plant-mediated synthesis of AgNPs reduces environmental harm by adsorbing natural organic matter, preventing oxidation and harmful ion formation. The biocompatibility of AgNPs further minimise their impact on animals and plant tissues (Kumar et al., 2021).

1.4 Objectives

The objectives of this study are:

1. To identify a potential medical plant and its corresponding solvent with strong antimicrobial and antioxidant properties for further study

2. To investigate the plant-mediated synthesis of silver nanoparticles and analyse their properties under various experimental conditions including temperature and pH

3. To prepare chitosan-gelatin based composite films incorporating medicinal plant extract and its mediated synthesis of silver nanoparticles at different ratios and analyses the water vapor permeability, physical, antimicrobial and mechanical properties

4. To analyse the physicochemical and biological properties of the selected ratios of chitosan-gelatin based bioactive composite films as well as to apply chicken breast preservation

1.5 Scope and limitation of the study

The study's scope and limitations are as follows:

1. This study sampled traditional medicinal plants (*Acacia concinna* (Willd.) DC pods and *Rhus chinensis* Mill. fruit) in Myitkyina, Kachin State, Northern Myanmar.

2. The antibacterial activity characterisation in this study was limited to *Escherichia coli (E.coli)* ATCC 25922 and *Staphylococcus aureus (S.aureus)* ATCC 43300.

3. The bioactive composite films were only tested for water vapour transmission. The gas vapour transmission rate is excluded due to equipment inaccessibility. Furthermore, the colour of the composite films was not considered in the study.

4. This study excluded factors related to raising chickens and developing feed formulations. Observation is used to assess the sensory quality of chicken breasts and shop sanitation practices. There is no set standard for selection.

1.6 Content of the thesis

The thesis is organised into seven chapters, as listed below.

The first chapter includes a general background, a problem statement, justification, objectives, scope and limitations, and flow chart of the study (Figure 1.1). The second chapter provides a comprehensive review of various topics, including active antimicrobial food packaging, antimicrobial and antioxidant agents, pharmacological properties, biological activities of RCM fruit and AC pods, and the green synthesis of silver nanoparticles. This chapter also discusses chitosan-gelatin (CG)-based bioactive composite films containing antimicrobial and antioxidant agents.

The third chapter discussed the phytochemical constituents and antimicrobial properties of RCM fruit and AC pods extracted with 80% ethanol and 80% methanol. Furthermore, the selected RCM fruit extract was used to analyse the Minimum Inhabitation Concentration (MIC) and Minimum Bactericidal Concentration (MBC), the antioxidant properties. The optimal ethanol solvent extract RCM also study the natural bioactive composition through gas chromatography-mass spectrometry (GC-MS).

The fourth chapter focusses on achieving optimal temperature and pH conditions for the plant-mediated synthesis of silver nanoparticles using RCM-E extract. In addition, the characterisation of these nanoparticles is discussed. The fifth chapter discusses the physicochemical and biological properties of CG-based active composite films containing RCM extract and RCM-AgNPs in varying ratios. The sixth chapter focusses

on the selected bioactive composite films and their application in the preservation of chicken breast. The seventh chapter concludes with recommendations for future research.

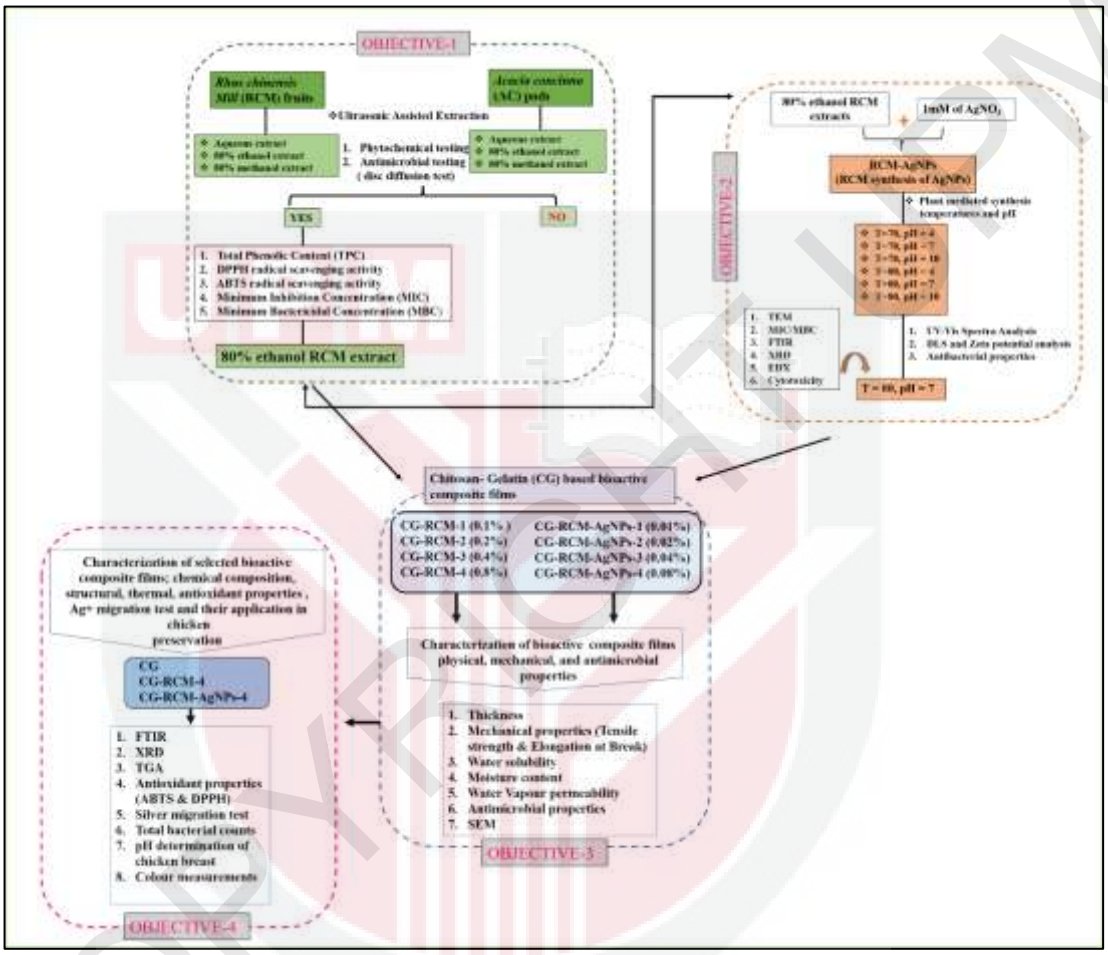

Figure 1.1: General flow chart of the research

CHAPTER 2

LITERATURE REVIEW

2.1 Food Packaging

Food packaging is essential for ensuring food quality and safety, prolonging shelf-life, and reducing food loss and waste. It serves as a barrier against environmental contamination and various factors, including aromas, temperature, shocks, dust, microorganisms, light, and humidity (Narayanan et al., 2017; Ribeiro-santos et al., 2017). The demand for clean, fresh, high-quality, minimally processed, and ready-to-eat produce with a long shelf life has risen due to customers' evolving lifestyles. This has led to a greater need for a contemporary packaging technique. The food sector is embracing innovative technologies like sustainable or green packaging, intelligent or smart packaging, and active packaging.

The food packaging industry is currently flooded with low-cost, single-use packaging materials made primarily from petroleum-based polymers (Anya et al., 2022). Unfortunately, only a small portion of these packaging materials are recycled (K. Huang & Wang, n.d.), resulting in negative environmental consequences such as pollution and the accumulation of waste in landfills. This distressing scenario poses a significant environmental challenge (Walker & Fequet, 2023). Given the gravity of these issues, there is a growing emphasis on environmental conservation, which corresponds to consumer demands for improved product quality and longer shelf life. This has fuelled a strong desire to advance the development of biodegradable,

compostable, or readily recyclable packaging materials.

Researchers are working to improve SOGP's environmental friendliness. Their goal is to reduce the environmental impact of the entire product packaging process while improving the overall sustainability of food packaging systems. The IOSP systems are intended to detect food freshness, expiration dates, quality, safety assessments, and storage conditions. They can also monitor microorganism growth. Using IOSP systems, such as time-temperature indicators (Mataragas et al., 2019), radio frequency identification system (Alfian et al., 2020), barcodes (Kalpana et al., 2019), gas indicators (Lyu et al., 2019), sensors (Dudnyk et al., 2018), and more, offers food producers the means to safeguard their food products in more convenient and secure ways. Nevertheless, the substantial costs and technical challenges associated with IOSP-based methods present significant barriers to their widespread adoption within the food industry. Consequently, the application of IOSP techniques remains limited in the food industry (Soltani Firouz et al., 2021).

It is critical to ensure the safety and sensory quality of packaged food during the preservation process. The AP system is critical in adjusting ambient conditions to maintain food quality. Figure 2.1 depicts the classification of various food packaging systems, as discussed by Han et al. (2018) and Soltani Firouz et al. (2021).

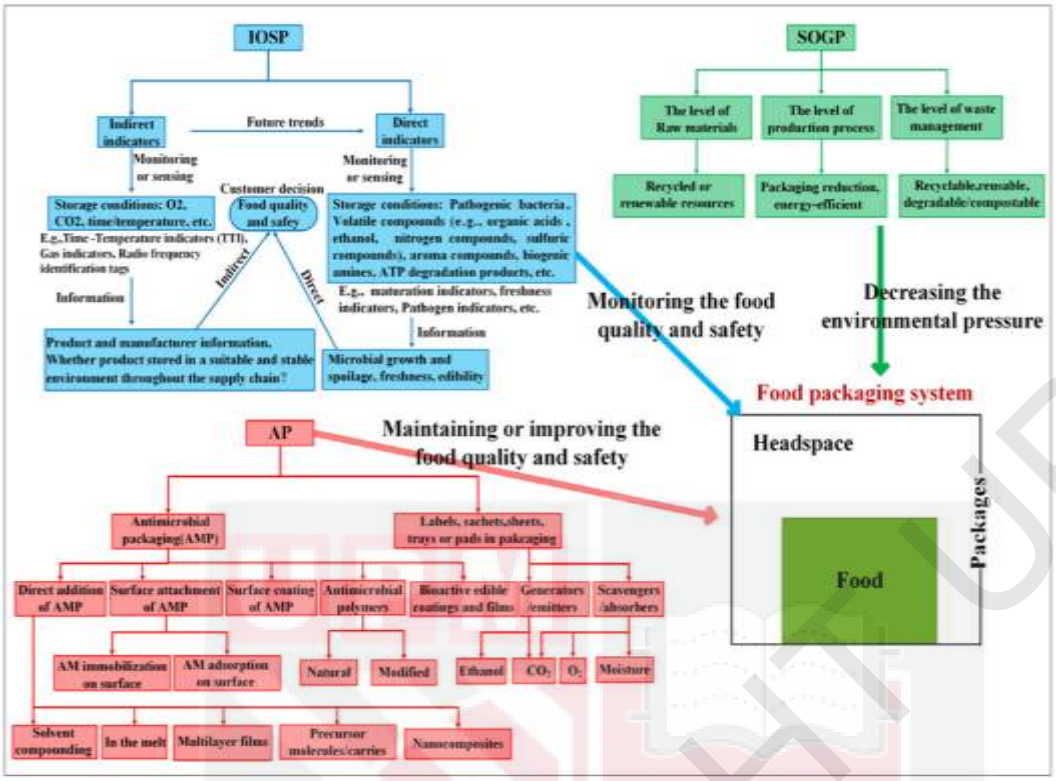

Figure 2.1 : Classification of various food packaging system (Han et al., 2018)

2.2 Active Food Packaging

The concept of "active packaging" refers to a shift from the traditional role of passive packaging, which is primarily defensive, to a more proactive and dynamic role. It serves as a channel for interactions between the environment, the product, and the packaging. Usually, these interactions encompass various physical, chemical, and biological processes that alter the natural environment in which the food is packaged, enhancing the sustainability, safety, quality, and shelf life of the product (Chawla et al., 2021). From a technical standpoint, active packaging involves deliberately incorporating structures that can absorb or release specific substances into or out of the enclosed environment or the packaged food (Bettina & Kvalv, 2017).

Active packaging can be classified into two categories based on the additives used in the food packaging material. Non-migratory active packaging involves scavengers that eliminate unwanted elements from the packaging environment without intentional migration. On the other hand, active releasing packaging involves emitters that allow controlled migration of desired substances into the packaging environment. Most nonmigratory active packaging systems used in food products have the ability to serve as ethylene absorbers, oxygen scavengers, and moisture absorbers (Ahmed et al., 2022). A ripening agent is ethylene gas. Fruit and raw vegetables can have their shelf lives extended by using ethylene scavengers (Wei et al., 2021). The presence of oxygen in food packaging promotes the development of aerobic microorganisms and results in undesired food modifications including rancidity of fat and browning of meat. Iron, titanium, zinc, and other oxygen-reactive elements are utilised as oxygen scavengers in packing materials (Sharma et al., 2020). Moreover, in the food industry, humidity moisture, and water are often factors, capable of causing detrimental effects at every stage, from the storage of raw materials and products in warehouses to transportation. To address this issue effectively, one practical solution involves incorporating moisture absorbers within the packaging. This helps regulate the presence and quantity of water within the package (Soltani Firouz et al., 2021). Active-release packaging technologies include carbon dioxide emitters, antimicrobial packaging, and antioxidant packaging. Carbon dioxide (CO2) is a gaseous molecule that can dissolve in the aqueous and fatty of food. The solubility of carbon dioxide in water causes the creation of carbonic acid, which then leads to the acidification of the food product. The beneficial antimicrobial properties of carbon dioxide are well known and commonly used in the food industry to maintain quality and prolong shelf life (Bettina & Kvalv, 2017).

The process of food oxidation is primarily caused by exposure to oxygen, which can create harmful free radicals that accelerate enzymatic browning and promote the growth of microbes, ultimately resulting in food spoilage (Liang et al., 2022). To mitigate these effects and ensure food safety, natural antioxidants derived from plant, fruit, and vegetable extracts have emerged as a promising alternative to synthetic antioxidant agents. By using natural antioxidants, food producers can effectively prevent oxidation and prolong the shelf life of their products while avoiding potential health risks associated with synthetic additives. The natural antioxidant compounds, such as Essential oil, vitamins, carotenoids, and polyphenols (eg., phenolic acids, flavonoids, tocopherols, lignins, and tannins), are commonly used in food packaging materials (A. A. Kadam et al., 2021). These compounds have antibacterial, antioxidant, and antifungal properties in different food packaging systems. Various microorganisms, including moulds, yeasts, bacteria, and other types, break down and spoil food, resulting in a decrease in its quality and shelf life. Antimicrobial agents can suppress the majority of these microorganisms (Fu & Dudley, 2021). The current trend in active packaging agents, which emphasises antibacterial and antioxidant agents, oxygen and ethylene scavengers, and carbon dioxide emitters, is shown in Figure 2.2.

Figure 2.2: Active food packaging (Vilela et al., 2018)

2.3 Antimicrobial agents

Food-borne microbial illnesses can be effectively addressed with the use of antimicrobial agents. In addition, they are used in the food packaging industry to produce antimicrobial packaging films that safeguard the structure, texture, colour, and nutritional value of food. In addition, antimicrobial compounds found in food can eliminate harmful bacteria and inhibit their growth. This not only enhances the safety of the food for consumers, but also helps to prolong the shelf life of food products. The capabilities of antimicrobial agents themselves determine their effectiveness and action against bacteria. These skills are influenced by the sources, both natural and manufactured, as well as the kind of source. The sources of these substances can be classified into three categories: organic acids and their salts, naturally occurring antimicrobial agents, and inorganic compounds as shown in Figure 2.3. Gram-positive and Gram-negative bacteria, as well as fungi and yeasts, have all been shown to be

susceptible to the action of organic acids and their salts. (Bra & Smaoui, 2021). The remarkable antibacterial activity of inorganic nanofillers is well known (Jafarzadeh et al., 2020; Qamar & Ahmad, 2021). The different types of antimicrobial agents are mentioned in Figure 2.3.

Botanically derived antimicrobial agents, animal-derived antimicrobial agents, and microorganism-derived antimicrobial agents are examples of natural antimicrobial agents (Oyom et al., 2022). Roots, seeds, leaves, bark, herbs, and spices are all sources of plant antibacterial components. The presence of the hydroxyl group and the high concentration of phenolic compounds, iso-flavonoids, terpenes, ketones, aliphatic alcohols, acids, and aldehydes in plant substances are what give them their primary antibacterial properties. In order to preserve fruit and vegetables, animal-based antibacterial compounds have been employed in edible coatings and films. Bio preservatives have been used to prevent food deterioration organisms using microorganisms and their derived antimicrobial metabolites (Yuan Zhao et al., 2022).

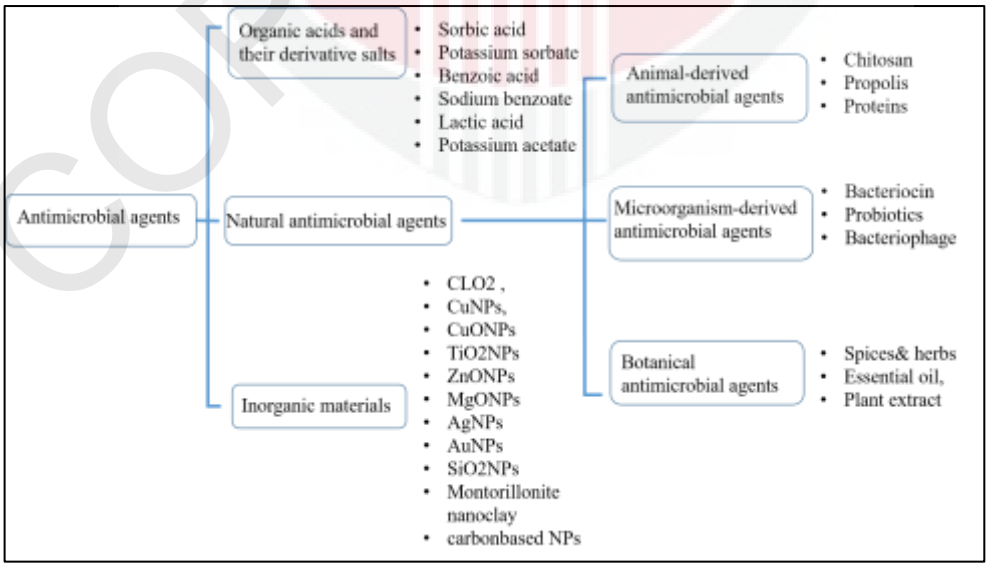

Figure 2.3: The different types of antimicrobial agents

2.4 Antioxidant agents

There has been considerable attention paid to antioxidant agents, as they have the potential to prolong the shelf life of food products that are susceptible to oxidation. Following microbial growth, oxidative degradation is the second most significant cause of food spoilage. The nutritional value of food is diminished as a result of oxidative reactions, which degrade essential fatty acids, proteins, and fat-soluble vitamins. In addition, it induces the development of unpleasant odours and tastes, as well as colour changes as a result of pigment degradation (Vilela et al., 2018).

There are numerous synthetic and natural antioxidant compounds that are acknowledged for their capacity to confer antioxidant properties on active packaging systems. Therefore, it is imperative to implement a prudent selection process that considers not only the specific attributes of the food but also health and safety concerns. However, concerns regarding potential hazards to human health have arisen as a result of the use of synthetic antioxidants such as butylated hydroxytoluene (BHT), butylated hydroxyanisole (BHA), and tert-butyl hydroquinone (TBHQ) (Fasihnia et al., 2020; Liang et al., 2022; Preparation, 2021).

The decline in research related to synthetic antioxidants is driven by the growing inclination to steer clear of or reduce the consumption of harmful artificial food additives. As a result, researchers are predominantly exploring healthier alternatives, particularly natural antioxidants, for the development of active food packaging films (Vilela et al., 2018).

The classification of natural antioxidants includes three distinct subgroups: (a) vitamins, specifically vitamins C and E; (b) carotenoids, which include carotenens and xanthophylls; and (c) polyphenols, which encompass flavonoids, phenolic acids, tannins, lignans, and stilbenes. In addition, polyphenolic derivatives are plentiful in various food and plant sources, such as vegetables, fruit seeds, berries, cereals, wine, olives tea, aromatic plants, and their byproducts (Rangaraj et al., 2021) .

The overall antioxidant efficacy of these substances typically relies on their chemical attributes and the methods used for their extraction, as a pointed out by Oroian and Escriche in 2015 (Oroian & Escriche, 2015). Conversely, the antioxidant qualities of phenolic concentrates and essential oils are closely tied to their polyphenolic content. Consequently, highly polyphenolic extracts and essential oils are deemed effective antioxidants for the development of active packaging and coatings. Furthermore, polyphenolic compounds serve as potent reducing agents and effectively neutralise free radicals present in food (Papuc et al., 2017). In addition, mechanical methods such as ultrasonication, pulse sonication, microwave, and ball milling are crucial in improving the extraction efficiency of these antioxidants, leading to an increase in the polar components in the extracts, as explained by Garcia-Vaquero and colleagues (Garcia-Vaquero et al., 2020).

However, a significant limitation associated with the use of natural antioxidants is the need for larger quantities to achieve equivalent antioxidant activity in the context of food systems, a trend similarly observed in the antimicrobial effectiveness of natural compound-based systems. The primary methodologies utilised to evaluate the antioxidant capacity of these compounds include the assessment of ferric reducing

antioxidant power (FRAP), DPPH radical scavenging, ferrous ion chelating (FIC) activity, ABTS radical scavenging, and oxygen radical absorbance capacity (ORAC). Furthermore, quantitative assessments were performed on various parameters, including total phenolic content (TFC), total flavonoid content (TFC), and total antioxidant capacity (TAC).

2.5 *Rhus chinensis* Mill. (RCM)

Figure 2.4: *Rhus chinensis* Mill. fruit, (a) pre-mature (b) mature stage

The Family Anacardiaceae, which includes more than 250 distinct species worldwide, includes the genus *Rhus* and the species *Rhus chinensis* Mill. (RCM). Common names include "Chinese sumac" and "Nutgall tree," which are both found in tropical, subtropical, and temperate climates, primarily in China, Japan, North-Eastern India, and South-east Asia. The fruit season lasts from October to December, and the tree can grow as tall as 25 feet, with an average height of 12 to 15 feet. The tree has strangely

complex, creamy-white leaves and blooms. It produces clusters of small fruit with seeds and a waxy coating. Figure 2.4 depicts RCM fruit of premature and mature stage.

RCM tree includes a wealth of nutrients and bioactive substances that have undergone extensive research in the fields of industry, food, and medicine. For example, RCM tree is used as a raw material for commercial colours, and its fruit and leaves are used to make vinegar, essential oils, sauces, appetisers, and beverages. Fruit oil can be used as a new source of edible oil because it has significant nutritional contents and health benefits. In Asia, folk medicine practitioners have long employed RCM tree. It is known that several substances, including leaves, roots, stems, bark, fruit, and especially the galls on its leaves (Galla chinensis), have both curative and preventative properties (Djakpo & Yao, 2010). Possible applications of different plant components in traditional medicine include the management and prevention of conditions such as diarrhoea, dysentery, colic, hepatitis, jaundice, kidney and urinary disorders caused by stones, malaria, coughs, haemostatic, diabetes mellitus, antiseptic astringent, persistent cough with blood, spontaneous sweating, and skin infections. The RCM tree reactive crystallisation method is used in functional foods, pharmaceuticals, nutraceuticals, and medications (Li et al., 2022). Table 2.1 shows the taxonomical classification of *Rhus chinensis* Mill., also known as Chinese Sumac.

Table 2.1: Classification of *Rhus chinensis* Mill. (Chinese Sumac)

Kingdom	Plantae (Plants)
Subkingdom	Tracheobionta (Vascular plants)
Super division	Spermatophyta (Seed plants)
Division	Magnoliophyta (Flowering plants)
Class	Magnoliopsida (Dicotyledons)
Subclass	Rosidae
Order	Sapindales
Family	Anacardiaceae (Sumac family)
Genus	Rhus L. (Sumac)
Species	*Rhus chinensis* Mill. (Chinese sumac)

Adapted from: United States Department of Agriculture (USDA)

2.5.1 Traditional Uses

The history of traditional medicine is vast. According to the World Health Organisation, traditional medicine encompasses "a wide range of knowledge, skills, and practices that are rooted in the theories, beliefs, and experiences of various cultures. It is utilised for maintaining health and addressing physical and mental illnesses through prevention, diagnosis, improvement, and treatment" (WHO, n.d.). RCM tree has been employed in Asian traditional medicine to treat a wide range of ailments for millennia. Ben Cao Shi Yi (Tang dynasty) first documented the medicinal properties of the root, rhizome, and leaves of RCM, attributing them to the treatment of colic, diarrhoea, dysentery, and hepatitis (Zhao, 2006). Other ancient Chinese texts state that the root, bark, fruit, leaves, and gall of RCM have the potential to be utilised in the treatment of diverse ailments.

While in Korea, the rhizome, bark, and leaves are employed as traditional treatments for diarrhoea and dysentery (Triterpenes et al., 2001) . Two or three times a day, fruit powder was applied topically to cure tinea. The fruit's acidic byproduct, when cooked with water, was either employed as a preservative or mixed with fresh eggs to treat

diarrhoea. Whereas in India, the fruit of RCM is traditionally used to treat diarrhoea and dysentery (Pampuinath & Meitei, 2021) In addition, the fruit is regarded as a type of culinary component used in chutney preparation. The water used to soak the fruit can be consumed as a beverage to ease gastrointestinal discomfort (Seal & Chaudhuri, 2014) (Tapan and Kausik, 2014). Gallnuts are frequently given as antidiarrheal medications in Thai traditional medicine, and a dental powder containing them is widely used in Thailand to treat aphthous ulcers (Sariozlu & Kivanc, 2011).

Moreover, the seed contains a significant percentage of linoleic acid (58–75%), making it suitable for use as a cooking oil and a key component in food production (Mingxing et al., 2013). The branch and foliage of RCM can be seen as a natural fertiliser due to its nutritious contents: nitrogen 0.43%, phosphoric acid 0.11%, and potassium oxide 0.43%. The high tannin content of GC causes its colour to behave like a dye that resembles light ink. In Japan, this dye is frequently employed to colour clothing and lighten hair, as well as for ink and pigment. It has been employed as the colour of mourning attire throughout history. The various components of the RCM tree that are employed as traditional medicines are summarised in Table 2.2.

Table 2.2: Different parts of RCM plant used as folk medicines (M. Li et al., 2022)

Part used	Traditional uses	Region
Root	Cold fever; cough; diarrhea; and malaria; wind-damp, Bi-syndrome; snakebite; ringworm sores; edema; jaundice; emission; measles; Pain and swelling; acute mastitis; deinebriating	China
Root bark (no cork)	Cough; edema; rheumatism; furuncle; jaundice; traumatic injury; snakebite; clearing heat; scattered blood stasis and removing toxicity; boiled with vinegar to treat bone stuck in the throat	China
Stem bark (no cork)	Bloody flux; furuncle; pyogenic infections; boiled with water to kill roundworm	China
Leave	Cough expectorant; sore; hemoptysis; diarrhea; bloody flux; hematochezia; eye disease; night sweat; laryngitis; emission; traumatic injury; detoxification of convergence	China

Gallnut	Arrest sweating; malaria; hemostasis; reduce phlegm; cough; diarrhea; relive pain; rectal cancer; emission and hemoptysis; diabetes; haemorrhoids; rectocele; scalds and burns; sore; night sweat; intestinal; eczema; cervical erosion; and uterine bleeding	China
	Used as astringent	Myanmar
Flower	Nasal eczema; carbuncle poison fester; source of honey.	China
Fruit	Cough; dandruff; tinea; night sweat; carbuncle; pharyngitis; jaundice; diarrhea; hernia and dysentery; hepatitis.	China
	Stomach ache; dysentery; allergies (rash) causes contact dermatitis; mushroom poisoning; high blood pressure and gas formation. Mixture with Zanthoxylum acanthopodium DC. leave extract to treat stomach ache.	India
	Gastric problem	India
	Diarrhea and dysentery Eaten	Nepal
	Eaten raw or add to food	Thailand
	Used to treat colic	Myanmar
Seed	Cough; dysentery and jaundice; malaria; hepatitis and rheumatism; drop cremation sputum; arrest sweating; promoting production of body fluid and nourishing the lung	China
Bark	Detumescence; sore; snakebite; bitten by dog	China
NA	Laryngitis; snakebite; stomach-ache traumati; diarrhea and dysentery	Nagaland

2.5.2 Phytochemical constituents

Various classes of compounds extracted from RCM fruit encompass flavonoids, phenolics, fatty acids, tannins, steroids, organic compounds, and additional types. The compounds are detailed in Tables 2.3.

Table 2.3: Phytochemical constituents in RCM Fruit

Name	**Molecular Formula**	**References**
Flavonoids		
Quercetin	$C_{15}H_{10}O_7$	Li et al. (2016)
Kaempferol	$C_{15}H_{10}O_6$	
Luteolin	$C_{15}H_{10}O_6$	Zhang et al. (2017)
Quercetin-3-O-rhamnoside (Quercitrin)	$C_{21}H_{20}O_{11}$	Li et al. (2016) Zhang et al. (2017)
Quercetin-3-O-arabinoside	$C_{20}H_{18}O_{11}$	Fu et al. (2021)
luteolin-7-O-glucoside	$C_{21}H_{20}O_{11}$	
myricetin-3-O-galactoside	$C_{21}H_{20}O_{13}$	
kaempferol-3-O-α-L-rhamnoside	$C_{21}H_{20}O_{10}$	Li et al. (2016)
apigenin	$C_{15}H_{10}O_5$	
myricetrin	$C_{21}H_{20}O_{12}$	
myricetin-3-O-(6″-galloyl) glycoside	$C_{28}H_{24}O_{16}$	Fu et al. (2021)
myricetin gallate	$C_{28}H_{24}O_{17}$	
kaempferol-3-O-hexoside	$C_{21}H_{20}O_{11}$	

Table 2.3: Continued

Phenolics		
Gallic acid	$C_7H_60_5$	Li et al. (2015)
Methyl gallate	$C_8H_8O_5$	
Propyl gallate	$C_{10}H_{12}O_5$	
Ethyl gallate	$C_9H_{10}O_5$	
Syringic acid	$C_9H_{10}O_5$	Nemkul et al. (2021)
3-pentadecylphenol	$C_{21}H_{36}O$	
(Z)-3-(heptadec-10-en-1-yl) phenol	$C_{21}H_{38}O$	
(Z)-3-(pentadec-8-en-1-yl) phenol	$C_{21}H_{34}O$	
Steroids		
β-sitosterol	$C_{29}H_{50}O$	Li et al. (2015)
Fatty acids		
Palmitic acid	$C_{16}H_{32}O_2$	Li et al. (2015)
α-monpalmitin	$C_{19}H_{38}O_4$	
citric acid, trimethyl ester	$C_9H_{14}O_7$	Nemkul et al. (2021)
oleic acid	$C_{18}H_{34}O_2$	
linoleic acid	$C_{18}H_{32}O_2$	
8,11-octadecadienoic acid, methyl ester	$C_{19}H_{34}O_2$	
cis-13-octadecenoic acid	$C_{18}H_{34}O_2$	
octadecanoic acid	$C_{18}H_{36}O_2$	
Table 2.3: Continued		
hexadecanoic acid, methyl ester	$C_{17}H_{34}O_2$	
2,3,6,7-tetrahydrooxepine-4-carboxylic acid, ethyl ester	$C_9H_{14}O_3$	
butanedioic acid, monomethyl ester	$C_5\ H_8O_4$	
hexadecanoic acid, methyl ester	$C_{17}H_{34}O$	
methyl (9Z,11E)-octadeca-9,11-dienoate	$C_{19}H_{34}O_2$	
hexadecanoic acid, ethyl ester	$C_{18}H_{36}O$	
Tannins		
di-O-galloyl-glucoside II	$C_{20}H_{20}O_{14}$	Fu et al. (2021)
trigalloyl glucose I	$C_{27}\ H_{24}O_{18}$	
digallic acid II	$C_{14}\ H_{10}O_9$	
trigalloyl glucose II	$C_{27}\ H_{24}O_{18}$	
digallic acid I	$C_{14}\ H_9O_9$	
tetragalonyl glucose I	$C_{34}\ H_{28}O_{22}$	
Organic compound		
citric acid	$C_6H_8O_7$	Zhang et al. (2018)
oxalic acid	$C_2H_2O_4$	Sharma et al. (2018)
D-tartarate	$C_4H_5O_6$	
malonic acid	$C_3H_4O_4$	
acetic acid	$C_2H_4O_2$	
Other types furfural		
3-methylfuran-2,5-dione	$C_5H_4\ O_3$	Nemkul et al. (2021)
maleic anhydride	$C_4H_2\ O_3$	
succinic anhydride	$C_4\ H_4O_3$	
3,5-dihydroxy-6-methyl-2,3-dihydro-4H-pyran- 4-one	$C_6H_8\ O_4$	
5-(hydroxymethyl) furan-2-carbaldehyde	$C_6\ H_6O_3$	
phthalic anhydride	$C_8H_4\ O_3$	
succinic acid	$C_4H_6O_4$	Sharma et al. (2018)
octadecanal	$C_{16}H_{32}O_2$	Nemkul et al. (2021)
octacosane	$C_{28}H_{58}$	
1-heptatriacotanol	$C_{37}H_{76}O$	
heptacosane	$C_{27}H_{56}$	
17-pentatriacontene	$C_{35}H_{70}$	

2.5.3 Pharmacological properties and biological activities

RCM fruit is widely recognised for its abundance of bioactive components and its ability to provide therapeutic benefits for a range of diseases. Numerous studies have uncovered the medicinal value of RCM medicinal tree and its biological activities. In a study conducted by Zhou and colleagues, it was discovered that the ethanol extract derived from RCM fruit exhibited a protective impact on liver fibrosis in mice that were induced with tetrachloromethane (Zhou et al., 2020). A different study revealed that Galla Chinensis exhibited anti-obesity properties, particularly in female C57BL/6J mice that were given a high-fat diet and orally administered Galla chinensis for a duration of 4 weeks.

The study findings indicate that Galla Chinensis effectively decreased fat accumulation in various body tissues, including the liver, gonads, and bone tissue. Moreover, it showed promising therapeutic potential in addressing postmenopausal obesity (Hwang et al., 2019). As per Liu et al. (2018), RCM fruit demonstrates antidiabetic properties. The researchers examined the impact of various extracts of RCM fruit, such as ethanol extract, free phenolic (TF), esterified phenolic (TE), and insoluble-bound phenolic (TI), on inhibiting α-glucosidase, dipeptidyl peptidase-4 (DPP-IV), and advanced glycation end-product (AGE) formation. According to the research conducted by X. Liu et al. (2021), it was found that TF had the highest level of inhibition on α-glucosidase and DPP-IV. On the other hand, TI exhibited the most powerful inhibition of AGEs. Furthermore, the water extract of Galla Chinensis (Galla Rhois) was discovered to have the ability to decrease lung metastasis of colorectal cancer (CRC) cells. This was observed in both laboratory and animal experiments, where it triggered AMPK-mediated apoptosis and hindered metastatic characteristics

like epithelial mesenchymal transition (EMT), migration, and invasion. According to a study conducted by Mun et al. in 2019, Galla chinensis was discovered to have potential as a treatment for CRC.

Studies have shown that the fruit of RCM possess potent antibacterial properties. For example, the 70% methanol extract clearly reduced the growth of *K. pneumoniae, S. dysenteriae,* and *E. faecalis* as well as *S. aureus, B. subtilis*, *E. coli,* and *P. aeruginosa*. Furthermore, obviously preventing the growth of these same bacteria was hexane extract. In conclusion, RCM fruit work as an antibacterial agent against bacteria that are connected to a variety of diseases, making them useful for treating diarrhoea, dysentery, pneumonia, and urinary tract infections.(Nemkul et al., 2021). Farmers in southern China employed RCM's roots, leaves, stems, and fruit as insecticides(L. Liu et al., 2015).

At 5.0 g/mL, 80% methanol, ethanol, and acetone extracts from RCM fruits scavenged over 60% of DPPH radicals, with IC_{50} values of 3.72 ± 0.19, 3.92 ± 0.22, and 3.64 ± 0.15 g/mL, respectively. The ABTS assay for radical scavenging yielded results that were comparable to the DPPH assay. In addition, three extracts showed a link between TPC and the capacity of DPPH and ABTS to scavenge free radicals, indicating that phenolic compounds may be the active elements of phenolic compounds that act as antioxidants (C. Zhang et al., 2018). A separate study showcased the potent antioxidant properties of the fruit extract, as evidenced by IC_{50} values of 5.31± 0.07 and 5.84 ± 0.17 g/mL for the DPPH and ABTS methods, respectively (Sharma et al., 2015). Sangtam et al. examined the aqueous extract of RCM fruit using two distinct concentration techniques: evaporation from a water bath at 50 °C and freeze-drying

using a lyophiliser. The IC_{50} values of the two method extracts in the DPPH scavenging assay were 3.792 g/ml and 3.282 g/ml, respectively, compared to the reference chemical BHA which had a value of 2.463 g/ml. Additional research has shown that freeze-dried fruit exhibits greater activity compared to aqueous-dried extract (Sangtam & Thanzami, 2020). In a study conducted by Nemkul et al., it was found that the fruit extract had a total phenolic content of 123.52± 1.29 mg GAE/g. Additionally, the 70% methanolic fruit extract showed hydrogen peroxide and DPPH scavenging rates of 42.69 ± 0.1 % and 63.20 ± 1.48 % at a concentration of 100 g/mL (Nemkul et al., 2021).

2.6 *Acacia-concinna (*Willd.) DC. (AC)

Figure 2.5: *Acacia concinna* (Willd.) DC pods

Acacia concinna (willd.) DC, commonly known as “Shikakai” or “Soap-Pod”, is a thorny, prickly, and scandent shrub native to the Asian Countries including India, Sri Lanka, Myanmar, and Thailand Figure 2.5. It is characterised by its broad and flattened base, with leaves that possess caducous stipules. The flowers of *Acacia concinna* are typically pink (or) creamy white and are accompanied by reduced subtending bracts.

The fruits season lasts from February to March, and the trees can grow to a height of up to 32 feet. The plant classification of *Acacia concinna* (Willd.) D.C can be found in Table 2.4, sourced from the Commonwealth Agricultural Bureaux International (CABI) digital library in the United Kingdom.

Table 2.4 Classification of *Acacica concinna* (Willd.) DC

Kingdom	**Plantae (Plants)**
Phylum	Spermatophyta (Seed plants)
Subphylum	Angiospermae (flowering plants)
Class	Dicotyledonae
Order	Fabales
Family	Fabaceae (Legumes, pea family)
Subfamily	Mimosoideae
Genus	Acacia
Species	*Acacia concinna*

2.6.1 Traditional uses

There are many traditional medicinal uses for elements of AC. A fragrant chutney made from the tender leaves of AC, combined with salt, tamarind, and chilies, is used to address different digestive issues, especially jaundice (Johnson, 2005). The solution derived from simmering the leaves in water is used to treat malaria, as well as to alleviate constipation and bloating (Raja & Sivaraj, 2012). It is used to treat skin infections, help with digestion, ease constipation, manage gastric problems, relieve stomachaches caused by gas, and address circulatory issues. Furthermore, mashed fruit plays a crucial role in recipes created to combat poisonous snakebites (DeFilipps & Krupnick, 2018).

Furthermore, AC ground fruit powder is well-known for its exceptional cleansing properties, making it an excellent hair care option. According to Wuthi-udomlert and

Vallisuta (2011), this powder not only gives hair a lustrous appearance, but it also promotes hair growth and effectively reduces dandruff. AC pods contain active components such as saponins, alkaloids, tannins, and malic acid, which are thought to be cleansing, stimulating, and astringent. This astringent action is essential for toning the scalp and conditioning the hair, as Johnson noted in 2005.

In Myanmar, the fruit is typically combined with the bark of the tree and pods to create a traditional shampoo known as “tayaw kinpun” in Burmese (Net, 2021). Additionally, Thai people hold the belief that this plant brings good luck and happiness, considering it an auspicious plant. In Thai traditions and festivals, such as “Songkran,” the pods of the “Som Poy” plant are utilised. During this festival, the plant is placed in holy water to wash away bad luck(Sombatsiri & Chairote, 2005).

2.6.2 Phytochemical constituents

Plant secondary metabolites possess distinctive chemical and pharmaceutical attributed that offer valuable benefits to human health. AC pods have been found to contain alkaloids, flavonoids, saponins, and tannins, while notably lacking anthraquionones and cyanogenic glycosides (Wuthi-udomlert & Vallisuta, 2011). Alkaloids, flavonoids, phytosterols, saponins, and phenolic compounds are consistently present across various extracts, including aqueous, benzene, chloroform, petroleum ether, butanol, and methanol (Gupta et al., 2013).

The synthesis of these chemical constituents in plants can be influenced by various factors beyond their growth and development. Secondary metabolites possess distinct

chemical properties that necessitate specialised extraction and analysis methods, ranging from polar to non-polar techniques. The utilisation of diverse analytical methods alongside various extraction processes facilitates the estimation of potential compound quantities (Todkar et al., 2011). As of now, a total of 15 phytochemical constituents have been extracted and identified from the pods, as outlined in Table 2.5. The exploration of other sections of the plant continues to be a potential area for further research.

Table 2.5: Phytochemical constituents in *Acacia concinna* (Willd.) DC.

Name	Molecular Formula
Furfural	$C_5H_4O_2$
5-Methyl-2-furfural	$C_6H_6O_2$
Phenyl acetaldehyde	C_8H_8O
Cis-Linalool oxide	$C_{10}H_{18}O_2$
Trans-Linalool oxide	$C_{10}H_{18}O_2$
Methyl salicylate	$C_8H_8O_3$
∝-Terpinolene (tentative)	$C_{10}H_{16}$
Geranyl acetone	$C_{13}H_{22}O$
Tetradecanoic acid	$C_{14}H_{28}O_2$
6,10,14-Trimethyl-2-pentadecanone	$C_{18}H_{36}O$
Methyl palmitate	$C_{17}H_{34}O_2$
Palmitic acid	$C_{16}H_{32}O_2$
Isopropyl palmitate	$C_{19}H_{38}O_2$
Methyl linoleate	$C_{19}H_{34}O_2$
Linoleic acid (tentative)	$C_{18}H_{32}O_2$

(Pazhamalai, 2019; Sombatsiri & Chairote, 2005)

2.6.3 Pharmacological properties and biological activities

AC pods are a rich source of secondary metabolites containing chemical compounds with potent antibacterial and antifungal properties (Pazhamalai, 2019). These compounds work by inhibiting and blocking crucial enzymes necessary for the growth and metabolism of microorganisms. The purification of these active compounds form

Acacia concinna pods holds the potential for utilisation as a chemotherapeutic agent (Todkar et al., 2011). The powder's characteristics include calcium oxalate crystals, oil globules, and cells containing saponins. The bark, specifically, has a high saponin content, recognised for its ability to produce foam. In these pods, a particular saponin contains trihydroxymonocarboxylic acid, showing both acidic properties and serving as a surfactant (Gupta et al., 2013; Pazhamalai, 2019).

Zhao and his fellow researchers made a notable discovery in their study. They found that the saponins derived from AC pods exhibit strong inhibition of pancreatic lipase activity, with an IC_{50} values of 7.9 /ml. Moreover, these saponins showed the capacity to reduce lipid accumulation in 3T3-L1 adipocytes, proving effective at a concentration of 6.3 /ml. In addition, it was discovered that saponins improve the lipolysis process in 3T3-L1 adipocytes when administered at concentrations of 3.1 or 6.3 /ml. This improvement was credited to their impact on the protein kinase A and extracellular signal-regulated kinase pathways. This observation indicates that changing these pathways is involved in decreasing lipid content in adipocytes. The results suggest that AC has the potential to serve as a future source of anti-obesogenic compounds for the treatment and prevention of obesity (Zhuoyue et al., 2021).

Furthermore, it was discovered that the dry fruit extract of AC possesses amphiphilic characteristics and exhibits surfactant properties. The surfactant that was extracted exhibited higher efficiency compared to synthetic surfactants such as sodium dodecyl sulphate (SDS) and cetyl trimethylammonium abromide (CTAB) due to its lower Critical Micelle Concentration (CMC) values. The efficacy of a single natural surfactant was found to be superior to that of commonly used synthetic surfactants in

terms of both working and interacting efficiency. Therefore, the use of a single natural surfactant derived from AC pods is proving to be a viable alternative to ionic surfactants, offering improved efficiency (Muhammad & Khan, 2018).

The AC Denture cleanser, which was recently developed, demonstrated remarkable efficacy in suppressing the activities of *S.aureus* and *E. coli* in contrast to the conventional Cefixime medication. According to Naik et al. (2019), this investigation underscores the potential of shikakai as a denture cleanser.

2.7 Synthesis of silver nanoparticles (AgNPs)

Professor Norio Taniguchi first used the word "nanotechnology" in 1974. The main focus of nanotechnology is the creation of nanoparticles for human use in a range of sizes, shapes, and controlled dispersities. Several researchers, scientists, and economists have seen a considerable increase in the usage of nanoparticles, which has been attributed to the development of novel materials to meet the demand that has formed in a variety of application areas. The extensive use of nanoparticles in the food, chemical, and cosmetics industries necessitates an environmentally acceptable and green method of synthesis (Ettadili et al., 2022; Siddiquee et al., 2020).

Traditionally, silver utensils have been a common feature in households due to their known health benefits. Modern research has confirmed the antibacterial properties silver, making them essential in many areas, particularly medicine (R. Khan et al., 2023). Particularly, silver nanoparticles are highly regarded for their unique properties, with applications in various fields like composite fibers, biosensors, pollution control, wastewater treatment, food packaging, cosmetics, and water purification (Dhaka et al., 2023).

Ali et al. (2021) classified the synthesis of silver nanoparticles into two main approaches. The bottom-up methods involve the aggregation of silver atoms or molecules to form AgNPs of different sizes and shapes. This technique is commonly utilised to generate nanoparticles with uniform distribution, morphology, and dimensions. This method utilises techniques such as supercritical hydrothermal processing (SHP), sol-gel synthesis, microwave heating, chemical vapour deposition (CVD), self-assembly of monomer/polymer molecules, laser pyrolysis, and biological synthesis. Conversely, the top-down approach employs physical methods including crushing, milling, grinding, etching, and lithography to transform substantial amounts of silver into AgNPs. Nevertheless, this approach is constrained by several drawbacks, such as the incapacity to generate smaller AgNPs, excessive energy consumption, difficulties in achieving nanoscale particles, and the potential for surface imperfections that can impact the characteristics of nanomaterial. In general, the production of AgNPs can be classified into three primary categories: chemical, physical, and biological methods. The categorisation is based on the specific preparation method employed (Ali et al., 2023).

Chemical synthesis methods use compounds like polyethylene glycol, sodium borohydride, sodium citrate, and element hydrogen as reducing agents to transform metal ions into metallic nanoparticles. This approach allows for easy production of a substantial quantity of nanoparticles (Rafique et al., 2017). However, it has drawbacks as it requires various chemicals and agents for stable colloid synthesis, which can be harmful to humans, including the substrate and chemical waste solution (Sportelli et al., 2018). Physical processes involve the use of mechanical pressure, thermal energy, electrical energy, and high-energy radiation to create nanoparticles through material

abrasion, evaporation, melting, or condensation. Physical methods necessitate a significant amount of energy, while both physical and chemical methods demand high temperatures, vacuum conditions, and expensive equipment to produce nanoparticles. These methods utilise stabilising agents, intense radiation, and concentrated reductants, resulting in potential health and environmental hazards (Dhaka et al., 2023). Conversely, biological methods utilise biomolecules, microorganisms, and phytochemicals as reducing and stabilising agents. The utilisation of phytochemicals for the synthesis of AgNPs is acknowledged for its environmentally friendly, cost-effective, convenient, and efficient attributes (Kumar et al., 2021).

2.7.1 Plant-mediated synthesis of AgNPs

Silver nanoparticles are formed using a range of phytochemical elements found in plant extracts, including phenolic acid, carbonhydrate, amino acids, carboxylic acid, terpenoids, and saponins etc which possess medicinal properties and environmentally friendly characteristics, serving as agents that both reduce and stabilise the nanoparticles, differing from the harmful chemicals used in traditional approaches (Figure2.6). Moreover, utilising plant extracts not only reduces the expense associated with microorganism isolation and culture media but also enhances cost competitiveness compared to nanoparticles synthesised by microorganisms which are vulnerable to biosafety problems (Bao et al., 2021). An important benefit of plant-mediated synthesis is its comprehensive utilisation of various plant components, such as the fruit, root, stem, peel, and so on, during the synthesis process (Ying et al., 2022). Furthermore, the unique characteristics of species diversity, the availability of biomass, the wide range of biomolecules with medicinal properties, and the

environmentally friendly nature of nanoparticles, which serve as both reducing and stabilising agents, distinguish them from the toxic chemicals employed in traditional methods (Bao et al., 2021).

Plant-based extracts offer potential for the mass production of extracellular AgNPs to fulfill the increasing demand for AgNPs. Factors such as the concentration of plant extract, silver nitrate, pH, the temperature and duration have obvious effects on the size and shape of AgNPs shown in Table 2.6. Moreover, plant mediated synthesis silver nanoparticles tends to functionalise the nanoparticles surfaces, leading to the nanoparticles surfaces, leading to the induction of synergistic effects that are essential for applications in antioxidant, antibacterial, antimicrobial, and cancer therapy (An et al., 2023; Muthu et al., 2020). Green synthesis methods typically allow for the production of nanoparticles in various shapes and sizes, including rods, spheres, cubes, and triangles, each of which can have distinct effects on microorganisms. Many studies have shown that the biocidal effect is inversely related to particle size, as smaller particles provide better contact or uptake (Rani et al., 2023) . As a result, these easily one-step-synthesised silver nanoparticles can serve as not only excellent biocompatible materials but also exhibit significant biological potential for a wide range of applications in agriculture, food science, bioengineering, cosmetics, medicine, and diagnostics (Saravanan et al., 2021).

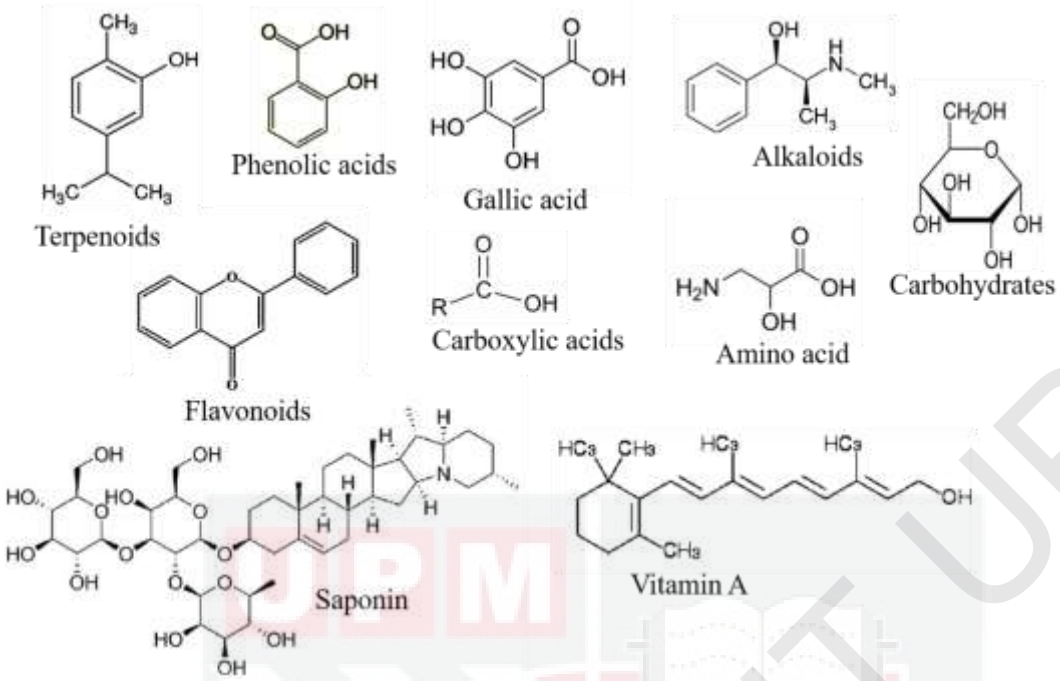

Figure 2.6: Phytochemicals using as reducing agent and stabilising agent for synthesis of silver nanoparticles

Table 2.6: Plant-mediated synthesis of AgNPs and their parameters

Part of the plants/ Biomass	pH	Temperature (C°)	Concentration ratio $AgNO_3$ and Extract	Time	Remark (optimal conditions)	Reference
Madhuca (*Madhuca latifolia*) oil cake	2,3 4,5 6,7 8	20,30 40,60 80	$AgNO_3$100 ml (1mM):10 ml	30 (mins)	Effect of temperature and pH confirmed by UV-Vis spectroscopic pH range 4 to 8 is more favorable to synthesis AgNPs 80 C° confirms uniform size of AgNPs (2 to 30nm/ spherical)	(Biswal & Pramila, 2020)
Kalanchoe pinnata (*Bryophyllum pinnatum*) leaves	5,6 7,8 9,10 11,12	10,20 30,40 50,60	$AgNO_3$ (1 mM, 2 mM, 3 mM and 4 mM) and plant extract ratio (1:10, 2:10, 3:10, 4:10)	05 (mins) 10 20 30 45 60	High $AgNO_3$, increase aggregation of nanoparticles Afters 60 mins synthesis time, no further change in observed for 24 hrs Alkaline pH suitable Higher temperature, small particles with uniform size (38nm/spherical)	(Aryan et al., 2021)
Cannabis sativa leaf extract	4,5 6,7 9,11	-	$AgNO_3$ (0.25mM, 0.5mM,1mM,1.5mM, 2mM,3mM)/ Extract to $AgNO_3$ (0.005:1,0.01:1 0.02:1,0.04:1,0.06:1 0.08:1,0.1:1)	0 hrs, 2 hrs 3 hrs, 4 hrs 5 hrs, 24 hrs, 48 hrs	3mM $AgNO_3$ 1:0.1 ($AgNO_3$ to plant extract) Neutral pH 24 hrs (Average 26.52nm/spherical)	(Chouhan & Guleria, 2020)
Plantago major L. leaf	10	60,70,80	$AgNO_3$(1mM) plant extract concentration (0.25,0.50,1%)	60 mins	0.25% plant extract and 70 C° was selected as the synthesis parameter for up-scale trail	(Sukweenadhi et al., 2021)
Givotia moluccana leaf extract and	4,6,7,9 11	-	1 to 5 mM $AgNO_3$ 0.01M to 0.0001M $AgNO_3$ 1ml, 2ml, 3 ml of leaf extract	1,2,3, 4, 5 hrs	1mM is the optimum concentration of $AgNO_3$ Basic condition pH,5 hrs (30-40 nm/ spherical)	(Sana & Dogiparthi, 2018)

2.7.2 Mechanism of AgNPs

The antibacterial mechanism of AgNPs is not yet fully understood. However, several factors affect their antimicrobial activity. These factors include the shape, size, and surface charge of the nanoparticles, the tolerance and sensitivity of different species to AgNPs, the type, genus, and species of bacteria, the concentration of the nanoparticles, and the duration of exposure to the pathogens. The antibacterial activity exhibited by the AgNPs is influenced by each of these elements. AgNPs exhibit antimicrobial effects against bacterial cells through seven previously documented mechanisms of action. These mechanisms, along with graphical representations, can be found in Figure 2.7 (Ashique et al., 2022; Ijaz et al., 2022; Kumar et al., 2021).

1. The breakdown of the cell wall and cytoplasmic membrane is caused by the passage of silver ions (Ag+) produced by silver nanoparticles (Alkhulaifi et al., 2020; Aryan et al., 2021; Gudimalla et al., 2021).

2. Degradation of ribosomes: Silver ions denature ribosomes, which prevents protein production (Rolim et al., 2019)

3. Interference with the production of adenosine triphosphate (ATP): Silver ions render respiratory enzymes on cytoplasmic membranes inactive, which inhibits the production of ATP (Lakkim et al., 2020)

4. Reactive oxygen species (ROS), which are created when an electron transport chain is disrupted, can damage membranes (Alomar et al., 2020; Mohammadalinejhad et al., 2019)

5. Replication of deoxyribonucleic acid (DNA) is inhibited by the binding of silver ions and reactive oxygen species (ROS) to DNA (Alomar et al., 2020; Aryan et al., 2021)

6. Membrane decomposition: Membrane denaturation is brought on by Ag-NPs aggregating into cell wall pits.(Rolim et al., 2019)

7. Membrane breaching: Cells generate organelles as a result of Ag-NPs immediately passing through the cytoplasmic membrane (Rolim et al., 2019)

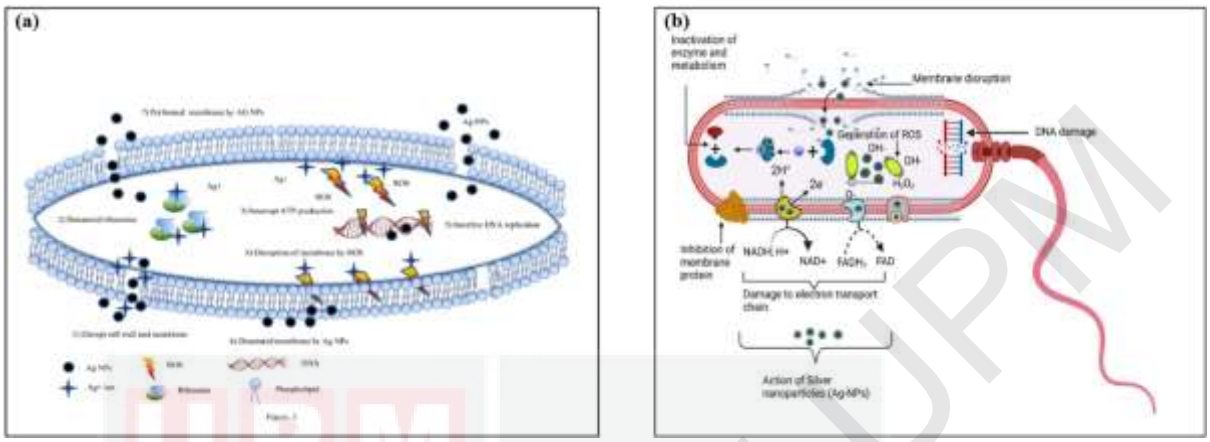

Figure 2.7: Schematic diagram of antibacterial mechanism of silver nanoparticles (a) and (b) (Ashique et al., 2022)

2.7.3 Toxicological and hazardous aspects of AgNPs

AgNPs have the potential to be used as antimicrobial agents to increase the longevity of food and effectively combat a range of harmful and spoilage-causing microorganisms. However, if Ag+ ion migration from packaging to food is not monitored, it could pose a risk to consumer health. According to the European Food Safety Authority (EFSA), it is important to ensure that the discharge of Ag+ ions from packaging does not exceed 0.05 mg/L in water and 0.05 mg/kg in food. In order to guarantee consumer safety, it is imperative to ascertain the quantity of Ag+ ions that are released from a nano-composite package based on AgNPs, as well as the amount that builds up in the packaged food (Kumar et al., 2021).

To evaluate the potential toxicity of food and packaging materials, researchers examined the effects of metal or metal oxide nanoparticles (NPs) on various human cell models. Cell viability, genotoxicity assessment, mutagenicity evaluation, and

apoptosis detection in human cell lines are frequently utilised cytotoxic assays (Rennan & Vieira, 2022). The cytotoxic profile of NPs can be influenced by several factors, including particle size, surface charge, concentration, and exposure duration to food packaging materials (Pereda et al., 2019).

Male and female mice were given AgNPs orally for three days at doses of 50, 150, and 300 mg/kg/day body weight to evaluate their toxicity and distribution in the body. According to the findings, most of the AgNPs were found to accumulate in the duodenum tissues before moving on to the liver, spleen, and kidney. TEM examination revealed that AgNPs were exclusively located in the cytoplasm or attached to the cell membrane, and did not penetrate the nuclei. Consequently, no genotoxic damage was observed in the internal organs and blood, as evidenced by the absence of any such evidence (Narciso et al., 2020). The complete analysis of the potential health risks associated with Ag+ ion migration from packages is still pending. However, instances of significantly hazardous levels of Ag+ ion migration from active packaging to food products are exceedingly uncommon.

In a recent study by Acharya et al. (2022), it was found that AgNPs exhibited promising anticancer effects when tested on human colon cancer (HCT-116) cells. Interestingly, the viability of normal human epithelial (FHM) cell lines remained unaffected by the exposure to AgNPs. In the study conducted by Yuetal. (2019), the researchers investigated the potential toxicity of AgNPs in CNF nano-composites. They utilised the human colorectal adenocarcinoma cell line (Caco-2) and human colon normal epithelial (FHC) cell lines, exposing them to different concentrations of the nano-composites (ranging from 50-1000 g/ml). In spite of the fact that AgNPs can

enter the endosomes of colon cells, neither FHC nor Caco-2 cells exhibited any adverse effects (Yu et al., 2019).

In addition, the process of plant-mediated synthesis has the advantage of reducing the environmental impact of AgNPs. This is due to the organic matter from nature that gets adsorbed onto the surfaces of the nanoparticles. This adsorption helps to prevent oxidation and the formation of harmful Ag+ ions. Furthermore, the biocompatibility of these nanoparticles ensures that they are not harmful to animal and plant tissues (Jorge de Souza et al., 2019). Based on the research conducted by R'onav'ari et al. (2017), it has been determined that AgNPs mediated by coffee extract do not have any adverse effects on human or mouse cells. It is possible that plant-mediated AgNPs may be a more effective alternative for antimicrobial purposes in sustainable food packaging (Rónavári et al., 2017).

2.8 Nanoparticles incorporated chitosan-gelatin composite film

Nanocomposites are created by utilising natural or synthetic polymers as a matrix and incorporating or dispersing organic or inorganic nanoparticles within the matrix. The majority of chitosan-gelatin nanocomposites are produced through the straightforward process of mixing and dispersing various nanoparticles within a chitosan-gelatin matrix.

Films made with a chitosan-gelatin mix incorporating 0.05% silver nanoparticles synthesized using *Mimusops elengi* fruit exhibited a smooth surface and adequate mechanical strength for commercial packaging. Films containing 0.1% AgNPs

demonstrated potential as protective packaging, extending the shelf life of red grapes by 14 days (Kumar et al., 2018). Ediyilyam and co-authors reported that adding *M.frondosa* leaf-mediated silver nanoparticles as nanofillers to chitosan-gelatin composite films enhances both mechanical and barrier properties, while also improving biological functions like antimicrobial activity, biosensing, and oxygen scavenging. The AgNPs slightly boosted the film's mechanical strength, likely due to a cross-linking effect that increased matrix density and reduced moisture retention, swelling, and water vapor transmission. CG-AgNPs films show potential as antimicrobial packaging, effectively extending the shelf life of carrot pieces (Ediyilyam et al., 2021).

In this study, incorporating chitosan nanofibers (CHNF) and ZnO nanoparticles (ZnONPs) introduced new interactions with gelatin chains, which reduced the free volume between polymer chains and created a denser, less permeable polymer network. Additionally, CHNF and ZnONPs reinforced the gelatin matrix, restricting polymer flexibility and segmental mobility. Their influence on thermal properties can be attributed to two main factors: (a) promoting heterogeneous nucleation to enhance overall crystallinity, and (b) increasing the regularity and compactness of the gelatin chains by filling in free spaces (Amjadi et al., 2019).

Advanced pH-sensing indicator films composed of chitosan/gelatin (CG) were created by integrating zinc oxide nanoparticles (nano-ZnO) (CGZ) and different quantities of black peanut seed coat anthocyanins (BPSCA) (CGZ-h), while preserving the original crystal structure. The incorporation of BPSCA augmented tensile strength and elongation at break, diminished water vapour permeability, and enhanced UV barrier

characteristics. The CGZ-h films exhibited robust antioxidant activity, primarily as a result of BPSCA, and antibacterial effects which were primarily attributed to nano-ZnO. The potential of CGZ-h films for real-time food freshness monitoring was underscored by a strong correlation between changes in total volatile basic nitrogen, pH, and total viable count in prawns and a distinct colour change in the CGZ-h2 film (Lu et al., 2022).

In this investigation, the primary substrates for film formation were chitosan and fish gelatin, with varying concentrations of TiO2-Ag being incorporated to generate composite films. At a TiO2-Ag concentration of 0.4%, the film exhibited the best water vapour barrier properties. However, the film's antibacterial and UV-blocking capabilities were improved by a higher concentration of TiO2-Ag (0.5%), but the tensile strength was reduced. The interactions between the film components were enhanced by the TiO2-Ag crystals in the film, as confirmed by XRD, XPS, and ATR-FTIR analyses. In general, the most appropriate concentration of TiO2-Ag for improving the functional properties of FG-Ch thin films was determined to be 0.4% (Lin et al., 2020).

All of the research studies mentioned above suggest that incorporating nanoparticles into the chitosan-gelatin matrix can lead to significant enhancements in the material's mechanical, electrical, thermal, chemical, optical, antimicrobial, and surface properties. Despite the fact that these NPs have well-established antibacterial properties, their high cost and toxic nature may restrict their application in the food industry (Gu et al., 2021). Plant-mediated synthesis is primarily used for synthesising nanoparticles of metals, metal oxides, and bio-metallic alloys. Composite packaging

films made with green nanoparticles biosynthesised from plant extracts demonstrated effective mechanical and barrier properties, reduced environmental impact, and provided efficient food protection. Furthermore, ZnONPs (Vieira et al., 2022), AgNPs (Kumar et al., 2021), and TiO2 NPs (Vieira et al., 2022) released metal ions into the contents at levels that were insufficient to harm human cells. This insight has the potential to help identify critical knowledge gaps and drive progress in the packaging industry.

2.9 Crosslinker in chitosan-gelatin composite film

Chitosan (polysaccharide) is well-known for its impressive qualities, such as its ability to fight against microbes, its antioxidant properties, its non-toxic nature, its ability to break down naturally, and its ability to form films. Nevertheless, the functional effectiveness of chitosan is influenced by several factors including the degree of deacetylation, molecular weight, pH, concentration, and source (Hosseinnejad & Mahdi, 2016). Although it naturally possesses antimicrobial properties, there is an ongoing effort to improve and expand its ability to fight against microorganisms. One way to accomplish this is by combining chitosan with botanical reagents (Bhowmik et al., 2022), nanoparticles (NPs), gamma-irradiation, and high hydrostatic pressure (Nair et al., 2020).

Polyphenols, which are widely present in various plants such as fruit, vegetables, and cereal grains, exhibit both functional and structural diversity. They encompass phenolic acids, flavonoids, polyphenolic amides, resveratrol, and lignans (Vieira et al., 2022). Extensive research has shown the wide range of biological functions of polyphenols, such as their ability to act as antioxidants, anticancers, combat obesity,

fight bacteria, regulate blood sugar levels, and prevent cardiovascular diseases. In addition, many studies have thoroughly examined the phenolic composition of different plant materials (Campos, 2016). The various phenolic constituents work together in coating formulations to enhance their antimicrobial and antioxidant potential. Polyphenols and plant extracts containing polyphenols are added to food products to improve their nutritional and functional characteristics, taking into account their biological functions. An important use case involves incorporating polyphenols into composite films, specifically polysaccharide-based systems utilised in food packaging (Zhu, 2021).

When polysaccharides are grafted with polyphenols, the nature of their interactions shifts towards covalent bonds (J. Liu et al., 2017). Conversely, water-soluble polyphenols tend to establish non-covalent interactions with polysaccharides. These non-covalent interactions include hydrogen bonding, electrostatic interactions, and hydrophobic interactions. The polar constituents of pequi (Caryocar brasiliense) extract interact with the amine hydroxyl groups of chitosan via hydrogen bonding and dipole-dipole interactions (Breda et al., 2017). The interaction between polysaccharides and polyphenols can affect their physical properties. For example, the incorporation of polyphenols derived from black soybean seed coat extracts into chitosan films results in a reduction in the crystallinity degree of chitosan due to non-covalent bonding (X. Wang et al., 2019). Furthermore, films made from a chitosan-gelatin blend were enriched with polyphenols extracted from Chinese hawthorn fruit. This addition led to a denser inner microstructure within the films, primarily driven by hydrogen bonds and electrostatic interactions between the film matrix and the polyphenol extract.

Zhang and collaborators integrated 4% banana peel extract into 2% chitosan films. The resulting films exhibited a smooth and compact structure, demonstrating enhanced mechanical properties, exceptional antioxidant activity, and high tensile strength. The enhanced stability of cross-linkage between phenolic compounds from banana peel and the chitosan matrix accounted for the observed increase in tensile strength. The chitosan films, in conjunction with phenolic compounds, functioned as efficient barriers to gaseous exchange due to their densely packed microstructure. Furthermore, the films exhibited a reduction in moisture and water vapour permeability. This phenomenon can be elucidated by the association between the -OH and -CHO groups of phenolic compounds and the chitosan matrix, which limits their interaction with water molecules. Furthermore, the interplay between the phenolic compounds' -OH and -CHO groups and the chitosan molecule's $-NH_2$ and -CHO groups contributed to the films' reduced water solubility. The use of chitosan films infused with banana peel extract on apple fruit resulted in a number of benefits, including reduced respiration rate, delayed changes in fruit weight, increased firmness, and the preservation of levels of total soluble solids (TSS), ascorbic acid content, and titratable acidity (TA) throughout storage and at room temperature (W. Zhang et al., 2020).

2.10 Molecular interactions between chitosan, gelatin and nanocomposite

The stability and texture of nano-composite materials are governed by molecular interactions between different functionalities (Strupiechonski et al., 2021). The strength of the interactions between chitosan and gelatin relies primarily on factors such as the pH and ionic strength of the environmental, along with the surface charge of the nanoparticles. The interactions that the C-G nano-composites may exhibit range

from electrostatic to hydrogen bonding, ionic, covalent, and Van der Waals (Gomez et al., 2021) .

During crosslinking interactions, a three-dimensional network is formed through the creation of covalent bonds. This happens when the free radical sites on the covalent cross-linker react with the free radical sites on the polymeric chains of chitosan and gelatin. The ionic interactions between the ionic cross-linkers influence the behaviour of chitosan and gelatin. Protonation or deprotonation of the functional groups (-COOH, $-NH_2$, and -OH) is essential for facilitating ionic interactions. Functional groups can undergo protonation and deprotonation by modifying the pH of the surrounding media. In an acidic pH, the $-NH_2$ group of chitosan and the $-CONH_2$ group of gelatin undergo protonation, resulting in the production of $-NH_3^+$ and $-CONH_3^+$, respectively. In addition, under basic pH conditions, functional groups such as the $-CH_2OH$ group in chitosan and the -COOH group in gelatin undergo deprotonation, resulting in the formation of $-CH_2O$ and -COO. Based on Figure 2.8, the charged functional groups on chitosan and gelatin interact through electrostatic interactions. The protonated primary amine group of chitosan enables it to dissolve when the pH value falls below its pKa (Rodríguez-rodríguez et al., 2019).

Strong electrostatic interactions are necessary for the interaction between the negatively charged polyanion and the resulting polycation. The overall charge of chitosan and gelatin can be screened by the presence of ionic salts in the aqueous media, which may impact the ionic interactions between them. The interplay between the surface charges of various nanoparticles and the charged functional groups on chitosan and gelatin can establish a robust and stable platform. This is contingent upon

the particular cationic and anionic groups incorporated onto the surfaces of the nanoparticles (López-Velázquez et al., 2019).

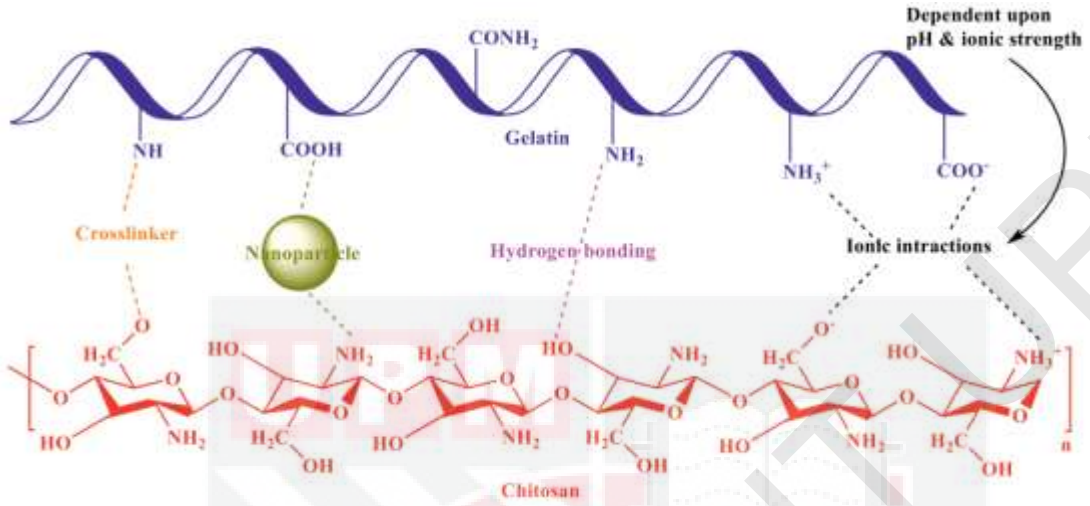

Figure 2.8: Types of molecular interactions (Sethi & Singh, 2022)

2.11 Chitosan-gelatin composite film for active food packaging

Deacetylating chitin, found in marine waste sources such as crustacean shells (shrimp, oysters, crabs, and lobsters), produces chitosan, a polymer known for its intriguing characteristics. These include its natural origin, biodegradability, non-toxicity, biocompatibility, cost-effectiveness, and excellent film-forming abilities. Extracting chitosan from marine wastes aligns with the circular economy concept, facilitating the production of value-added commodities from seafood waste. Chitosan, the world's second most abundant biopolymer, has outstanding properties that make it ideal for a variety of applications (Bhowmik et al., 2022). When the positively charged chitosan molecule interacts with the negatively charged microbial cell membrane, internal bacterial components may leak out. Given its capacity to interact with other molecules and produce beneficial outcomes, chitosan can be utilised as an active biological substance (Azmana et al., 2021; Duan et al., 2019).

However, the low thermal and mechanical stability of chitosan pose significant limitations for its industrial-scale application as a biodegradable material (Silva et al., 2021). To address this issue, different strategies have been employed to improve the thermal and mechanical stability of chitosan. One method includes the addition of various plasticizers like water, ethylene glycol, glycerol, and sorbitol. The plasticizers mentioned in the study by Vlacha et al. (2016) were used to enhance the flexibility, stretchability, and workability of chitosan films, thereby reducing their brittleness. In order to minimise its susceptibility to humidity, chitosan is frequently mixed with various bio-based substances such as gelatine, collagen, why protein, casein, zein, and botanical agents (Bhowmik et al., 2022). By combining chitosan with these materials, its overall properties can be improved expanding its potential applications.

Extensively investigating the integration of natural and biodegradable chitosan (polysaccharide) into the gelatin (protein) system has become a notable and popular approach. After the slaughter and processing of an animal, a fibrous and insoluble collagen residue remains, which is meticulously hydrolysed to produce gelatin, an animal derived protein. Gelatin is a highly popular protein choice for creating food packaging films. It is highly accessible and possesses a robust capacity for film formation. Furthermore, it demonstrates remarkable barrier properties against light, oxygen, and lipids. Chitosan's cationic properties enable it to establish electrostatic interactions with negatively charged substances under acidic conditions. Chitosan and gelatin (C-G) demonstrate compatibility within the film matrix due to electrostatic interactions and hydrogen bonding. This compatibility arises from the positive charge of chitosan and the negative charge of gelatin at specific pH values. It is worth noting that films made from a combination of C-G mix exhibit superior mechanical and

barrier properties when compared to films made from their individual components (Lu et al., 2022; Shi et al., 2022).

Natural bioactive chemicals have shown promise in the development of active packaging, meeting a growing consumer demand for products with the fewest chemical components. Plant extracts are especially intriguing because they are frequently high in bioactive compounds. Polyphenols, which are found in a wide variety of plants including fruit, vegetables, and cereal grains, have both functional and structural diversity. They encompass phenolic acids, flavonoids, polyphenolic amides, resveratrol, and lignans (Vieira et al., 2022). Extensive research has shown the wide range of biological functions of polyphenols, such as their ability to act as antioxidants, anticancers, combat obesity, fight bacteria, regulate blood sugar levels, and prevent cardiovascular diseases (Campos, 2016). The various phenolic constituents work together in coating formulations to enhance their antimicrobial and antioxidant potential. An important use case involves incorporating polyphenols into composite films, specifically polysaccharide-based systems utilised in food packaging (Zhu, 2021).

In addition, the direct incorporation of bioactive compounds into food may be restricted due to their interaction with food components, which neutralises their activity and causes rapid degradation of food quality (Al-maqtari et al., 2022). Researchers have attempted to augment the properties and efficacy of edible films by integrating bioactive substances such as antioxidants, phenolic compounds, and antimicrobials. The altered films can subsequently serve as dynamic packaging films for the controlled release and management of substances during storage (Tessaro et al.,

2021). C-G blend films can experience significant improvements in their physical, mechanical, barrier, and antioxidant properties when pure polyphenols and plant extracts rich in polyphenols are incorporated.

The C-G matrix is combined with nanoparticles to create the nano-composites. By incorporating nanoparticles into the chitosan-gelatin matrix, the resulting materials can experience significant improvements in their mechanical, electrical, thermal, chemical, optical, and surface properties. In recent studies, there have been promising developments in the field of environmentally friendly NP preparation techniques. These advancements have shown potential for active food packaging by utilising plant extracts and biomolecules as reducing and complexing agents in nanocomposite films. In a novel approach to the development of exceptional materials with potent antibacterial and antioxidant properties, inorganic nanoparticles are combined with plant extracts or essential oils in biodegradable polymer matrices. The antibacterial properties of inorganic NPs are well-established and effective against a diverse array of Gram-positive and Gram-negative bacteria. Furthermore, it is worth noting that metallic nanoparticles have the ability to act as antioxidants. This property can be enhanced further by combining it with natural antioxidants, as shown in Figure 2.9 (Pirsa et al., 2020).

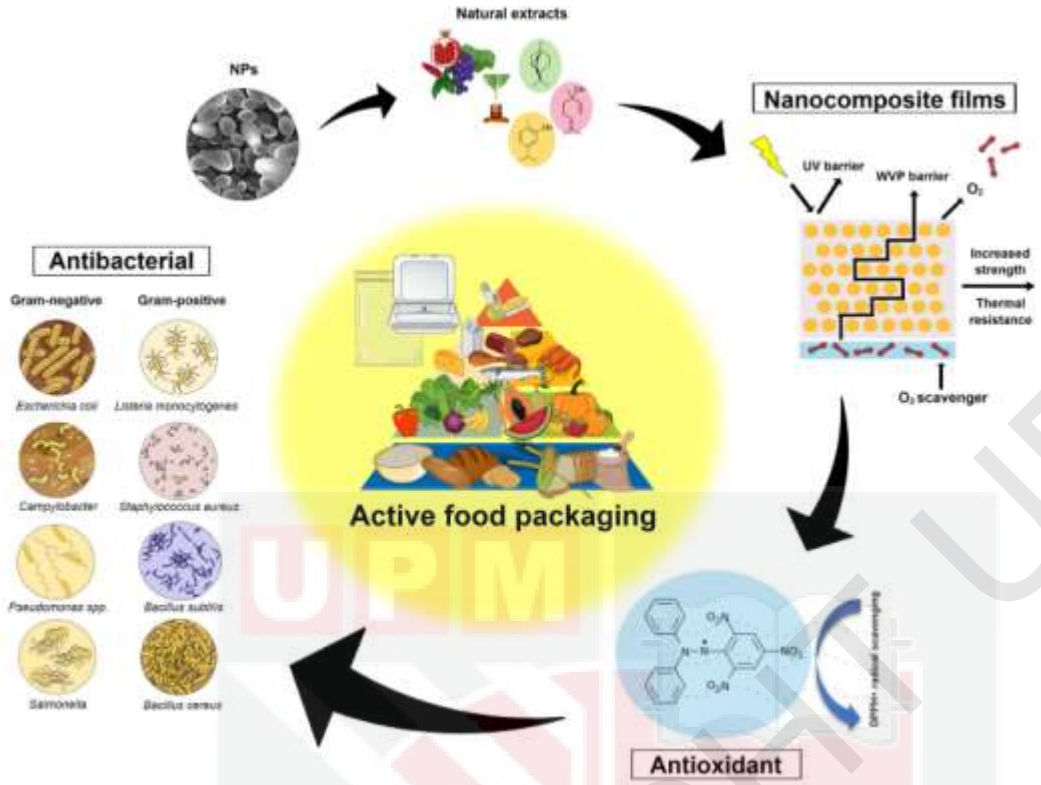

Figure 2.9: Application of nanoparticles and natural extracts in nano-composite films for active food packaging (Vieira et al., 2022)

2.12 Summary

The synergistic effects of combining chitosan and gelatin are explored, particularly in physicochemical properties. Numerous studies have investigated the use of chitosan-gelatin composite in biomedical applications (Sethi & Singh, 2022), while a few have explored their potential in food packaging. While chitosan and gelatin together have promising properties for food applications (H. Wang et al., 2021), further research is needed to fully explore their potential active properties. Consumer health concerns, awareness of extending product shelf-life, and the importance of safety and freshness have driven the development of antimicrobial and antioxidant food packaging systems. Previous research has indicated that synthetic preservatives such as nitrates, benzoates,

sulfites, sorbates, parabens, formaldehyde, BHT, and BHA may pose serious health risks, including hypersensitivity, allergic reactions, cancer, asthma, and neurological issues(Anand & Sati, 2013). The use of synthetic antimicrobial and antioxidant agents in packaging remains controversial due to these potential adverse effects (Felter et al., 2021; Hauser et al., 2016), prompting a growing interest in natural preservative alternatives.

The classification of food packaging and its functional properties were discussed, with a particular emphasis on active food packaging and its antimicrobial and antioxidant properties. In addition, this literature review includes a detailed discussion of silver nanoparticle synthesis, antibacterial mechanism, and toxicological and hazardous aspects. The mechanism and properties of chitosan-gelatin biopolymer-based active food packaging have also been explored. The selection of *Rhus chiensis* Mill fruit and *Acacia concinna* (Willd.) DC pods extracts was based on their biological properties and popular folk medicinal plants in Asia. There is no comprehensive work on the use of selected plant extracts in serving as bioactive agents for food preservations as well as reinforcing biopolymer composite films. This study also intended to analyse the plant extract mediated synthesis of silver nanoparticles, concentration of Ag+ ions released from selected bioactive composite film and apply chicken breast preservation.

CHAPTER 3

CHARACTERISATION OF BIOACTIVE PROPERTIES PROFILES IN VARIOUS SOLVENTS OF *RHUS CHINENSIS* MILL. FRUIT AND *ACACIA CONCINNA* (WILLD.) DC PODS

3.1 Introduction

Extraction is one of the most critical steps in herbal product manufacturing, as it impacts both the quality and quantity of active ingredients in the sample (Huie, 2002). The extraction of biologically active compounds relies on several factors, including the extraction method, choice of raw materials, and type of solvent used (Tiwari, 2015). Ultrasonic-assisted extraction efficiently extracts bioactive components from plants, achieving high-purity yields in minutes while reducing extraction time, solvent use and enhancing both quality and reproducibility, making it an ideal method for sustainable practices (Shen et al., 2023). Furthermore, we provide a variety of extraction solvents, including distilled water, 80% ethanol, and 80% methanol, which are known for their high yields and eco-friendliness, making them environmentally friendly options (Chemat et al., 2019).

The two of the most popular edible traditional medicinal plants in Myitkyina, the Northern part of Myanmar; *Acacia concinna* (willd.) DC, commonly known as shikakai, and *Rhus chiensis* Mill, known as Chinese sumac. Previous research has shown that *Acacia concinna* (Willd.) DC and *Rhus chinensis* Mill. have traditional medicinal uses, phytochemical constituents, pharmacological properties, and biological activities (Johnson, 2005; Raja & Sivaraj, 2012; Y. Zhang et al., 2023). These plants merit to be further investigate as currently there is no published research on the use of their extracts as bioactive agents for food preservation.

This chapter develops into characterising the profiles of bioactive properties in distilled water, 80% ethanol, and 80% methanol solvents extracted from both *Rhus Chinensis* Mill. fruit and *Acacia concinna* (Willd.) DC pods using Ultrasonic-assisted extraction methods and to identify a potential medical plant and its corresponding solvent with strong antimicrobial and antioxidant properties for further study. Figure 3.1 depicts the research layout for this chapter.

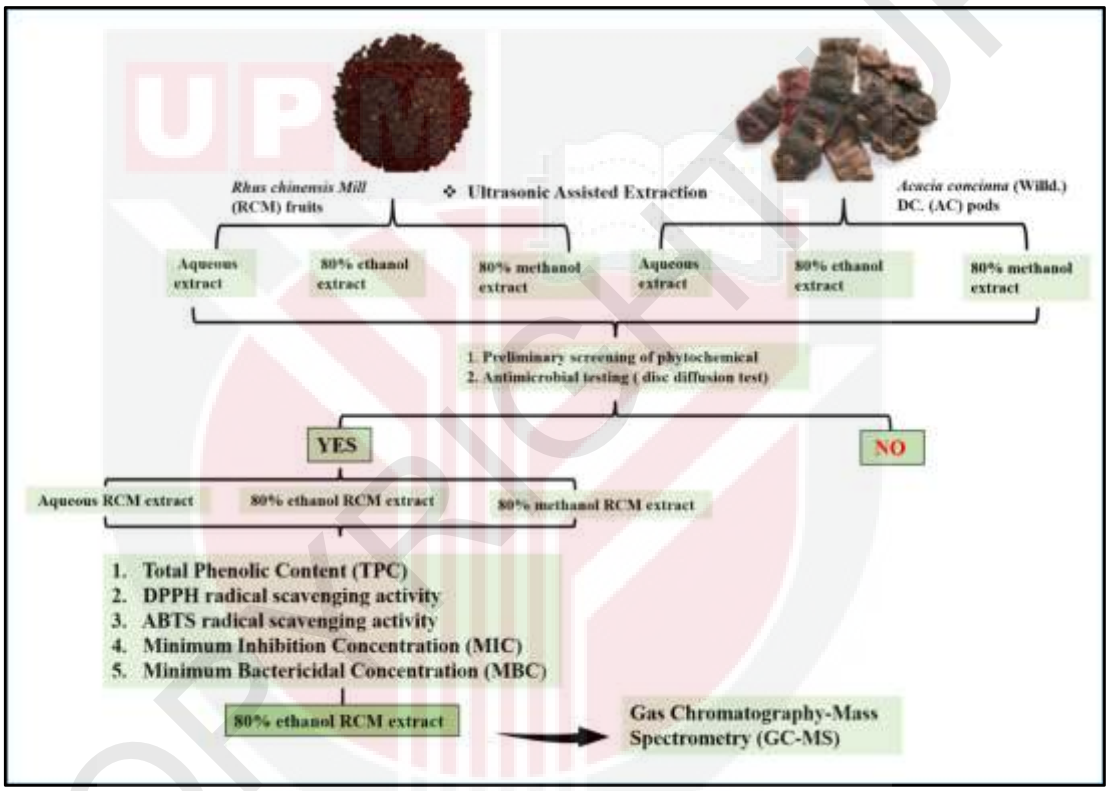

Figure 3.1: Flow chart of chapter (3)

3.2 Materials and methods

3.2.1 Plants sample collection and identification

Fruit of *Rhus chinensis* Mill. (RCM) and pods of *Acacia concinna* (Willd.) DC. (AC) were procured from Myitkyina, Kachin State, and the northern region of Myanmar. The plant samples were taxonomically identified by botanist Dr. Khairil Mahmud, and

the voucher specimens with accession numbers KM0002/22 and KM0012/22 were deposited at the Biodiversity Unit, Institute of Bioscience, Universiti Putra Malaysia (Appendices A1 and A2).

3.2.2 Chemicals, solvents and reagents

This chapter presents the chemicals and solvents listed in Table 3.1.

Table 3.1: Chemicals and solvents used

Chemicals/Solvents/Reagent	Manufacturer
0.5 N sodium hydroxide	R&M Chemicals, UK
ABTS (2,2-azin bis (3-ethylbenzothiazoline-6-sulfonic acid))	Sigma, USA
Ampicillin (10 µg)	Oxoid Ltd, England
Ascorbic acid	R&M Chemicals, UK
Chloroform	R&M Chemicals, UK
Dimethyl sulfoxide (DMSO)	R&M Chemicals, UK
DPPH (2,2-diphenyl-1-picrylhydrazyl)	Sigma, USA
Dragendroff's reagent	R&M Chemicals, India
Ethanol (80%)	R&M Chemicals, India
Ferric chloride (30% w/v)	R&M Chemicals, India
Folin-Ciocalteu reagent	R&M Chemicals, UK
Gallic acid	R&M Chemicals, UK
Hydrochloride (37%)	R&M Chemicals, India
Methanol (80%)	R&M Chemicals, India
Potassium persulfate	Sigma, USA
Sodium carbonate	R&M Chemicals, India
Sulphuric acid (99%)	R&M Chemicals, UK
Vancomycin (30 µg)	Oxoid Ltd, England

3.2.3 Preparation of extracts

RCM fruit and AC pods were air-dried in the shade at ambient temperature for the research. Subsequently, the desiccated fruit and pods were meticulously powdered using a Waring laboratory blender and subsequently sifted through a 60-mesh sieve to guarantee adequate refinement. Preparation was conducted for the 60-

mesh sieve of RCM fruit and AC pods for extraction via ultrasound-assisted extraction (P. Tiwari et al., 2011). The RCM fruit and AC pods were initially macerated in aqueous solutions of 80% ethanol and 80% methanol (at a material to solution ratio of 1:5) at 500 rpm, utilising a WiseStir MSH-20D hotplate stirrer from Korea, and stirred at room temperature overnight. During the second stage, each solution underwent ultrasonic extraction at a frequency of 20 kHz and an amplitude of 50 percent (Sonifier® SFX550, Branson Ultrasonics, USA) for 15 minutes in an ice bath (Nn, 2015). The filtrate was gathered, and the residue underwent two further extractions employing the identical second stage procedures, with the solvents being replenished each time. In the final stage, the entire collected solution was filtered using a Buchner funnel attached to a vacuum pump. The filtrates were concentrated using a rotary evaporator (Heidolph HB Digital, Germany) at 45°C to eliminate the organic reagents and subsequently stored at 4°C for future utilisation. The yield percentage was ascertained as follows.

$$\text{Extraction of yield (\%)} = \frac{The\ weight\ of\ extract\ (g)}{The\ weight\ of\ sample\ powder\ (g)} \times 100\ \% \qquad \text{Equation (3.1)}$$

3.2.4 Preliminary screening of phytochemicals of RCM fruit and AC pods

The phytochemicals of RCM fruit and AC pods were screened in three different extracts: aqueous, 80% ethanol, and 80% methanol, to detect the presence of phenols, flavonoids, alkaloids, tannins, terpenoid, saponins, and steroids. Table 3.2 shows the procedure for qualitatively determining phytochemicals in plant samples.

Table 3.2: Preliminary screening of phytochemicals

No	Phytochemical name	Method	Observation	References
1.	Phenols	Sample + 5 drops of 2%(W/V) $FeCl_3$	black or Blue green colouration	(Patle et al., 2020)
2.	Flavonoid	Sample + 5 drops dilute.NaOH + dilute HCL	Yellow solution with NaOH turned colourless with HCL	(Kilonzo & Munisi, 2021)
3.	Alkaloid	Sample + 5 drops of Dragendroff's reagent	The orange colour was formed	(Kilonzo & Munisi, 2021)
4.	Tannins	Sample + 2ml 2% $FeCL_3$	Blue-green or black colouration	(R. Yadav & Agarwala, 2011)
5.	Terpenoid	Sample + 3ml chloroform+ 2ml Con.H_2SO_4	Reddish brown colour	(Kilonzo & Munisi, 2021)
6.	Saponin	Sample + 4ml distilled water(shaken)	Foam formation	(Kilonzo & Munisi, 2021)
7.	Steroids	Sample + 4 drops Chloroform + Conc H_2SO_4	The red colour in the chloroform layer	(D. M. Heirangkhongjam & Iboyaima, 2021)

3.2.5 Antimicrobial activity of RCM fruit and AC pods extracts

3.2.5.1 Preparation of media and chemicals

The media, chemicals, and bacterial strain were prepared as outlined in Table 3.3 prior to conducting the antibacterial activity assays.

Table 3.3: Preparation of media and chemicals

Media/chemical/Strain	Instruction for preparation
Muller Hinton Agar (Oxoid, England)	Suspend 38 g of media powder into 1L of distilled water. Autoclave (121°C, 15 min).
Muller Hinton Broth (Oxoid, England)	Suspend 21 g of media powder in 1L of distilled water. Autoclave (121°C, 15 min)
E.coli (ATCC 25922**)** *S.aureus* (ATCC 43300)	The strains were grown on Muller Hinton Broth media and incubated for 18-24 h at 37°C. The stock of the cultures was prepared for further used.
Dimethyl sulfoxide	10% dimethyl sulfoxide (DMSO) was used as negative control.
RCM fruit and AC pod extracts	The crude extracts were diluted in 10% of DMSO to obtain 100 mg/ml. (Natural antimicrobial agents)
Bacterial maintenance & prepare inoculums	Bacterial stock cultures were grown on Muller Hinton agar at 37°C for 12 to 24 hours. The bacteria were sub-cultured every 2-3 weeks due to the high risk of cross-contamination in a laboratory environment. A loop of three to five single colonies of each bacterium from Muller Hinton agar plates were transferred to 5 mL of sterile saline water (0.85% NaCl). To reach the desired turbidity level according to the 0.5 McFarland criterion, adjustments were made to the turbidity of the colony suspension. Consequently, a suspension of 1-2 10^6 CFU/mL is generated. Additional analyses were performed using standardised suspensions of activated bacteria.

3.2.5.2 Disc diffusion test

We employed the disc diffusion method on Muller Hinton Agar (MHA) medium to evaluate antibacterial efficacy. The examination concentrated on *S. aureus* and *E. coli* (Umaira et al., 2022). Before placing the disc paper in the specified area at the top of the MHA medium, 100 µl of a 1-2×10^8 CFU/mL bacterial suspension was uniformly dispersed throughout the medium. A 40 µl sample was positioned at the centre of each disc. Ampicillin disc (10 µg) served as the positive control, whereas DMSO at a concentration of 10% functioned as the negative control. Following 18 hours of incubation at 37°C, the diameter of the clear zone was recorded. The procedure was conducted three times separately.

3.2.6 Total Phenolic Content of RCM fruit extracts

The Folin-Ciocalteu reagent (FCR) was used to measure the total phenolic compounds (TPC) using a UV-Vis spectrophotometer following the methods recommended (Nemkul et al., 2021) with slight modifications. The extract samples were diluted with Folin-Ciocalteu reagent and 4mL 7.5 % (w/v) Na_2CO_3 solution, then incubated for 30 minutes at 45°C. With a UV-Vis spectrophotometer, the mixture was analysed at 760 nm using pure methanol as the blank. The calibration curve, with the equation y = 0.0085x + 0.0084 (R2 = 0.99), served as the standard calibration for gallic acid concentrations. After measuring absorbance, the phenolic content was calculated as mg of Gallic acid equivalent (GAE) in mg per g of dry weight (DW). All tests are conducted three times.

3.2.7 DPPH radical scavenging activity of RCM fruit extracts

Aqueous, 80% ethanol and 80% methanol RCM fruit extracts were evaluated for their capacity to scavenge DPPH radicals following the procedure outlined by Lee and colleagues, with a slight adjustment (K. J. Lee et al., 2015). Each sample was dissolved in methanol before analysis, and then centrifuged at 5500 rpm for 10 minutes at 4°C. Afterward, the gathered supernatants underwent additional testing. The DPPH reagent consists of 8 mg of DPPH dissolved in 100ml of methanol, resulting in a solution concentration of 80 µl/ml. The assessment of scavenging activity involved the combination of 100 µl of DPPH reagents with 100 µl of supernatant in a 96-well plate. The mixture was then incubated for 30 minutes at room temperature. The absorbance was measured at 514 nm subsequent to incubation utilising an ELSA reader (TECAN

Grodig, Austria), with a control solution consisting of 100% methanol. The formula provided was utilised to ascertain the DPPH scavenging effect.

$$\text{DPPH radical scavenging activity (\%)} = \left[\frac{(S)control-(S)sample}{(S)control}\right]\times 100 \quad \text{Equation (3.2)}$$

The IC_{50} values for DPPH (the concentration of the sample required to inhibit 50% of DPPH radicals) were calculated through extrapolation and regression analysis. The IC_{50} value was used to evaluate the antioxidant's efficacy.

3.2.8 ABTS radical scavenging activity of RCM fruit extracts

The method described by Lee and colleagues was used to evaluate each extract's ABTS radical scavenging activity, with a few minor modifications (K. J. Lee et al., 2015). Individual samples were dissolved in methanol before analysis, which was followed by centrifugation (5500 rpm/10 min/4°C). The collected supernatants were later subjected to additional examination. The ABTS reagents were produced by combining 88 ml of 140 mM potassium persulfate with 5 ml of 7 mM ABTS. The mixture was diluted with water (1:44, v/v) and left to sit in the dark at room temperature for 16 hours to facilitate the production of free radicals. A combination of 100 ml of ABTS reagent and 100 µL of samples was mixed in a 96-well microplate to assess the scavenging activity. The mixture was incubated at room temperature for 6 minutes. The absorbance at 734nm was measured following incubation using a TECAN ELISA reader from Groding, Austria. A 100% methanol control was implemented.

$$\text{ABTS radical scavenging activity (\%)} = \left[\frac{(S)control-(S)sample}{(S)control}\right]\times 100 \quad \text{Equation (3.3)}$$

The IC_{50} values for ABTS were calculated using extrapolation and regression analysis, indicating the sample concentration required to inhibit 50% of DPPH radicals. The antioxidant's effectiveness was assessed using its IC_{50} value.

3.2.9 Determination of minimum inhibitory concentrations (MIC) of RCM fruit extracts

The minimum inhibitory concentration (MIC) of the RCM fruit 80% ethanol, 80% methanol, and aqueous extracts was determined against the bacterial strains *S.aureus* and *E.coli* using the two-fold serial dilution method (CLSI, 2012).The colony suspension was created by suspending 10 to 20 isolated colonies in 5 ml of saline solution (0.85% NaCl). Subsequently, the turbidity of the colony suspension was adjusted to meet the 0.5 McFarland standard. This results in a suspension with a concentration of 1-2 $\times 10^8$ CFU/mL. Dilute the prepared inoculum to 1:20 in MH broth to obtain an approximate 2-8 $\times 10^6$ CFU/mL. In a microtiter plate, add 100 µL of inoculum to columns 1 to 11 and 100 µL of MH broth to column 12 as a sterility control. Column 11 was used to control growth. Column 1 contained the highest concentration of samples (50 mg/ml), which was stirred and serially two-fold diluted until column 10 (0.097 mg/ml). The incubation period extended for 24 hours at a temperature of 37°C. The MIC value was established by identifying the minimal extract concentration that did not induce turbidity in the broth.

3.2.10 Minimal bactericidal concentrations (MBC) of RCM fruit extracts

The minimum bactericidal concentration (MBC) of the RCM fruit 80% ethanol, 80% methanol and aqueous extracts against the bacterial strains *S.aureus* and *E.coli* was determined by sub-culturing 10 µL of each suspension from the microtiter plates (columns 1 to 12) onto an LB agar plate and incubating at 37°C for 12-24 hours. The MBC value was calculated as the lowest concentration at which there was no discernible growth.

3.2.11 Profiling of phytochemical composition of RCM fruit 80% ethanol extract of Gas chromatography-mass spectrometry (GCMS)

The 80% ethanol extract was combined with methanol in a 1:5 ratio. An aliquot of the resultant solution was injected into a QP2010 Ultra gas chromatograph-mass spectrometer (Shimadzu Corporation, Kyoto, Japan) equipped with a BP5MS column (30.0 m in length, 0.25 mm i.d, and a film thickness of 0.25 µm) for compound separation. Helium was used as the carrier gas, with a slow increase of 3℃/min until it reached 300 ℃, and then maintained for 10 minutes. Both the injection and ion-source temperatures were kept at 200℃. In order to determine the peaks, their retention times and mass fragment patterns were compared to the standard spectra found in the Shimadzu GC-MS NIST17/Wiley library and FFNSC2. The components' identities, molecular weights and structures of the extract under test were determined.

3.2.12 Statistical analysis

The data was gathered utilising IBM-SPSS version 25 and analysed through one-way analysis of variance (ANOVA). The Least Significance Difference (LSD) method was employed to ascertain differences in means.

3.3 Result and discussion

3.3.1 Extraction yield and phytochemical constituent of RCM fruit and AC pods

For phytochemical extraction techniques, the primary solvents are distilled water, 80% ethanol, and 80% methanol. Also, the literature suggests that these solvents be employed to extract the most bioactive components from plants (Lojkova et al., 2023). Table 3.4 provides the phytochemical composition and percentage of yield of the aqueous, 80% ethanol, and 80% methanol extracts of RCM fruit and AC pods.

In the case of RCM fruit, the yield percentages for aqueous, 80% ethanol, and 80% methanol extracts were 10.16%, 14.57%, and 16.8%, respectively. In line with this, the yield percentages of AC pods extracted in aqueous, 80% ethanol, and 80% methanol were 13.2%, 10%, and 14%, respectively. The percentage of extract yield is typically influenced by a variety of solvents and extraction methods. Saleh et al. (2016) found that using ultrasound-assisted extraction increased the yield of chlorogenic acid extracted from *Cynara scolymus* L. leaves by 50% compared to the conventional maceration process conducted at room temperature.

Table 3.4: Phytochemicals screening and yield percent

Parameters	*Rhus chinensis* Mill. (RCM)			*Acacia concinna* (Willd.) DC (AC)		
	Aqueous Extract	80 % Ethanol Extract	80% Methanol Extract	Aqueous Extract	80% Ethanol Extract	80% Methanol Extract
Yield %	10.16	14.57	16.8	13.2	10	14
Phytochemical						
Phenols	+	+	+	+	+	+
Flavonoid	+	-	-	+	-	-
Alkaloid	+	+	+	+	+	+
Tannins	+	+	+	+	+	+
Terpenoids	+	+	+	-	+	+
Saponins	-	-	-	+	-	-
Steroids	+	+	+	+	+	+

+ = Presence, - = Absence.

According to past research, the yield percentages for RCM aqueous extract obtained through the reflux extraction method were 0.75% (R.-R. Wang et al., 2006). The percentages of yield for the 70% methanol extract obtained through the Soxhlet extraction method were 11.54% (Nemkul et al., 2021), while for the 80% methanol, 80% ethanol, and 80% acetone extracts obtained through the ultrasonic extraction method were 10.55 ± 1.18%, 10.39 ± 1.04%, and 11.40 ± 1.62%, respectively (C. Zhang et al., 2018). According to prior research, the ethanolic extract yields of AC were 8.73% and 14.18% when using the Soxhlet extractor and maceration, respectively. In addition, Badi and colleagues discovered that the AC aqueous extract generated 8.3% through hot maceration (Bhadauria & Gupta, 2019). The current yield percentage of the extract is 4-6% higher than that of the previous study as a result of the modified extraction method. Additionally, the percentage of RCM fruit extract is higher (0.57 to 6.8%) than that of AC pods extracts.

Tannins, phenols, alkaloids, terpenoids, and steroids were found in the aqueous, 80%

ethanol, and 80% methanol solvent extracts of RCM, as well as AC. Flavonoids were observed only in the aqueous extracts, while saponins were present only in the aqueous extract of AC. According to research, the preliminary phytochemical analysis includes antioxidant, hormonal, enzyme-stimulatisng, DNA replication-interfering, and antimicrobial effects (Poudyali & Singh, 2020).

3.3.2 Antimicrobial properties of RCM fruit and AC pods extracts

The antimicrobial activity of aqueous, 80% ethanol, and 80% methanol extracts of RCM fruit and AC pods were assessed using the disc-diffusion assay. Table 3.5 shows that RCM fruit exhibited higher antibacterial activity, with inhibition zones ranging from 8.46 ± 0.30 to 10.53 ± 0.25 mm for *E.coli* (Gram-negative) and from 6.51 ± 0.20 to 11.86 ± 0.72 mm for *S.aureus* (Gram-positive), compared to AC's antibacterial activity. AC exhibited antibacterial activity only against *S.aureus*, with inhibition zones ranging from 7.02 ± 0.37 to 13.20 ± 0.18 mm. The RCM fruit extracts had similar antibacterial properties to the positive control, Ampicilline. Additionally, Ramli (2018) suggests that certain bioactive compounds may be unable to fully express their activity when using discs due to their immobilisation in the disc pores and their inability to traverse the inoculation medium. However, the antibacterial properties of both extracts are noteworthy.

According to Nemkul et al., the 70 % methanol RCM fruit extract shown significantly antibacterial activities against Gram positive bacteria (*S. aureus, B. subtilis* and *E. faecalis* with inhibition zone rates with 20.25 ± 0.75, 20.66 ± 0.33 and 17.83 ± 0.16 mm) and Gram-negative bacteria (*E. coli*, and *P. aeruginosa*, *K. pneumoniae*, and *S.*

dysenteriae with inhibition zone diameters of 23.00 ± 0.57, 16.33 ± 0.33, 14.66 ± 0.33 and 14.66 ± 0.33 mm). While, the hexane extract was found effective against *S.aureus*, *B. subtilis, E.coli* and *P. aeruginosa* (14.00 ± 0.57, 15.66 ± 0.33, 16.00 ± 0.33 and 12.33 ± 0.33 mm) (Nemkul et al., 2021). However, a recent study found that the antibacterial activity of RCM fruit extract against *S.aureus* and *E.Coli* decreased in the following order: methanol extract was the most effective, followed by ethyl acetate extract and then the aqueous extract. An inhibition zone was observed in all the solvent extracts of RCM fruit when tested at a concentration of 400 mg/ml (Poudyali & Singh, 2020).

The aqueous extract of AC exhibited antibacterial activity, with inhibition zones of 10.4 mm for *B.subtilis* and 5.4 mm for *S.aureus*. It also inhibited *K.pneumoniae*, *P.aeruginoda*, and *E.coli*, with zone of inhibition measuring 12.5 mm, 5.4mm, and 10.2 mm, respectively (Todkar et al., 2010). On the other hand, the methanol extract of AC showed antibacterial effects against *B.subtilis* (10.2mm) and *S.aureus* (6.2 mm), as well as against *K.pneumoniae*, *P.aeruginosa*, and *E.coli*, with inhibition zones of 11.4 mm, 5.2 mm, and 10.2 mm, respectively.

The antimicrobial properties of plants have been demonstrated through research on phytochemicals, which are abundant in a variety of phytochemicals such as tannins, terpenoids, alkaloids, phenol, and flavonoids (Kilonzo & Munisi, 2021) (Table 3.4). In addition, phenolic compounds possess a phenolic structure that includes an aromatic benzene ring and at least one hydroxyl (O-H) group (Ong et al., 2021). By accumulating hydroxyl groups that interact with membranes, phenols primarily disrupt the plasma membrane, thereby exerting their antibacterial effects. The hydrophobicity

and surface charge of the membrane are altered by this accumulation, which leads to localised ruptures, pore formation, and leakage, among other disruptive effects (Álvarez-Martínez et al., 2021). Stearic acid and palmitic acid, which are fatty acids, have antimicrobial properties that defend against a variety of infections, as indicated by prior research on *P. betle* leaf extracts (Umaira et al., 2022). Flavonoids have the ability to regulate the function of bacterial enzymes that are essential for cell survival, including those that catalyse the production of cell wall components, cell membrane fatty acids, or ATP (adenosine triphosphate) (Makarewicz et al., 2021).

The findings of this study may vary from past research on the antibacterial properties of RCM fruit and AC pods extracts, possibly due to various factors. This study took into account a variety of factors, including the geographic location of the plant materials, variations in the diffusion capacity of the active substances, and the use of diverse extraction methods. Additionally, the antibacterial properties of the RCM fruit extract may have been affected by the use of various organic solvents in this study. It is essential to evaluate these factors when analysing the results of this study and comparing them with prior findings. RCM fruit extracts exhibit a more potent antibacterial effect on the candidates compared to AC pod extracts. Consequently, RCM fruit extracts were subjected to further analysis to ascertain the Minimum Bactericidal Concentration (MBC) and Minimum Inhibitory Concentration (MIC) values regarding their antimicrobial efficacy.

Table 3.5: The antibacterial activities of RCM fruit and AC pods aqueous, 80% ethanol and 80% methanol extract

Solvent extract	Inhibition Zone (mm)	
	E.coli	***S.aureus***
RCM fruit		
Aqueous	8.46 ± 0.30^{C}	6.51 ± 0.20^{D}
80% ethanol	8.75 ± 0.21^{C}	11.86 ± 0.72^{B}
80% methanol	10.53 ± 0.25^{B}	9.9 ± 0.42^{C}
AC pods		
Aqueous	0^{D}	7.02 ± 0.37^{D}
80 % ethanol	0^{D}	10.51 ± 0.71^{C}
80 % methanol	0^{D}	13.20 ± 0.18^{A}
Ampicilline (10 µg)	11.15 ± 0.14^{A}	6.51 ± 0.24^{D}
DMSO (10%)	0^{D}	0^{E}

Note: Values are means ± SD of three determinations. Means within each column with different letters differ significantly ($P < 0.05$).

3.3.3 Total Phenolic Content and antioxidant properties of RCM fruit

The antioxidant activity of plant-derived extracts can be evaluated through various in vitro antioxidant assays that utilise chemical reaction methods, including those based on hydrogen atom transfer (HAT) or single electron transfer (SET) mechanisms. The HAT-based method assesses an antioxidant's ability to counteract free radicals by releasing hydrogen and forming stable molecules, whereas SET-based assays assess the antioxidant's ability to transfer one electron and reduce various compounds (Razali, 2019). In order to determine the antioxidant properties of RCM fruit aqueous, 80% ethanol and 80% methanol extracts were subjected to TPC, DPPH and $ABTS^{+}$ radical scavenging assays.

TPC is a commonly used method to assess antioxidant activity in plant extracts, as it measures the concentration of polyphenolic compounds present. Phenolic compounds

are a key class of plant components that possess redox properties, which enable their antioxidant action. In particular the hydroxyl groups' presents in plant extracts are capable of scavenging free radicals (Hinokidani et al., 2022). According to the findings of this study, it was observed that 80% methanol and 80% ethanol were much more effective in extracting phenolic compounds from plants compared to aqueous extract ($P < 0.05$). These two solvents showed higher efficiency than the other polar solvents commonly used for this purpose. The TPC content in the aqueous extract, 80% ethanol, and 80% methanol of the fruit of RCM were measured to be 259.01±9.41, 461.36 ± 13.26, and 410.77 ± 11.52 mg GAE/g dry extract, respectively.

In a previous study, it was found that the TPC of methanol, 80% ethanol, 80% methanol, and 70% methanol extracts from RCM fruit were 172.84 ± 15.33, 374.27 ± 12.28, 278.09 ± 6.11, and 123.52 ± 1.29 mg of GAE/g of dried extract, respectively(Nemkul et al., 2021; C. Zhang et al., 2018) . These values were significantly lower than that of the 80% methanol extract of RCM fruit in the current study. Poudyali et.; reported 1.2 ± 0.05 (µg GAE) (Poudyali & Singh, 2020), Chhetri et al. reported 49.24 ± 4.35 mg of GAE /g (Chhetri et al., 2020) and Heirangkhongjam et al., reported 725 ± 2.64 mg of GAE /100 g (M. D. Heirangkhongjam & Ngaseppam, 2019) of aqueous extract of RCM fruit respectively. The data suggests that our findings show a greater phenolic content in comparison to the earlier study. We noticed differences in the phenolic content values between our study and what has been reported in the literature. The variations may be due to different concentrations, regional disparities, or variations in extraction methods, all of which can impact the phenolics' concentration.

Table 3.6 shows the DPPH and ABTS+ radical scavenging capabilities of RCM fruit extracts with aqueous, 80% ethanol, and 80% methanol. These radicals are frequently used to evaluate the ability of antioxidants, plant extracts, and food items to scavenge free radicals. For ABTS, the IC_{50} values for aqueous, ethanol, and methanol were 144.01 ± 6.28, 26.21 ± 0.09, and 46.23 ± 0.69 µg/ml, respectively. These values were significantly different from one another ($P > 0.05$). In the DPPH free radical scavenging activity assay, a liner curve was created for standard ascorbic acid ($y = 15.77 x + 9.9671$, $R^2 = 0.9974$) using inhibition values and standard ascorbic acid concentrations. Ascorbic acid had an IC_{50} of 2.52 ± 0.03 µg/ml under current DPPH assay conditions. The IC_{50} values for aqueous, ethanol, and methanol were 33.03 ± 0.19, 16.08 ± 0.006, and 8.44 ± 0.3 µg/ml, respectively. These values significantly varied from one another ($P > 0.05$). In the DPPH assay, Heirangkhongjam and Ngaseppam additionally presented IC_{50} results for RCM fruit extracts: 86.54 ± 0.64 µg/ml for aqueous extract, 10.35 ± 0.13 µg/ml for acetone extract, 11.19 ± 0.22 µg/ml for ethanolic extract, and 12.27 ± 0.04 µg/ml for methanolic extract (M. D. Heirangkhongjam & Ngaseppam, 2019). Differences in the choice of solvent, regional different and extraction conditions can also influence the results (Chhetri et al., 2020).

Table 3.6: TPC, $ABTS^+$, DPPH values of different solvent extraction of RCM fruit

Solvents	TPC (mg GAE/g)	$ABTS^+$ Radical Scavenging Assay IC_{50} (µg/ml)	DPPH Radical Scavenging Assay IC_{50} (µg/ml)
Aqueous	262.89 ± 4.91^{C}	144.01 ± 6.28^{A}	33.03 ± 0.19^{A}
80% ethanol	461.36 ± 13.26^{A}	26.21 ± 0.09^{B}	16.08 ± 0.06^{C}
80% methanol	426.94 ± 13.13^{B}	46.23 ± 0.69^{C}	8.44 ± 0.3^{B}

Note: Data are represented as mean ± standard deviation (n = 3). Letters $^{A, B, C}$ in the same column are statistically significant from each other ($P < 0.05$)

A strong positive correlation ($r = 0.978$, $P < 0.001$) was noted between the TPC and the DPPH radical scavenging activities across all samples in the present experimental

conditions. The correlation indicates that phenolics are most likely the main bioactive compounds that are responsible for the DPPH radical scavenging activity of RCM fruit extract. Moreover, a significant correlation ($r = 0.777$, $P < 0.01$) was found between TPCs and ABTS radical scavenging activities in three distinct extracts. This suggests that phenolic compounds may have a crucial impact on the ABTS radical scavenging activity of RCM fruit. These findings clearly show that the three different solvent extracts of RCM fruit are abundant in phenolic compounds and demonstrate powerful antioxidant properties, positioning them as a potential option for antioxidant agents. Although both the 80% methanol and 80% ethanol extracts exhibited comparable antioxidant activities, the 80% ethanol extract appears to be more appropriate for food and health applications due to its lower toxicity compared to the 80% methanol extract.

3.3.4 Determination of MIC/MBC of RCM fruit

Figure 3.2 presents quantitative analyses of the antibacterial activities of aqueous, 80% ethanol, and 80% methanol RCM fruit extracts against *E. coli* and *S. aureus*, measured by MIC and MBC values. Reduced MIC and MBC values signify a more potent antibacterial effect. MBC refers to the minimum concentration of an antibacterial agent that is capable of completely eliminating the entire bacterial population, without any signs of viable growth observed when streaked on agar plates. The MIC value is the concentration of the extract that is the most diluted and still maintains its antimicrobial activity against the tested microorganism. MBC values may be equivalent to or greater than MIC values; however, they are not permitted to be less than MIC values.

Aqueous RCM fruit extract exhibited broad-spectrum activity against both *E.coli* and *S.aureus*, demonstrating the same MIC values at a concentration of 6.25 mg/ml. In contrast, 80% methanol RCM fruit displayed differing MIC values: 0.391 mg/ml for *S.aureus* and 3.125 mg/ml for *E.coli*. Additionally, 80% ethanol showed MIC values of 0.195 mg/ml for *S.aureus* and 1.563 mg/ml for *E.coli*. MBC values, in 80% methanol was 3.125 mg/ml for *E.coli* and 0.781 mg/ml for *S.aureus*. In contrast, 80% ethanol resulted in MBC values of 1.563 mg/ml for *E.coli* and 0.391 mg/ml for *S. aureus*. In contrast, the aqueous extract had inhibitory effects on both *S.aureus* and *E.coil*, with MBC values of 6.25 mg/ml. These findings showed that the 80% ethanol extract had the highest level of antibacterial activity.

A previous study reported the MIC values for *Rhus chinensis* Mill. methanol, ethyl acetate, and aqueous extracts against *E.coli* to be 12.5, 12.5, and 50 mg/ml, and against *S.aureus* to be 12.5, 12.5, and 50 mg/ml. Meanwhile, the MBC values for *Rhus chinensis* Mill. methanol, ethyl acetate, and aqueous extracts were 25, 25, and 200 mg/ml for *E.coli*, and 50, 25, and 200 mg/ml for *S.aureus* (Poudyali & Singh, 2020). Additionally, Nemkul and coauthors found that 70% methanolic extract of *Rhus chinensis* Mill. fruit exhibited MIC and MBC values of 3.12 mg/ml for *S.aureus* and 25 mg/ml for *E.coli* (Nemkul et al., 2021).

The observed differences in MIC values between Gram- negative and Gram-positive bacteria may be attributed to variances in their respective cell surface structures. Gram-negative bacteria possess an outer membrane consisting of lipopolysaccharides, and molecular transfer occurs through the cell membrane. The efficacy of antimicrobial agents is linked to their capacity to infiltrate the outer membrane based on their shape

and size, thereby accessing their targeted site (Kavak et al., 2010). The hydrophilic cell wall of Gram-negative bacteria plays a crucial role in reducing their sensitivity to extracts and essential oils by impeding the penetration of hydrophobic oils and the accumulation of substances within the bacterial cell membrane. According to a previous study, plant extracts such as *Arum maculatum* leaves, rosemary, lavender, oregano, henna, and cinnamon have a lower impact on Gram-negative bacteria than Gram-positive bacteria (Farahmandfar et al., 2019).

While it is widely assumed that the Gram distinction is a determining factor in growth inhibition for many essential oils, new research suggests that this is not always the case. In fact, certain herbs and spices have been shown to be equally effective against both groups of bacteria. Furthermore, according to Ramli, porin proteins found in Gram-negative bacteria's outer membrane layer can form channels that allow phenolic compounds with molecular masses less than 600 Da to enter the plasma membrane (Ramli, 2018). By extending the duration of contact between the bacterial sample and the active compounds present in the extract, it is possible to achieve equivalent effects on both bacterial types (Witkowska et al., 2013). As an example, our current study found that the ethanol extracts of clove (Witkowska et al., 2013) and *S. polyanthum* (Ramli, 2018), as well as the aqueous extract of RCM fruit were equally effective against both Gram-positive and Gram-negative bacteria.

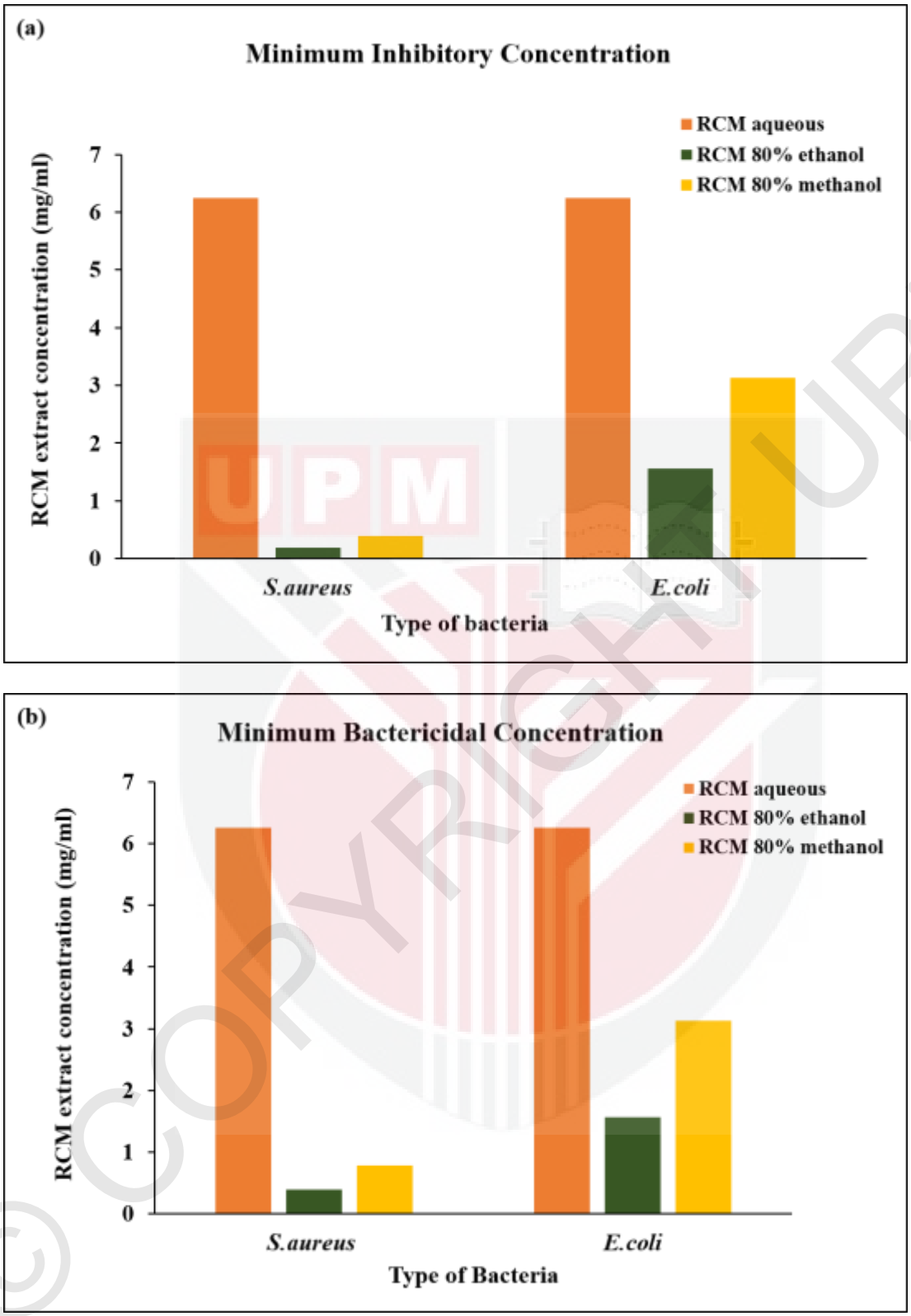

Figure 3.2: Minimum inhibitory concentration (a) and Minimum bactericidal concentration (b) for aqueous, 80% ethanol and 80% methanol RCM fruit extract against *S.aureus and E.coli.*

3.3.5 Phytochemical composition of 80% ethanol RCM fruit extract

The GC-MS analysis of the RCM fruit's 80% ethanol extract revealed that 97.97% of the total extract composition consisted of various phytochemical components. The retention times and mass spectral patterns of the chromatogram peaks were used to qualitatively identify them. Table 3.7 displays the components of the GC-chromatogram that have been identified based on the NIST17, FFNSC2, and WILEY229 Mass Spectral Libraries databases, as determined by various retention times and mass spectral patterns. The 80% ethanol extract contained sixteen compounds, the majority of which were organic acids (32.96%), followed by phenols (24.9%) and fatty acids (13.64%).

Malic acid (an organic acid) is a significant component in the RCM fruit, and it has been reported to possess antioxidant properties (Rob et al., 2018) and antimicrobial properties in previous studies. Malic acid, an organic acid, is a significant component in RCM fruit. Previous studies have reported its antioxidant and antimicrobial properties (Rob et al., 2018). According to Taylor, this particular type of fruit also contains malic acid. Furthermore, research discovered that malic acid can prevent the growth of *Listeria monocytogenes, Salmonella Enteritidis, and Escherichia coli* O157:H7 (Taylor et al., 2009). According to some researchers, the hydroxyl group in malic acid may interfere with cell membrane permeability, potentially offering a mechanism of action (Duangjai et al., 2016).

It is worth noting that the presence of pyrogallol (1, 2, 3-benzene-triol), a phenolic compound, has not been previously reported in RCM fruit extract. Interesting,

pyrogallol can be formed when gallic acid is decarboxylated (Li and Wang, 2015). Furthermore, there is ongoing research into the potential of pyrogallol as an antimalarial candidate (H & N, 2020).This finding is supported by (Mir et al., 2023), who reported pyrogallol could be considered as good antimalarial medicine, anti-inflammatory, and anti-biotic. Phenolic compounds demonstrate various pharmacological activities, notably antioxidant activity and antimicrobial properties (Presenza et al., 2023).

Fatty acids, along with lipids, are ubiquitous in plant cells, serving as membrane components, storage products, metabolites, and an energy source. Some fatty acids, such as linoleic acid (9,12-Octadecadienoic acid (Z,Z)), are well-known for their antibacterial and antifungal properties, as confirmed by previous researchers (Preez-Bruwer et al., 2022). Linoleic acid is a crucial element in the human body due to its potential anticancer activity, particularly in the treatment of breast cancer, as reported by (Qadir et al., 2022). In addition, linoleic acid possesses anti-inflammatory, anti-androgenic, and cancer- preventive properties, as well as reducing cholesterol levels and improving cardiovascular health (Nemkul et al., 2021). Linoleic acid can also be used in food to treat atopic eczema and breast pain, according to (Marangoni et al., 2020). RCM fruit extract also contains N-Hexadecanoic acid (palmitic acid), which has antimicrobial activity against *E.coli*, *B.subtilis*, *S.aureus*, and *C.albicans*, as isolated from *Canthium parviflorum* leaves (Krishnan et al., 2016). Palmitic acid is a promising component for inhibiting colon and prostate cancer cell growth by inducing apoptosis and cell cycle arrest, respectively (Bharath et al., 2021; Zhu et al., 2021).

Previous studies have reported the presence of 2, 5- furandione, 3- methyl compound with anticancer activity in the methanolic peel extract of *Punica grantanum* and

ethanol extract of *C.orchiodes* (Nandhini et al., 2021). Additionally, the 80% methanol extract of RCM fruit contains 2,3-dihydro-3,5-dihydroxy-6-methyl-4H-pyran-4-one, a compound known for its ability to inhibit the growth of microorganisms, reduce inflammatory responses, and exhibit antioxidant properties (Preez-Bruwer et al., 2022).

The 80% ethanol extract of RCM fruit contains significant compounds that exhibit antimicrobial, antioxidant, and other biological properties. Previous studies have identified 22,23, and 33 compounds/peaks of CG-MS in methanol, ethanol and benzene/ethanol (1:1) extracts of RCM leaves (Suo et al., 2020). Furthermore, Nemkul and colleagues (2021) found 16 compounds in the hexane and 18 compounds in the 70% methanol extract (Nemkul et al., 2021). The study discovered minor differences in the RCM fruit extract composition compared to previous research, possibly influenced by regional variations in the samples, choice of solvent, plant parts used, and extraction methods.

Table 3.7: Phytochemical constituents of 80% ethanol extract of RCM fruit

No	Retention time	Name of the compound	Molecular formula	Nature of the compound	Peak area (%)
1	5.377	Furfural	$C_5H_4O_2$	Aldehyde	1.50
2	6.079	Maleic acid anhydride (malic acid)	$C_4H_2O_3$	Organic acid	32.96
3	8.837	2,5-Furandione, 3-methyl	$C_5H_4O_3$	Anhydride	10.15
4	12.470	2,5-Furandione, 3-methyl (Citraconic anhydride)	$C_5H_4O_3$	Anhydride	3.37
5	14.685	Furyl hydroxymethyl ketone	$C_6H_6O_3$	Heterocyclic Compound	0.96
6	15.896	Formic acid, ethenyl ester	$C_3H_4O_2$	Ester	2.92
7	17.531	2,3-dihydro-3,5-dihydroxy-6-methyl 4H-Pyran-4-one	$C_6H_8O_4$	Flavonoid	2.51
8	21.728	5 Hydroxy methyl furfural	$C_6\ H_6\ O_3$	Aldehyde	2.06
9	28.546	1,2,3-Benzenetriol (Pyrogallol)	$C_6H_6O_3$	Phenol	15.39
10	51.181	N-Hexadecanoic acid (palmitic acid)	$C_{16}H_{32}O_2$	Fatty acid	6.72
11	56.719	9,12-Octadecadienoic acid (Z,Z)- (linoleic acid)	$C_{18}H_{32}O_2$	Fatty acid	5.40
12	56.864	Cis 9-Hexadecenal	$C_{16}H_{30}O$	Fatty aldehyde	3.01
13	57.555	n-Octadecanoic acid (Stearic acid)	$C_{18}\ H_{36}O_2$	Fatty acid	1.52
14	66.862	(Z)-3-(pentadec-8-en-1-yl) phenol	$C_{21}H_{34}O$	Phenol	3.08
15	67.83	Unknown compound	-	-	0.91
16	71.769	3-((4Z,7Z)-Heptadeca-4,7-dien-1-yl) phenol	$C_{23}H_{36}O$	Phenol	1.91
17	71.98	Unknown compound	-	-	1.12
18	72.366	(Z)-3-(Heptadec-10-en-1-yl) phenol	$C_{23}H_{38}O$	Phenol	4.52

3.4 Conclusion

Throughout this chapter, we explored the potential bioactive properties of extracts from *Rhus chinensis* Mill. fruit and *Acacia concinna* (Willd.) DC pods using aqueous, 80% ethanol, and 80% methanol solvents. We used ultrasound-assisted extraction methods to increase the yield of both extracts. Following an initial phytochemical analysis and evaluation of antimicrobial effects, RCM fruit extracts are preferred over AC pod extracts. In addition, ethanol at 80% and methanol at 80% extract of RCM

fruit showed better DPPH and $ABTS^{+}$ radical scavenging abilities and higher TPC values than the aqueous extract. When using 80% ethanol, the MBC values against *E. coli* and *S. aureus* were enhanced, measuring 1.563 mg/ml and 0.391 mg/ml, respectively. Identified through CG-MS analysis, the main active compounds responsible for these effects include organic acids, polyphenols, and fatty acids. Nonetheless, there is a preference for bio-based solvents in the food and nutraceutical industries, not only because they are less toxic to humans. In this case, 80% ethanol could be a better solvent than 80% methanol.

The 80% ethanol extract was selected as a natural antimicrobial and antioxidant agent (bioactive properties) for a comprehensive investigation due to its efficacy. In Chapter 4, this extract will be employed as a stabilising and reducing agent in the green synthesis of silver nanoparticles. Additionally, it will be integrated into bioactive films in Chapter 5.

CHAPTER 4

PREPARATION AND CHARACTERISATION OF PLANT MEDIATED SYNTHESIS OF SILVER NANOPARTICLES USING PLANT EXTRACT OF *RHUS CHINENSIS* MILL. (RCM) FRUIT

4.1 Introduction

The goal of this chapter was to synthesise silver nanoparticles (AgNPs) using 80% ethanol RCM fruit extracts in order to provide a low-cost and environmentally friendly solution. Experiments were conducted to determine the optimal synthesis conditions for RCM-AgNPs, including varying temperatures (70℃ and 80℃) and pH values (pH=4, pH=7, and pH=10). These parameters were chosen based on previous research (Aryan et al., 2021; Biswal & Pramila, 2020) for plant-mediated synthesis to improve antimicrobial properties for potential use in food preservation and related applications. We believe that this is the first study to show plant-mediated AgNP synthesis using RCM fruit extract. Figure 4.1 depicts the detailed preparation, characterisation, and selection of optimised conditions for plant-mediated synthesis in this chapter.

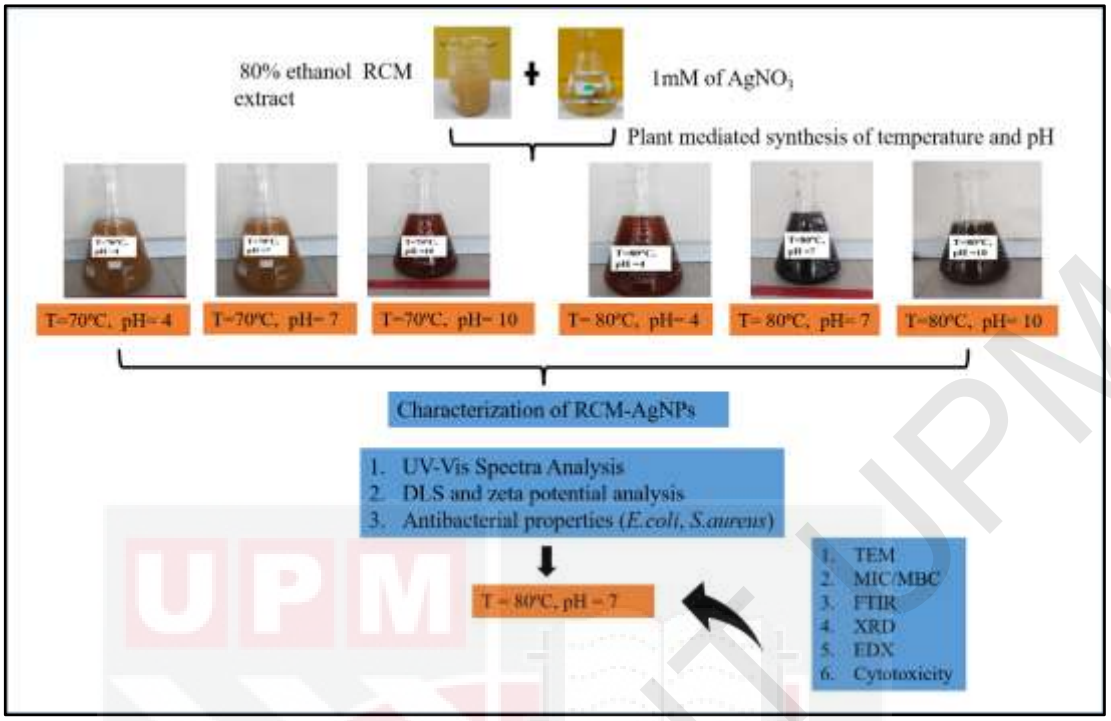

Figure 4.1: Flow chart of plant-mediated synthesis of RCM-AgNPs

4.2 Materials and methods

4.2.1 Materials

Silver nitrate ($AgNO_3$) was supplied by system. Sodium hydroxide (NaOH) purchased from R&M chemicals.

4.2.2 Plant sample collection and identification

Explanation of Plant Sample Collection and Identification is provided in Section 3.2.1.

4.2.3 Preparation of extracts

Rhus chinensis Mill. (RCM) fruit were extracted with 80% ethanol, as described in Section 3.2.2.

4.2.4 RCM fruit extract mediated synthesis of AgNPs (RCM-AgNPs)

With some adjustments, 80% ethanol extract of RCM fruit facilitated the synthesis of AgNPs following the literature (Aryan et al., 2021; Biswal & Pramila, 2020). A 900 ml solution of aqueous silver nitrate was combined with 100 mL of the RCM 80% ethanol extract, which was then stirred continuously at a temperature of 70 or 80°C on a magnetic stirrer (Wise Stir MSH-20D, Korea) for 60 minutes. The solution's pH was adjusted to 4, 7, and 10 by the addition of 1 N NaOH solution. When RCM-AgNPs were generated, the solution changed from pale yellow to either reddish or dark brown. The RCM-AgNPs were isolated using centrifugation. Following precipitation, the RCM-AgNPs were decanted and rinsed three times with distilled water.

4.2.5 Characterisation of various parameters of synthesised RCM-AgNPs

4.2.5.1 UV-Vis spectrophotometry

The UV-visible spectrum in the 300-700 nm range was analysed for various parameters of RCM-AgNPs solution and RCM fruit 80% ethanol extracts using a Shimadzu UV-1800 spectrophotometer. Quart cuvettes were used for the analysis.

4.2.5.2 Dynamic Light Scattering

An analysis of various parameters of RCM-AgNPs solutions was conducted using a Zetasizer Nano series instrument from Malvern, UK to determine average particle size and zeta potential.

4.2.5.3 Dis diffusion test

The antibacterial properties of various parameters (20 mg/ml) were tested following the procedures outlined in Section 3.2.4.

4.2.6 Characterisation of selected parameter of synthesised RCM-AgNPs

4.2.6.1 Transmission Electron Microscopy (TEM)

The morphology of selected parameters of synthesised RCM-AgNPs was investigated using a TEM (Hitachi H-9500, Japan) operating at 100 kV.

4.2.6.2 Fourier Transform Infrared (FTIR) Spectroscopy

The Fourier transform infrared (FT-IR) emissions of both RCM fruit 80% ethanol extract and selected parameter of synthesised RCM-AgNPs were measured using a Thermo Scientific Nicolet iS5 spectrometer with an iD5 ATR attachment.

4.2.6.3 X-ray diffraction Analysis (XRD)

The crystalline structure of selected parameters of synthesised RCM-AgNPs was analysed utilising an X-ray diffractometer (XRD – 6000, Shimadzu, Japan) within the 30° to 80° range, employing a scanning rate of 2°/min.

4.2.6.4 Energy-Dispersive X-ray Spectroscopy (EDX)

The elemental composition of the selected parameters of synthesised RCM-AgNPs was analysed using Energy-Dispersive X-ray Spectroscopy (Oxford Instruments, X-Max 20 mm^2).

4.2.6.5 Determination of minimum inhibitory concentrations (MIC)

The MIC testing for a concentration of 20 mg/ml of selected parameter of synthesised RCM-AgNPs was conducted as previously described in Section 3.2.8.

4.2.6.6 Determination of minimum bactericidal concentrations (MBC)

The MBC testing for a concentration of 20 mg/ml of the selected parameter of synthesised RCM-AgNPs was carried out following the method outlined in Section 3.2.9.

4.2.6.7 Cytotoxicity analysis

The cytotoxicity assessment was conducted utilising the 3T3 mouse embryonic fibroblast cell line. The 3T3 cell was cultured in DMEM medium (Sigma Aldrich, U.S.A) supplemented with 85% DMEM, 10% fetal bovine serum (FBS), and 5% antibiotics. The cells were subcultured and incubated at 37°C in a humidified atmosphere containing 5% CO_2. Cells achieving over 80% confluence were utilised

for seeding (Kothandaraman et al., 2023). The MTT proliferation assay was employed to assess cell viability and identify any cytotoxic effects of RCM-AgNPs. Cell cultures were established at a concentration of 1.0×10^4 cells/ml and subsequently dispensed into 96-well plates at (100 µl/well). Different concentrations of RCM-AgNPs (2.5, 5, 10, 20, 80, and 160 µg/ml) were introduced to each well and subsequently incubated for 24 hours. Following the incubation period, MTT solution was administered to the cells, which were subsequently incubated for an additional 3 hours. After solubilising the purple formazan crystals with DMSO, the Optical Density (OD) was measured using an ELSA reader at a wavelength of 570 nm. The cytotoxicity was assessed by calculating the IC_{50} value, which denotes the drug concentration that results in a 50% reduction in cell growth. This calculation was conducted using the formula provided.

$$Cell\ viability = \frac{Absorbance\ sample\ (mean)}{Absorbance\ control\ (mean)} \times 100\% \qquad \text{Equation (4.1)}$$

4.2.7 Statistical analysis

The data was collected using IBM-SPSS version 25, applying one-way analysis of variance (ANOVA). Mean differences were assessed using the Least Significance Difference (LSD) method.

4.3 Results and discussion

4.3.1 UV–Vis Spectra Analysis

Recent research on the production of AgNPs utilising plant extracts has generated considerable interest. Various herbal extracts have been employed to enhance the synthesis of AgNPs for diverse applications. This study revealed the capability of RCM fruit extract in the green synthesis of AgNPs for the first time. The colour change of the silver nitrate and plant extract solution acts as an initial indicator for the synthesis of Ag NPs. Following incubation, the colourless silver nitrate solution and the pale green fruit extract transformed into a dark brown hue. This behaviour is in line with other methods that have been reported to use plant extracts that contain polyphenolic compounds as well as chemicals like tannic acid, a polyphenolic plant-derived substance.

Phenolic chemicals in the plant extract oxidise to Quinone, providing free electrons for the reduction of the Ag^{+} ion to Ag^{0} and production of NPs (Nouri et al., 2020). Phenolic compounds with carboxylic and hydroxyl groups can attract silver ions. Polyhydroxylic compounds and water-soluble heterocyclic components have a significant impact on the bio-reduction and stability of Ag ions. Phenolic chemicals derived from plants can have an impact on the surface of NP by creating steric and electrostatic forces, acting as a capping agent, and hindering their growth (Mohammadalinejhad et al., 2019).

UV-Vis spectroscopy was employed to verify the synthesis of RCM-AgNPs. Figure 4.2a shows the absorption spectra of RCM-AgNPs and the plant extract. The band

observed at approximately 419 nm signifies the high surface plasmon resonance (SPR) of the silver nanoparticles. The emergence of SPR was ascribed to the resonant oscillation of conductive electrons on the surface of nanoparticles resulting from their interaction with electromagnetic waves (Rolim et al., 2019). Experiments performed at varying temperatures (70°C and 80°C) and pH levels (pH 4, pH 7, and pH 10) enabled the identification of optimal synthesis conditions for RCM-AgNPs.

The parameters were chosen based on previous research (Aryan et al., 2021; Biswal & Pramila, 2020). When the temperature was 70°C, the solution of RCM-AgNPs showed peak absorbance wavelengths at 438nm, 436nm, and 435nm for pH values of 4, 7, and 10, respectively (Figure 4.2b). On the other hand, when the temperature was 80°C, the RCM-AgNPs solution showed peak absorbance at wavelengths of 430 nm, 419 nm, and 420 nm for pH values of 4, 7, and 10, respectively (Figure 4.2c). There was an increase in the intensity of the SPR peak as the pH changed from 4 to 7. At pH 4, the SPR peak broadened with reduced intensity. Yet, at a pH of 7, the SPR peak became narrower and showed the most intense signal. Increasing the pH even more to 10 led to a wider SPR peak, moving towards longer wavelengths, while also decreasing the intensity of the SPR peaks. Khalil and his colleagues observed a rise in the absorbance of AgNPs produced from olive leaf extract as the pH of the solution increased from 2 to 8. Nevertheless, as the pH rose, the absorbance decreased (Khalil et al., 2013). The study identified pH 7 as the best levels for synthesising small-sized nanoparticles.

The optimisation can be credited to alterations in the dissociation constant values of functional groups in the biomolecules, which are responsible for decreasing the silver ions. At the same time, the temperature rise caused the SPR peak to become more

intense. The increased temperature caused a more intense reaction, resulting in the quick reduction of Ag^{+} ions. This led to the formation of AgNPs through homogeneous nucleation, resulting in smaller particle sizes. However, above 90°C, the strength of the SPR peak decreased, confirming that 90°C is the optimal temperature for AgNPs synthesis (Ramesh et al., 2018).

Comparable results were noted in the synthesis of AgNPs utilising Kalanchoe pinnata leaf extract (Aryan et al., 2021) and Piper nigrum seed extract (Kanniah et al., 2021a). Studies by Lakkin et al. and Malini et al. indicate that AgNPs with absorption maxima near 440 nm generally display a spherical morphology (Lakkim et al., 2020; Malini et al., 2020). Silver nanoparticles (AgNPs) were synthesised utilising extracts from *Ocimum tenuiflorum*, *Centella asiatica*, and *Clonorchis sinensis*. The absorbance at 420 nm was quantified utilising a UV spectrophotometer (Venkatadri et al., 2020).

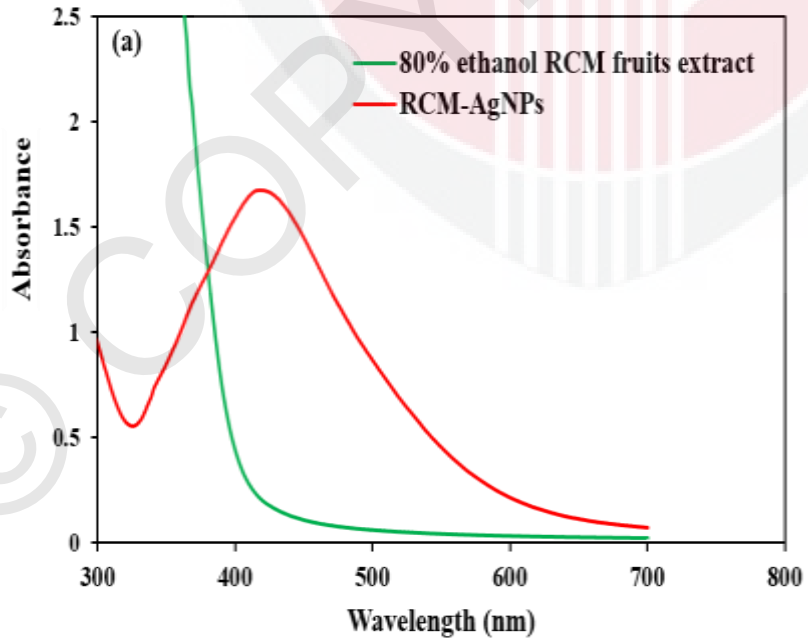

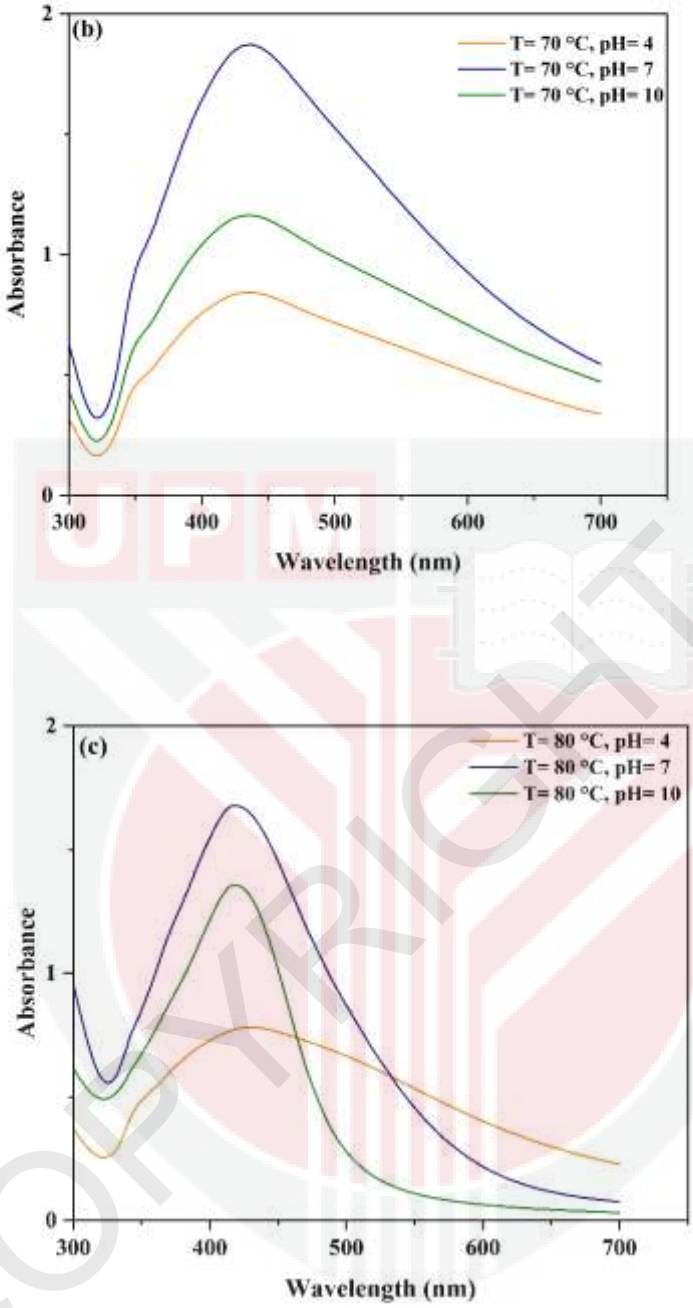

Figure 4.2: The absorption spectra of 80% ethanol RCM fruit extract, and RCM-AgNPs (a) and RCM-AgNPs with different pH at (b) 70°C and (c) 80°C.

4.3.2 Dynamic Light Scattering (DLS) and zeta potential analysis

Dynamic light scattering (DLS), also known as photon correlation spectroscopy, proves to be a highly promising scattering method for determining both the average particles size and the size distribution of nanoparticles, as detailed in Table 4.1. The average particles size for various RCM-AgNPs parameters ranged from 43.77 ± 0.94 nm to 173.33 ± 3.5 nm. Notably, the green synthesis at T= 80°C, pH7 resulted in the smallest particle sizes.

The particle size distribution was evident from the Polydispersity Index (PDI) values. The PDI for different parameters of green synthesised RCM-AgNPs ranges from 0.298 ± 0.002 to 0.5 ± 0.019, indicating moderate agglomeration and size variation (Alomar et al., 2020; Sukweenadhi et al., 2021). When nanoparticles have a high positive or negative zeta potential, they can improve dispersion, creating a colloidal solution that remains stable over time and prevents agglomeration (Hashemitabar et al., 2023). The Zeta potential of RCM-AgNPs synthesised using green methods under optimal conditions exhibited a remarkable level of stability, with values ranging from -25.56 ± 2.1 to -61.86 ± 1.85 mV (as demonstrated in Table 4.2). Specifically, the Zeta potential of RCM-AgNPs achieved under ideal process conditions was - 61.86 ± 1.85 mV, providing additional evidence of robust stability attributed to the phytochemicals present in the ethanol extract (Prema et al., 2022). However, previous studies have demonstrated that nanoparticles with potential values around ± 30 mV are considered to be within a more stable colloidal range due to the electrostatic attraction/repulsion among the particles (Aryan et al., 2021; Wadia et al., 2022).

Plant-mediated synthesis at pH 7 and 80℃ resulted in small particles with moderate PDI values and enhanced stability. Furthermore, the UV-vis spectra of RCM-AgNPs revealed that pH7 was the optimal level for synthesising small nanoparticles.

Table 4.1: Average Particle Size, Polydispersity Index (PDI), and Zeta Potential on RCM fruit 80% ethanol extract mediated synthesis AgNPs

Samples of RCM-AgNPs	Average Particle Size (nm)	PDI	Zeta Potential (mV)
T= 70 °C, pH= 4	164.43 ± 2.1^{B}	0.403 ± 0.02^{D}	-38.33 ± 0.8^{D}
T= 70 °C, pH= 7	105.26 ± 1.7^{D}	0.44 ± 0.025^{C}	-30.96 ± 0.7^{B}
T= 70 °C, pH= 10	133.43 ± 3.5^{C}	0.298 ± 0.002^{D}	-61.86 ± 1.85^{F}
T= 80 °C, pH= 4	173.33 ± 3.5^{A}	0.443 ± 0.02^{A}	$- 36.6 \pm 0.6^{C}$
T= 80 °C, pH= 7	43.77 ± 0.94^{F}	0.5 ± 0.019^{C}	$- 25.56 \pm 2.1^{A}$
T= 80 °C, pH= 10	72.89 ± 1.37^{E}	0.43 ± 0.01^{B}	$- 44.3 \pm 1.5^{E}$

Note: Values are means ± SD of three determinations. Different superscripts in the same column indicate significant differences ($P < 0.05$)

4.3.3 Antibacterial properties

Currently, the mechanism behind AgNPs'antibacterial activity is unknown. According to many researchers, antibacterial activity was higher in smaller particle size of AgNPs (Kumar et al., 2021). Since the nano particle functions as a molecule, it can readily pass through bacteria's tough and inflexible cell wall and alter their essential molecular pathways (Biswal & Pramila, 2020). The diameter of the clear zone region in Table 4.2 indicates that each parameter of RCM-AgNPs, DMSO 10%, and ampicillin (10µg) shows significantly different antibacterial activity against both *E. coli* and *S. aureus* ($P < 0.05$). In comparison to ampicillin (10µg), which serves as the standard control, RCM-AgNPs demonstrate potential for application in the medicinal field and other related research. Among the parameters, pH values of 7 at a temperature of 80 °C showed the highest inhibition zones against *E.coli* and *S.aureus*. This result is consistent with DLS findings, as the synthesis of AgNPs via RCM fruit mediated at pH 7, temperature 80°C, yields nanoparticles of smaller size. So, this RCM-AgNPs

synthesis parameter was further tested using TEM, MIC, and MBC to determine the optimal particle size and antibacterial properties.

Table 4.2: Antibacterial properties of RCM-AgNPs synthesis at different temperature and pH

Samples of RCM-AgNPs	Inhibition Zone (mm)	
	E.coli	***S.aureus***
T= 70 °C, pH= 4	6.86 ± 0.13^{E}	6.33 ± 0.17^{D}
T= 70 °C, pH= 7	7.64 ± 0.21^{D}	7.06 ± 0.09^{C}
T= 70 °C, pH= 10	6.91 ± 0.10^{E}	7.00 ± 0.19^{C}
T= 80 °C, pH= 4	6.19 ± 0.18^{F}	6.72 ± 0.19^{C}
T= 80 °C, pH= 7	11.14 ± 0.59^{B}	10.73 ± 0.36^{A}
T= 80 °C, pH= 10	8.51 ± 0.23^{C}	9.98 ± 0.43^{B}
Ampicilline (10µg)	13.53 ± 0.42^{A}	7.1 ± 0.13^{C}
DMSO (10%)	0^{G}	0^{E}

Note: Values are means ± SD of three determinations. Means within each column with different letters differ significantly ($P < 0.05$)

4.3.4 Characterisation of selected parameter of synthesised RCM-AgNPs

Based on UV-Vis analysis, particle size, PDI values, zeta potential, and antibacterial properties, RCM-AgNPs synthesised at T = 80°C, pH= 7 were selected for further characterisation.

4.3.4.1 Transmission Electron Microscopy Analysis

The size and morphology of RCM-AgNPs were analysed using transmission electron microscopy (TEM), as demonstrated in Figure 4.3a. The agglomeration was the result of the adsorption and aggregation of the chemicals identified onto the surface of the RCM-AgNPs. Size variations and aggregation of RCM-AgNPs were observed, as evidenced by DLS results revealing a polydispersity index of approximately 0.5 (Alomar et al., 2020).

The size distribution histogram of RCM-AgNPs in the TEM image reveals that the majority of particles were within the 7 nm to 30 nm range, with an average size of 17.4 nm (Figure.4.3b). Furthermore, it is worth noting that the DLS results typically yield slightly larger sizes compared to TEM measurements, attributed to the hydrodynamic diameter of the nanoparticles (Saravanakumar et al., 2021; Wadia et al., 2022).

This conclusion finds support in a study that produced silver nanoparticles with a variety of shapes, including spherical, and an average size of approximately 30 nm using *Arachis hypogaea* root extract (Sankaranarayanan et al., 2017). On the contrary, Periasamy and co-authors reported larger dimensions for AgNPs synthesised using *Hibiscus rosasinensis* extract, ranging from 200 nm to 1 µm (Periasamy et al., 2022). This illustrates that the size of the synthesised silver nanoparticles can be significantly influenced by experimental parameters and their optimisation.

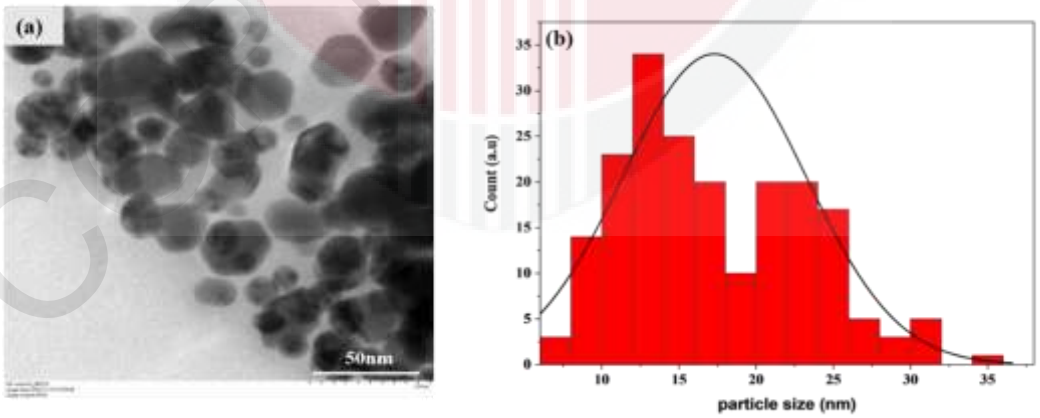

Figure 4.3: TEM image and particle size distribution histogram for RCM-AgNPs

4.3.4.2 Fourier Transformed Infrared spectroscopy

Fourier Transformed Infrared spectroscopy (FTIR) analyses were performed on both the RCM fruit 80% ethanol extract and the RCM-AgNPs to identify the specific functional groups of the biomolecules responsible for reducing the silver ions and then capping/stabilising the synthesised AgNPs. Figure 4.4 demonstrated that the RCM extract generated peaks at 3416, 2920.36, 2849.54, 1699, 1606, 1187, and 1028 cm^{-1}. The broad peak at 3416 cm^{-1} signifies the presence of the aromatic hydroxyl group. The absorption peak at 2920.36 cm^{-1} is attributed to the SP3 C-H stretch. The carboxylic acid group may account for the absorption peaks at 2860.23 cm^{-1}.

An intense aromatic OH hydroxyl stretch at 3428.27 cm^{-1} enhances the probability of the presence of a phenolic group (Odeniyi et al., 2020). The pronounced absorption peak between 1699 and 1606 cm^{-1} is attributed to the C=O bond. Aldehydes, ketones, and carboxylic acids serve as indicators for the presence of carbonyl compounds. A prevalent reducing agent is ketone, which effectively converts metal ions into metal nanoparticles (Suo et al., 2020). The peak at 1028, 1141.86 cm^{-1} revealed that bands were due to C-N stretching and aliphatic amines, respectively. Despite the presence of RCM fruit 80% ethanol extract in the RCM-AgNPs, the FTIR spectra show peaks at 3400, 3237, 2980, 1638, 1080, and 1043.65 cm^{-1}. The stretching vibrations of O-H in alcohol, phenol functional groups, and the -C-O stretching vibration of alcoholic groups were associated with the bands at 3237, 2980, and 1043.65 cm^{-1}, respectively.

The N-H bond of the amine groups in RCM-AgNPs, as evidenced by the absorption signal peaks at approximately 3400, 1638, and 1080 cm^{-1} in the spectrum. When

proteins and enzymes specific to the N-H group appear, $AgNO_3$ is reduced to Ag. Additionally, the presence of phytochemicals like phenolic, tannins, alkaloids, steroids, and proteins in the RCM extract was attributed to the characteristic peaks in the FTIR spectrum of the as synthesised RCM-AgNPs, confirming that these substances could function as both reductants and oxidants (Nouri et al., 2020; Sankaranarayanan et al., 2017).

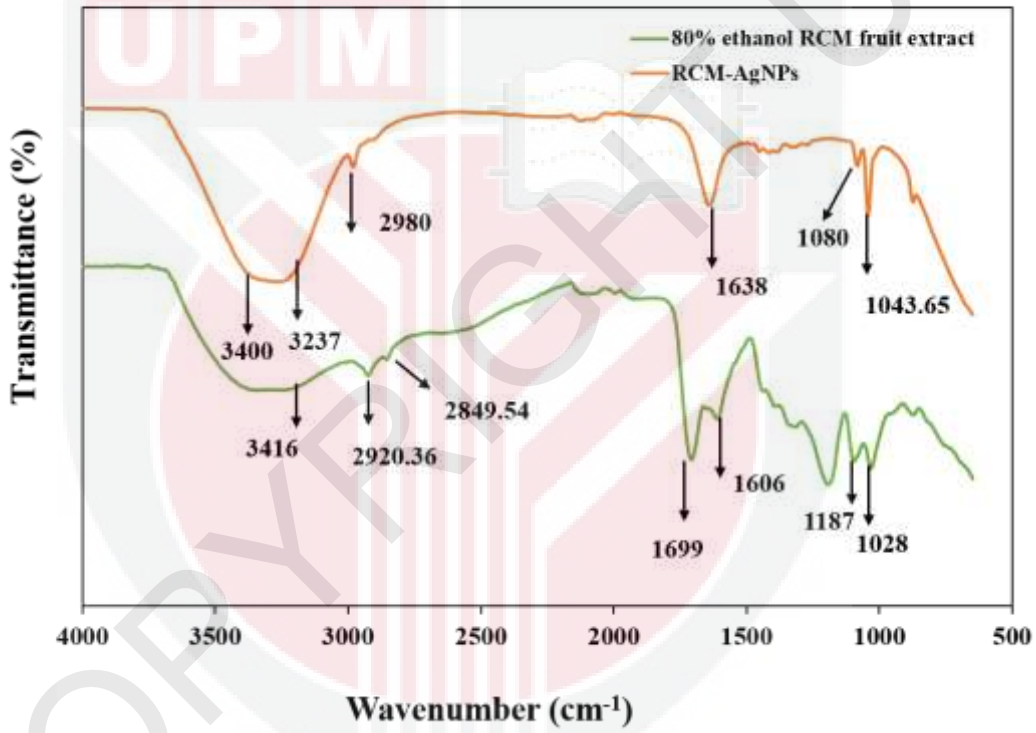

Figure 4.4: FTIR spectra of silver nanoparticles 80% ethanol RCM fruit and RCM-AgNPs

4.3.4.3 X-ray diffraction Analysis

Figure 4.5 depicts the X-ray diffraction (XRD) pattern of RCM-AgNPs synthesised with 80% ethanol extract from RCM fruit. The spectrum analysis using the XRD technique revealed distinct peaks, indicating that the RCM-AgNPs are crystalline. The XRD pattern's Bragg reflections suggested face-centered cubic (fcc) silver at ,38.1°, 44.14°, 64.4°, and 77.3°, which corresponded to (111), (200), (220), and (311) in the lattice which is depicted in Figure 4.5. The current study's XRD pattern were compared to crystalline silver from the Joint Committee on Powder Diffraction Standards (File no. 04- 0783). Similar lattice pattern (111), (200), (220) and (311) was also obtained in AgNPs synthesised from *piper nigrum* seed extract (Kanniah et al., 2021) and *Kalanchoe pinnata* leaves (Aryan et al., 2021).

RCM fruit 80% ethanol extract's phytomolecules are present, as evidenced by the emergence of a few additional peaks alongside RCM-AgNPs. Plant extract phytochemicals may serve as an electron donor during the creation of nanoparticles. As a result, Ag^{+} to Ag^{0} are shifted. Additionally, these silver atoms are grown through Ostwald ripening or coalescence to generate silver nanoparticles (Biswal & Pramila, 2020; Odeniyi et al., 2020). The XRD outcome aligns well with reported values linked to the cubic structure of plant mediated synthesised AgNPs (Biswal & Pramila, 2020) , thus providing strong evidence for the formation of these silver nanocrystals.

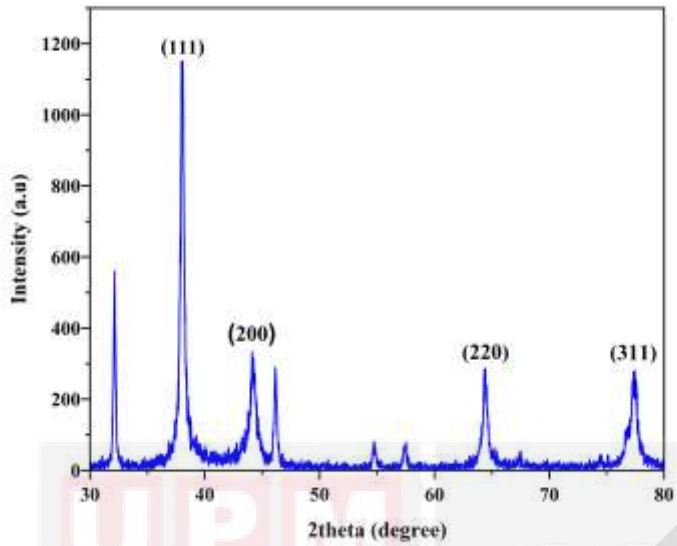

Figure 4.5: XRD spectrum of RCM-AgNPs

4.3.4.4 Energy-Dispersive X-ray Spectroscopy (EDX)

The elemental composition analysis was performed to determine the presence of metallic RCM-AgNPs in the reaction mixture of silver nitrate and RCM fruit 80% ethanol extract. The presence of silver nanoparticles is confirmed by the robust signal observed at 3 keV in the EDX analysis (Figure.4.6). Additionally, the appearance of signals for other elements such as carbon (C), potassium (K), chlorine (Cl), sodium (Na), oxygen (O) alongside silver suggests the presence of phytochemical constituents from the RCM fruit extract. These findings align with previous studies in the literature (Alomar et al., 2020; Arumai Selvan et al., 2018) . Furthermore, the results are closely correlated with XRD and FTIR analysis.

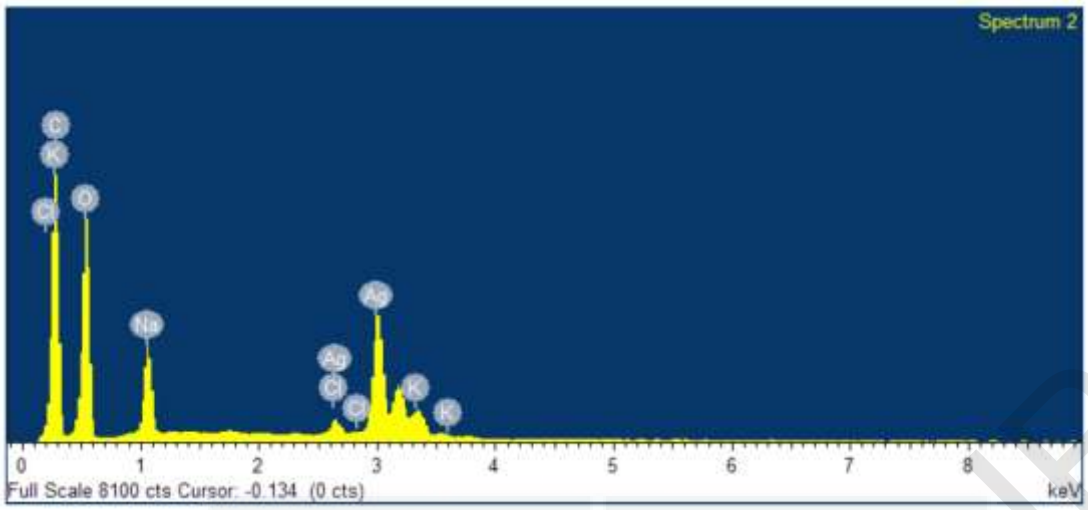

Figure 4.6: EDX analysis of RCM-AgNPs

4.3.4.5 Determination of MIC/MBC

Table 4.3 presents the MIC and MBC values that were determined following a 24-hour incubation of *E.coli* and *S.aureus* with RCM-AgNPs. *E.coli* showed a greater susceptibility to the RCM-AgNPs, with MIC and MBC values of 39 µg/ml. On the other hand, *S.aureus* showed reduced sensitivity to the RCM-AgNPs, with MIC values of 39 µg/ml, and MBC values of 156 µg/ml. The observed results aligned with the study on the production of AgNPs by *Crossopteryx febrifuga* (CR-FE) leaf extract (Kambale et al., 2020). Due to variations in the composition of their cell walls, gram-negative bacteria are generally more susceptible to Ag invasion compared to gram-positive bacteria. Interestingly, gram-negative bacteria possess only a single peptidoglycan layer, which renders their cell wall susceptible to damage from Ag ions. The dense cell wall of Gram-positive bacteria, composed of linear polysaccharide chains and peptide cross-linkages, acts as a barrier that prevents the AgNPs from entering the bacterial cells (Liao et al., 2019; Moteriya & Chanda, 2017).

Although AgNPs have been demonstrated to be effective against a number of bacteria, the precise mechanism is yet unknown. The concentration, size, shape, pH, temperature, and test microorganisms are some of the factors that affect AgNPs' antibacterial activity. Moreover, it was discovered that the size of AgNPs is crucial in limiting microbial growth (Kumar et al., 2021). This results in increased bacterial sensitivity and lower MIC and MBC values, as evidenced by TEM and DLS results. Uddin and Akrema (2016) discovered comparable relationships between nanoparticle size and antibacterial activity in AgNPs mediated by *C. viminalis* leaves (Rahisuddin & Akrema, 2016). Nanoparticles with smaller sizes are more toxic, but they allow for the faster release of silver ions, which enter the microbial cell and act on its DNA. The molecules in DNA may get condensed, which could disrupt DNA replication and cause bacterial dysfunction (Yan et al., 2018). In addition, silver ions with a positive charge can interact with the negatively charged components of bio-macromolecules, such as phosphate and disulfide or sulfhydride of enzymes and nucleic acids. This interaction leads to structural changes in bacterial cell walls and disrupts the metabolic process, ultimately resulting in cell death. Furthermore, the AgNPs become attached to the cell surface of bacteria and modify the physical and chemical properties of the cell membrane (Moteriya & Chanda, 2017) . As a result, the membrane's structural makeup is changed, it becomes more permeable, and it stops functioning (Carson et al., 2020; Jing et al., 2022).

The final mechanism is based on reactive oxygen species (ROS) that are created when free Ag^+ ions are taken up by cells and render the respiratory enzymes ineffective. The increase of cellular components and DNA damage are both significantly influenced by ROS. The disintegration of cytoplasmic ribosomal elements caused by the Ag^+ ions

can also result in protein production (Ashique et al., 2022).

Panpaliya et al. (2019) discovered that AgNPs synthesised using green methods exhibited stronger antibacterial properties against specific human pathogens and lactic acid bacteria that cause food spoilage when contrasted with synthetic/chemical antibacterial compounds such as chlorohexidine. Hence, AgNPs derived from plants extracts may be a valuable antibacterial bioresource with prospective applications in the food sector and other relevant fields (Kumar et al., 2021).

Table 4.3: Minimum inhibitory concentration (MIC) and minimum bactericidal concentration (MBC)

Bacterial type	MIC (µg/ml)	MBC (µg/ml)
E.coli	39	39
S.aureus	39	156

4.3.4.6 Cytotoxicity Study

In recent efforts, researchers have focused on developing strategies to reduce the cytotoxic impact of AgNPs, which are toxic to both microorganisms and human cells. Notably, exposure to specific concentrations can produce a variety of reactions. This study evaluated the cytotoxic effects of RCM-AgNPs on a 3T3 mouse embryo fibroblast cell line at various concentrations (2.5, 5, 10, 20, 40, 80, and 160 µg/ml). The MTT assay, a common method for measuring cellular metabolic activity that is frequently used in cytotoxicity assessments, was used to conduct the evaluation.

In vitro experiments revealed that silver nanoparticles synthesised using RCM fruit 80% ethanol extract exhibited a cell viability of over 70% in 3T3 cells at a

concentration of 20 µg/ml in Figure 4.7. Previous reports suggest that an average relative cell viability above 70% is generally considered safe. In a study by Arokiyaraj and colleagues, the silver nanoparticles synthesised from the aqueous flower extract of *C.indicum* demonstrated no significant impact on cell viability, showing 93.33% at a concentration of 25 µg/ml. However, at a higher concentration of 50 µg/ml, the cell viability dropped notably to 45.14% (Arokiyaraj et al., 2014) . Furthermore, the chemical synthesis of silver nanoparticles employing $NaBH_4$ as reducing agent resulted in NIH 3T3 cells treated with 10 µg/ml of AgNPs for 24 hours, displaying a substantial increase in dead cells (56.8%) (Y. H. Lee et al., 2014) . Therefore, it seems that the synthesis of nanoparticles through plants makes them less harmful to the environment. The prevention of oxidation and the creation of harmful Ag^+ ions is attributed to the absorption of natural organic matter on their surface. Furthermore, these nanoparticles exhibit a high level of compatibility with animal and plant tissues (Jorge de Souza et al., 2019).

Ronavari et al. reported that, the IC_{50} for AgNPs produced through green synthesis using green tea extract in the case of the 3T3 mouse embryo cell line was 5 µg/ml. On the other hand, the IC_{50} for AgNPs against the same cell line while using coffee extract for green synthesis was found to be 272.14 ± 0.09 µg/ml (Rónavári et al., 2017).

This study indicated that RCM-AgNPs decreased 3T3 cell viability in a dose-dependent manner, with an IC_{50} of 46 µg/ml while maintaining over 70% cell viability at 20 µg/ml, a level considered safe by previous standards. Our findings align with prior research indicating that an escalation in concentration heightens toxicity to the cells (Majeed et al., 2022).As a result, the biological activity or toxicity profiles of the

nanoparticles produced can vary significantly depending on the plant extract used.

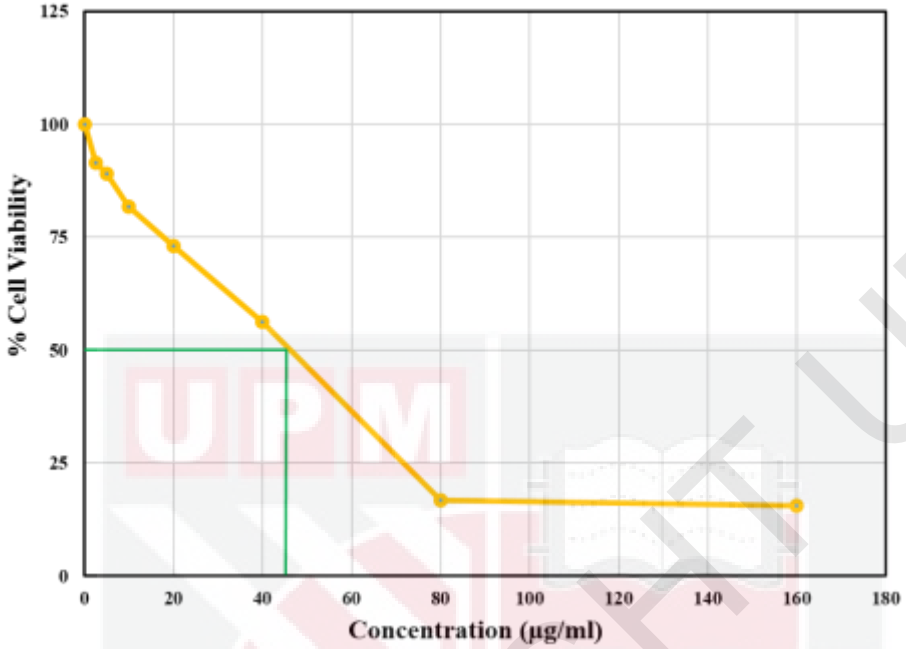

Figure 4.7: Effect of RCM-AgNPs on 3T3 cells after 24 hours exposure

4.4 Conclusion

In this chapter, we employed a cost-effective and straightforward plant-mediated synthesis method to successfully produce silver nanoparticles. To our knowledge, this is the first study to synthesise AgNPs using extracts from *Rhus Chinese* Mill fruit, traditional medicinal plant. Our previous study (Chapter 3) revealed that the extracts contained essential compounds such as tannins, terpenoids, alkaloids, phenolic compounds and steroids, acting as primary reducing and stabilising agents in the RCM-AgNPs synthesis. To identify the optimal synthesis conditions for RCM-AgNPs, we conducted experiments varying the experimental parameters, including different temperatures (70°C and 80°C) and pH values (pH 4, pH 7, pH 10), in accordance with the previous study. The RCM-AgNPs synthesised at 80°C and pH of 7 exhibited

absorption peaks around 419 nm. DLS analysis revealed that at parameters, smaller particle sizes were formed, measuring 43.77 ± 0.94 nm with moderate PDI values, indicating enhanced stability but also higher antibacterial activity against *E.coil* and *S.aureus*.

The TEM results revealed that the sizes of RCM-AgNPs ranging from 7 to 30 nm and the MIC and MBC values of RCM-AgNPs against *E.coil* and *S.aureus* were ranging from 39 to 156 µg/ml. A thorough analysis involving FTIR, XRD, EDX, and cytotoxicity assessments was conducted to validate its composition, crystalline structure, functional groups, and cytotoxicity properties. The FTIR analysis revealed that the biomolecules present in the plant extract acted as the primary reducing and stabilising agents during the synthesis of AgNPs. The crystalline nature of AgNPs was confirmed by XRD, while EDX revealed a dominant Ag peak at 3.0 kV, indicating the elemental composition of AgNP. In the cytotoxicity assessment utilising the 3T3 cell line, RCM-AgNPs exhibited no toxic effects at 20 µg/ml. Consequently, AgNPs obtained from plant extracts exhibit considerable antibacterial potential, with applications in medicine, pharmacology, and food science.

CHAPTER 5

PREPARATION AND CHARACTERISATION OF PHYSICOCHEMICAL PROPERTIES, SURFACE MORPHOLOGY AND ANTIMICROBIAL EVALUATION OF CHITOSAN-GELATIN BASED BIOACTIVE COMPOSITE FILMS

5.1 Introduction

Biopolymers sourced from natural and renewable origins, encompassing polysaccharides (e.g chitosan, starch, cellulose, alginate, and pectin) as well as proteins (eg. gelatin, whey protein, and soy protein isolate), have been extensively researched for creating edible films. These films can be composed of single biopolymers or blends. Notably, chitosan and gelatin are biopolymers with excellent properties such as film forming abilities, non-toxicity, high biocompatibility, biodegradability, stability, renewability, cost-effectiveness, and widespread commercial availability (Kumar et al., 2020; H. Wang et al., 2021). The gelatin-chitosan composite films in a 1:1 ratio exhibit optimal physico-chemical properties (Al-maqtari et al., 2022; Bonilla & Sobral, 2018). Furthermore, these films offer an excellent platform for integrating various active agents, like antimicrobial and antioxidants, transforming them into active films suitable for food preservation applications (Luis et al., 2018).

In Chapters 3 and 4, the 80% ethanol extract of RCM fruit and RCM-AgNPs were shown to be excellent natural sources of antioxidant and antimicrobial components in the production of these materials. The properties of the films are significantly improved by combining chitosan-gelatin with a bioactive agent and a nano-filler sourced from plants. This produces antimicrobial and antioxidant properties, as well

as improved mechanical strength and barrier properties. However, in order to produce films with exceptional properties, a uniformly dispersed and homogeneous film-forming solution is required. Unfortunately, composite films prepared using simple stirring methods frequently have poor barrier properties, low mechanical strength, and an unappealing appearance. Furthermore, decreasing particle size is critical for increasing the accessibility of additives like antimicrobials and antioxidants. Researchers have successfully demonstrated the effectiveness of the ultrasonic mixing technique in film formulation (Ajesh et al., 2023; Yuan et al., 2021).

The main goal of this chapter was to create composite films by combining RCM 80% ethanol fruit extracts and RCM-AgNPs with chitosan-gelatin (CG) biopolymers in different ratios, with the help of ultrasound treatment. Moreover, the study highlights the importance of enhancing the characteristics of composite films and conducting a detailed analysis of the physical, mechanical, surface morphology, and antimicrobial properties of both CG-RCM composite films and CG-RCM-AgNPs composite films. Figure 5.1 provides a comprehensive overview of the research approach discussed in this chapter.

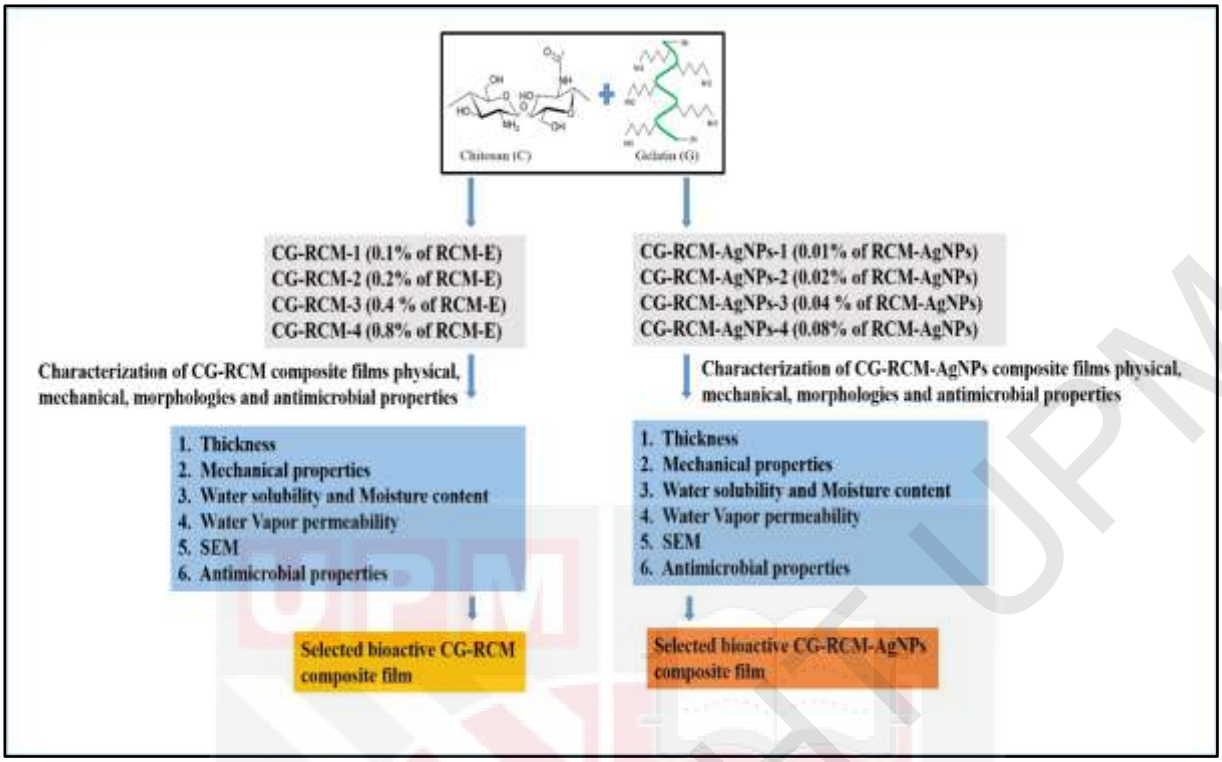

Figure 5.1: Research methodology flow chart for Chapter 5

5.2 Materials and methods

5.2.1 Materials

Acetic acid (99.8%), gelatin and glycerol were purchased from R&M Chemicals UK. Chitosan (85% deacetylation degree) was purchased from thermoscientific, US.

5.2.2 Fabrication of chitosan-gelatin based bioactive composite films

The chitosan-gelatin based bioactive composite films were prepared using a 20 kHz ultrasonic processor with a probe diameter of 12 mm (VC 500, Sonics Vibra Cell, US). Initially, a chitosan solution was prepared by stirring 2% w/v chitosan with 1% v/v acetic acid at room temperature overnight. Subsequently, glycerol, the plasticizer, was added at a rate of 30% per chitosan basis. Meanwhile, in a separate process, glycerol

(30 wt% on gelatin) was dissolved in a 2% w/w gelatin solution and stirred for one hour at 50 °C. At the same time, RCM-AgNPs (0.01%, 0.02%, 0.04 % and 0.08 % w/v) were created by mixing RCM-AgNPs powder in distilled water with an ultrasonic processor set at an amplitude of 50% for 15 minutes. The chitosan and gelatin solutions were mixed in a 1:1 ratio, combined with the RCM-AgNPs dispersion, and sonicated for 30 minutes. During the process, the temperature of the film-forming solutions was kept at 20 ± 5°C by utilising an ice water bath. Later, the final film solution was poured into 100 mm glass petri dishes and left to dry overnight in an oven set at 50 °C. The dried bioactive composite films were carefully removed from the petri dishes and conditioned at 50% relative humidity (RH) for 48 hours before undergoing further experimental analysis. Each composite film containing 0.01%, 0.02%, 0.04 % and 0.08 % RCM-AgNPs, were assigned a distinct name: CG-RCM-AgNPs-1, CG-RCM-AgNPs-2, CG-RCM-AgNPs-3 and CG-RCM-AgNPs-4, respectively. Additionally, chitosan-gelatin and RCM fruit methanol extract (0.1%, 0.2%, 0.4% and 0.8%) bioactive composite films, prepared using a similar procedure, and were labelled as CG, CG-RCM-1, CG-RCM-2, CG-RCM-3 and CG-RCM-4, respectively.

5.2.3 Thickness and mechanical properties

The film thickness was measured at five different points using an electronic vernier calliper with a precision of 0.01 mm (Mitutoyo Absolute, Tester Sangyo Co., Ltd., Tokyo, Japan). The outcome was described using an average value. The mechanical properties (tensile strength and elongation at break) of composite films were evaluated using a universal testing apparatus from Shimadzu Corporation, Japan. The testing apparatus was equipped with a 100 N load cell and a 0.5 mm/min strain rate. Film

specimens (dumbbell-shaped pieces measuring 2.5 cm × 8 cm) were placed in an environmental chamber and left to condition at a relative humidity of 50 ± 5% for 48 hours prior to testing. Each film was tested with at least five-time samples.

5.2.4 Moisture Content

The composite films were first cut into 2×2 cm pieces, and then they were pre-weighed. Afterward, the pre-weighed pieces were dried in an oven set at 105°C for 24 hours. For precise measurements, three replications were conducted for each film, and the moisture content was calculated using these replicates.

$$\text{Moisture content (\%)} = \frac{Wp - Wd}{Wp} \times 100 \qquad \text{Equation (5.1)}$$

Where Wp represents the initial weight of the film (g), and Wd represents the weight of the film after drying (g).

5.2.5 Water Solubility

The film was evaluated in triplicate using the method established by Hanani and colleagues (Hanani et al., 2019) . At first, the films were cut into 2×2 cm squares with great precision. The pre-weighted sample films were placed in 30 ml of distilled water. Following that, any remaining films were dried at 105°C until a consistent weight was reached. The solubility was calculated using the following equation:

$$\text{Water Solubility (\%)} = \frac{Wp - Wu}{Wp} \times 100 \qquad \text{Equation (5.2)}$$

Where Wp is the initial weight of the film (g) and Wu is the weight of undissolved film after drying in the oven.

5.2.6 Water Vapour Permeability

The water vapour permeability (WVP) of the films was determined gravimetrically at 25°C in accordance with the ASTM E96-80 standard (ASTM, 1989), with slight modifications. The film sample was enclosed within a 20 ml vial (inner diameter of 16 mm) containing silica gel (RH = 0, vapour pressure = 0 Pa). The sealed vials were subsequently positioned in desiccators containing distilled water (RH = 100%, vapour pressure = 3, 1691 kPa). The vial's weight was measured and recorded every 24 hours for a duration of seven days. The WVP of the film was determined using the subsequent equation:

$$\text{WVP} = \frac{W \times L}{t \times A \times \triangle P} \qquad \text{Equation (5.3)}$$

Where W signifies the augmented weight of the vials sealed with the film (g), L denotes the mean thickness of the film (m), t represents the experimental duration in seconds (s), 'A' indicates the permeation area (m^2), and $\triangle P$ signifies the partial pressure differential across the films. The WVP results of the films were presented in units of $g \cdot m^{-1} \cdot s^{-1} \cdot Pa^{-1}$.

5.2.7 Scanning Electron Microscopy

The morphology of bioactive composite films was analysed via scanning electron microscopy (SEM) at an accelerating voltage of 15 kV. The assessment was performed using a Hitachi TM3000 SEM from Hitachi Ltd., Tokyo, Japan. Prior to the SEM examination, the film surfaces were coated with platinum via a vacuum sputtering instrument (Magnetron sputter MSP-1S, Japan) to augment their conductivity and improve imaging quality.

5.2.8 Antimicrobial properties

The bacterial strains selected for this experiment were *E. coli* and *S. aureus*. The bacterial strain was cultured in Muller Hinton broth for 24 hours. Next, a Muller Hinton (MH) agar plate was uniformly coated with 40 µL of a bacterial culture containing 1-2 $\times 10^8$ CFU/mL. Before conducting antimicrobial testing, the films were punched into 9 mm diameter discs, sterilised using UV irradiation, and subsequently pressed firmly onto the MH agar. Measurement of the inhibitory zone size (mm) after 24 hours of incubation at 37°C was done using an electronic vernier calliper with a 0.01 mm resolution (Mitutoyo Absolute, Tester Sangyo Co., Ltd., Tokyo, Japan). Each experiment had three duplicates (X. Zhang et al., 2019) .

5.2.9 Statistical Analysis

The data was analysed using one-way analysis of variance (ANOVA) and was collected using IBM-SPSS version 25. The Least Significance Difference (LSD) method was employed to determine the differences in means.

5.3 Results and discussion

5.3.1 Films thickness, Moisture Content and Water Solubility of CG-RCM composite films

Table 5.1 shows the results for film thickness, moisture content, and water solubility in CG-RCM. The amount of solids in the film-forming solution directly correlates with film thickness, with the RCM ethanol extract producing a thicker film ($P < 0.005$).

Moisture content is the total volume of free space within the film network that is occupied by water molecules. Significant variations in moisture values ($P < 0.05$) were observed among the films under investigation, ranging from 28.49% to 18.58%. Comparing CG-RCM films to the control film revealed that the incorporation of RCM extract markedly decreased moisture content in relation to the extract concentration. This reduction is due to the incorporation of polyphenol extract, which enables the formation of intermolecular interactions between the extract and chitosan/gelatin, including hydrogen bonding and electrostatic interactions. According to Kan et al. (2019), these interactions prevent moisture from interacting with chitosan/gelatin. In addition, Al-Maqtari and his co-authors reported that the moisture content of chitosan-gelatin films was decreased by the incorporation of *Pulicaria jaubertii* extract (Al-maqtari et al., 2022).

Water solubility serves as an indicator of film stability, resistance to water, and potential for biodegradability. It is crucial to minimise water solubility because films should neither disintegrate upon contact with water nor permit water to pass through. It's worth noting that all the films tested exhibited slight solubility in water. The water

solubility of CG film was 26.26 ± 0.92%, aligns with the values previously reported by Romanelli (Romanelli et al., 2022). The higher concentration of RCM extract decreased water solubility of CG-RCM films (24.94 ± 2.22 to 21.64 ± 0.66%). Other researchers have obtained results consistent with our study (Luangapai & Iwamoto, 2023). Furthermore, Haghighi and co-authors have noted that water solubility in films can influence various types of secondary metabolites found in plants with diverse bioactive compounds (Haghighi et al., 2019).

CG-RCM-4 composite film showed significant improvement in thickness, moisture content, and water solubility ($P < 0.05$). As a result, CG-RCM-4 composite film was selected as the best condition for further analysis among the CG-RCM composite films for packaging applications.

Table 5.1: Thickness, moisture content and water solubility of the CG-RCM composite films

Sample	Thickness (mm)	Moisture Content (%)	Water Solubility (%)
CG	0.087 ± 0.00^{C}	28.49 ± 1.90^{A}	26.26 ± 0.92^{A}
CG-RCM-1	0.082 ± 0.01^{D}	25.17 ± 1.95^{A}	24.94 ± 2.22^{A}
CG-RCM-2	0.092 ± 0.008^{C}	24.68 ± 2.43^{B}	24.45 ± 3.96^{A}
CG-RCM-3	0.118 ± 0.01^{B}	22.91 ± 2.36^{B}	23.76 ± 1.42^{A}
CG-RCM-4	0.126 ± 0.01^{A}	18.58 ± 0.32^{C}	21.64 ± 0.66^{B}

Values are means ± SD. Different lowercase superscripts in the same column denote significant difference ($P < 0.05$).

5.3.2 Film thickness, Moisture Content and Water Solubility of CG-RCM-AgNPs composite films

Table 5.2 presents the findings of the tests conducted on the thickness, moisture content, and water solubility of the CG-RCM-AgNPs films. The film thickness shows a slight increase, which is influenced by the solid content of RCM-AgNPs in the film-forming solution ($P < 0.05$).

The neat CG film had the highest moisture content value (28.49 ± 1.9%). This is due to the abundance of hydrophilic natural compounds in chitosan, gelatin, and glycerol, which interact with water molecules via hydrogen bonds (Kan et al., 2019; W. Zhao et al., 2022) The moisture content of CG-RCM-AgNPs showed a significant decrease when RCM-AgNPs were incorporated into the CG film ($P < 0.05$). This decrease could be explained by the possibility of a coordination effect between the silver atoms in AgNPs and the hydroxyl groups, which might limit the interaction of the AgNPs with moisture (You et al., 2022). Comparable findings have previously been reported, indicating that the inclusion of AgNPs in a polymer matrix can lead to a decrease in moisture content (Kadam et al., 2019; Qin et al., 2019). For water solubility testing, compared to the CG film, the CG-RCM-AgNPs films initially exhibited a dramatic decrease in water solubility, but with an increase in the concentration of RCM-AgNPs, the water solubility of the films only slightly decreased. On the contrary, Kadam et al. reported that the water solubility of chitosan/Ag nanocomposite films increased as the AgNPs content increased (Kadam et al., 2019). The results of this study showed that AgNPs were significantly beneficial in terms of reducing moisture content and improving water resistance.

Table 5.2: Thickness, moisture content and water solubility of the CG-RCM-AgNPs composite films

Sample	Thickness (mm)	Moisture Content (%)	Water Solubility (%)
CG	0.087 ± 0.00^{B}	28.49 ± 1.90^{A}	26.26 ± 0.92^{A}
CG-RCM-AgNPs-1	0.081 ± 0.01^{B}	25.24 ± 0.812^{A}	22.50 ± 0.46^{B}
CG-RCM-AgNPs-2	0.092 ± 0.014^{B}	24.17 ± 3.0^{B}	22.78 ± 0.25^{B}
CG-RCM-AgNPs-3	0.095 ± 0.002^{B}	23.39 ± 2.12^{B}	22.88 ± 0.84^{B}
CG-RCM-AgNPs-4	0.112 ± 0.028^{A}	20.06 ± 0.91^{C}	22.08 ± 0.21^{B}

Note: Values are means ± SD. Different superscripts $^{A, B, C}$ in the same column denote significant difference ($P < 0.05$).

5.3.3 Water Vapour Permeability of CG-RCM composite films

Water vapour permeability (WVP) measures the speed at which water vapour moves through the film's surface. Generally, for food preservation films, it's desirable to minimise WVP to prevent moisture exchange between the food and its surroundings, ultimately extending the food's shelf life (Haghighi et al., 2019).

The WVP value of control CG film was 9.39 ± 0.47 $\times 10^{-12}$ g $m^{-1}s^{-1}Pa^{-1}$. Figure 5.2 illustrates that the WVP of CG-RCM films markedly diminished upon the incorporation of RCM 80% ethanol extract ($P < 0.05$). The results were predominantly attributed to the phenolic constituents of the RCM 80% ethanol extract. These phenolic compounds interacted with proteins to form a densely interconnected structure. This structure effectively reduced the available space within the polymer matrix and added complexity to the path that water molecules had to traverse. Consequently, this led to a decrease in the rate at which water molecules diffused through the film (Ramziia et al., 2018).

Tagrida et al. and Hu et al. demonstrated that WVP of chitosan-gelatin films could be effectively lowered by introducing betel leaf or amaranth ethanol extract. This reduction in WVP can be attributed to the presence of phenolic compounds, which may enhance the cross-linking of gelatin and chitosan, ultimately resulting in a decrease in the number of hydrophilic functional groups (Hu et al., 2020; Tagrida et al., 2023). Notably, when the extract concentration grew, the WVP of CG films initially declined and subsequently increased. This was due to the extract's ability to effectively disperse at low concentration (0.1, 0.2, and 0.4%) in the film matrix, which

prevented the transfer of water vapour. Additional extract could agglomerate, though, and somewhat disturb the matrix of the compact film. Thus, when the extract content of CG-RCM films reached 0.8%, the WVP dropped. The same effect on the behaviour of WVP was observed when Chinese hawthorn ethanol extract added to the chitosan-gelatin films (Kan et al., 2019). On the contrary, Al-Maqtari and colleagues reported that as the concentration of microcapsules containing *Pulicaria jaubertii* extract (MPJE) increased gradually, the WVP of chitosan-gelatin films also increased. This effect was attributed to the swelling of the granules and the expansion of inter-chain gaps within the resulting film matrix, caused by unlinked components present in MPJE. This resulted in an increase in WVP values form 6.23 ± 0.10 to 7.30 ± 0.27 g mm/kPa hm^2(Al-maqtari et al., 2022)

Furthermore, Huixia and colleagues discovered a reduction in WVP of the composite film made from chitosan and gelatin based amaranth extract, dropping from 34.9 ± 0.1 to 31.6 ± 3.5× 10^{-11} g $m^{-1}s^{-1}Pa^{-1}$ (Hu et al., 2020). In comparison to previous films created without ultrasound treatment, the current ultrasound-assist composite film samples had lower WVP values. Several important factors influence WVP value. These encompass the structural and chemical attributes of the polymer base, the existence of hydrophobic interactions within the film, and the type and concentration of additives (S. Yadav et al., 2020). This is essential to comprehend, as it elucidates that the microstructural composition of a film is inextricably linked to its capacity to function as a barrier. The utilisation of ultrasound-assisted methods is increasing, primarily to improve the compatibility and cross-linking between the components of films. This has resulted in a substantial reduction in particle size and dense structure form (Ajesh et al., 2023; Yuan et al., 2021).

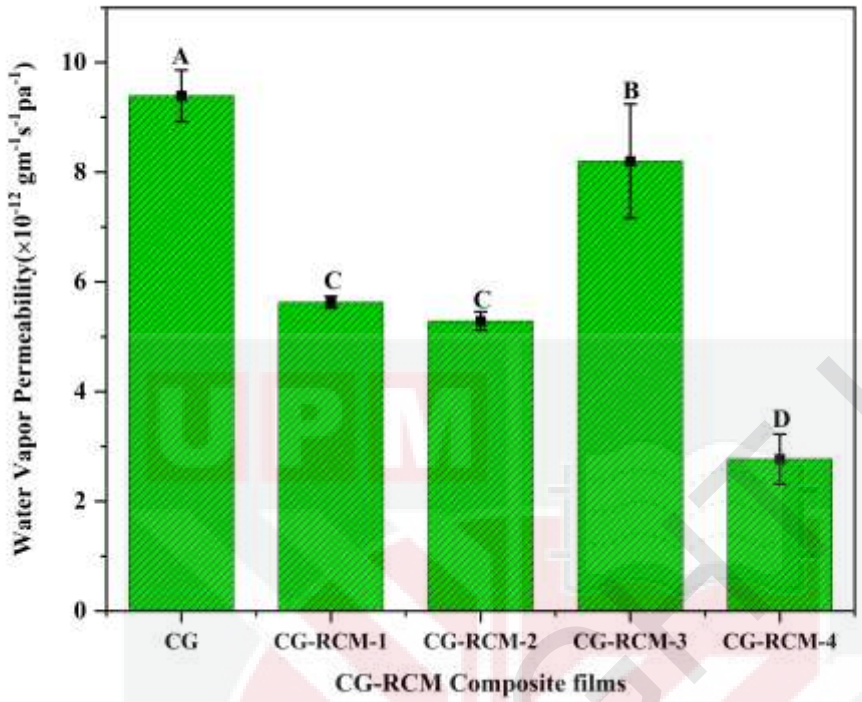

Figure 5.2: WVP of CG-RCM composite films
Note: Means followed with the different letters $^{A, B, C}$ represent significant differences among CG-RCM composite films ($P < 0.05$) according to LSD.

5.3.4 Water Vapour Permeability (WVP) of CG-RCM-AgNPs composite films

The WVP value of control CG film was 9.39 ± 0.47 $\times 10^{-12}$ g $m^{-1}s^{-1}Pa^{-1}$. With an increase in RCM-AgNPs content, the WVP decreased from 9.244 ± 1.13 to 6.642 ± 0.867$\times 10^{-12}$ g $m^{-1}s^{-1}Pa^{-1}$ **(**Figure 5.3). A Similar decrease in the WVP was also observed in chitosan composite films containing tea phenolic synthesised AgNPs (W. Zhang & Jiang, 2020) and catechol-grafted chitosan/gelatin blend films (CSCT-G) incorporated with CSCT-AgNPs (Cao et al., 2020). This phenomenon can be attributed to the impervious nature of AgNPs which increases the tortuous pathway for water vapour diffusion, consequently enhancing the barrier properties (Yang et al., 2023).

Additionally, Yang and his team showed that the presence of AgNPs altered the internal network, resulting in decreased WVP values for chitosan/polyvinyl alcohol films loaded with AgNPs, reducing from 21.6 to 16.9 ($\times 10^{-11}$ g·m^{-1}·s^{-1}·Pa^{-1}) (Yang et al., 2023). Furthermore, the alterations in structure evident in SEM images suggest a denser configuration brought about by the infusion of both RCM 80% ethanol extract and RCM-AgNPs.

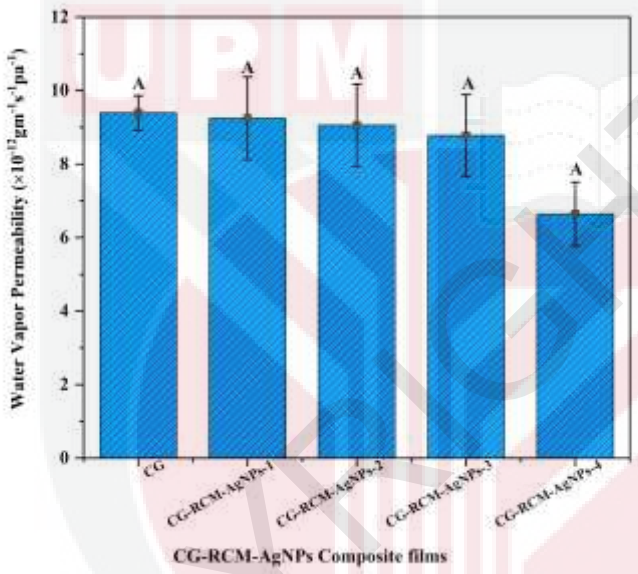

Figure 5.3: WVP of CG-RCM-AgNPs composite films
Note: Same letters are not significantly different among CG-RCM-AgNPs ($P < 0.05$) according to LSD.

5.3.5 Mechanical properties of CG-RCM composite films

Ensuring film integrity relies heavily on mechanical strength, specifically the assessment of tensile strength (TS) and elongation at break (EAB). These two parameters play a crucial role in evaluating the mechanical properties of polymeric films (S. Li et al., 2022) .

CG-RCM films exhibited significant changes in TS and EAB values compared to control CG films after the addition of RCM 80% ethanol extract ($P < 0.05$). The increase in TS and the decrease in EAB of CG-RCM films were observed in relation to the concentration of RCM 80% ethanol extract (Figure 5.4). This phenomenon is likely attributable to the electrostatic interaction between the RCM 80% ethanol extract and CG, as well as the formation of hydrogen bonds, which contributed to the enhancement of the tensile properties. In contrast, the EAB of CG-RCM films decreased significantly from 31.09 to 7.382 MPa. This result can be attributed to the reduction in chain mobility within CG-RCM composite films due to the formation of hydrogen bonds between the polyphenol plant extract and the CG film. Consequently, this decreased chain mobility resulted in reduced flexibility. Kan and co-authors observed similar phenomena in chitosan-gelatin blend films incorporated with Chinese hawthorn fruit extract (Kan et al., 2019). Additionally, Zhang and colleagues also found that increasing the concentration of tannic acid into chitosan gelatin based films directly impacts the mechanical properties of the films (C. Zhang et al., 2021).

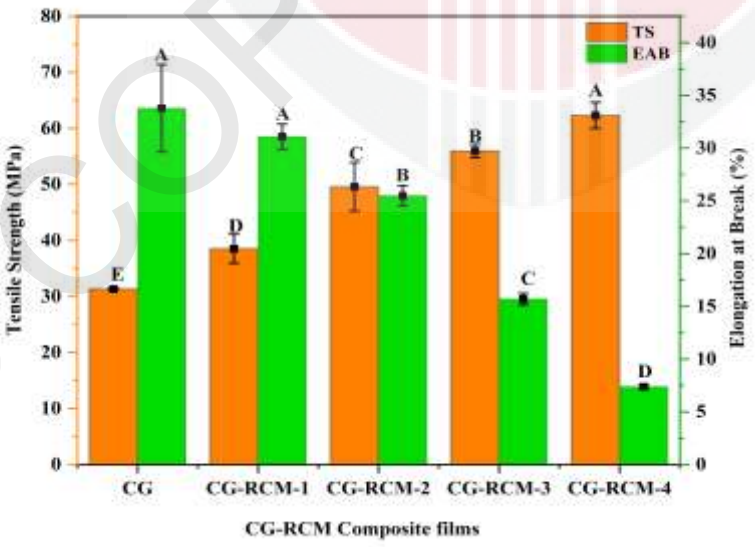

Figure 5.4: Mechanical properties of CG-RCM composite films
Note: Different letters $^{A, B, C...}$ indicated significant differences within each parameter ($P < 0.05$).

5.3.6 Mechanical properties of CG-RCM-AgNPs composite films

In Figure 5.5, incorporating RCM-AgNPs into the CG film, the TS of the resulting CG-RCM-AgNPs films exhibits a pattern of initial increase followed by a notable decrease ($P<0.05$). Especially, as the concentration of RCM-AgNPs is raised to 0.02%, the TS of CG-RCM-AgNPs reaches maximum value of 64.15 ± 1.82 MPa. The EAB of the films initially decreased, and then increased significantly from 6.21 ± 1.33% to 30.98 ± 1.62%. The increase in TS observed in the CG-RCM-AgNPs films is likely attributed to the capability of RCM-AgNPs to form uniform dispersion at low concentrations, facilitating interaction with specific amino acids within the CG film.

Conversely, elevated concentrations of RCM-AgNPs tend to induce agglomeration within the film, potentially admonishing the contact surface and interaction between the nanomaterial and the polymer. As a consequence, this agglomeration leads to a decline in the film's TS (Lin et al., 2020). Similar behaviour was also observed where the TS of the chitosan-gelatin based nanocomposite film decreased as the concentration of *Mimusops elengi* fruit-synthesised silver nanoparticles increased (Kumar et al., 2018). However, the EAB value of the CG-RCM-AgNPs biocomposite films showed an upward trend with increasing silver nanoparticles concentration, likely due to the plasticising effect of silver nanoparticles in the CG film. The extensive specific surface area of silver nanoparticles facilitates the development of an interfacial polymer layer bonded to the particle core. This layer's presence will diminish the maximum nanoparticle filling capacity within the polymer matrix. The presence of repulsive forces between particles and the interfacial layer enhances polymer chain mobility, resulting in a plasticising effect that reduces the Glass Transition

Temperature (Tg). This could be determined by measuring Tg change with DMA. Normally, the mechanical properties of bioactive composite films predominantly depends on factors such as the size, shape, and quantity of nanoparticles, alongside the level of inter and intra-molecular interactions among polymer chains or the interplay between nanofillers and polymeric chains (Nguyen et al., 2023).

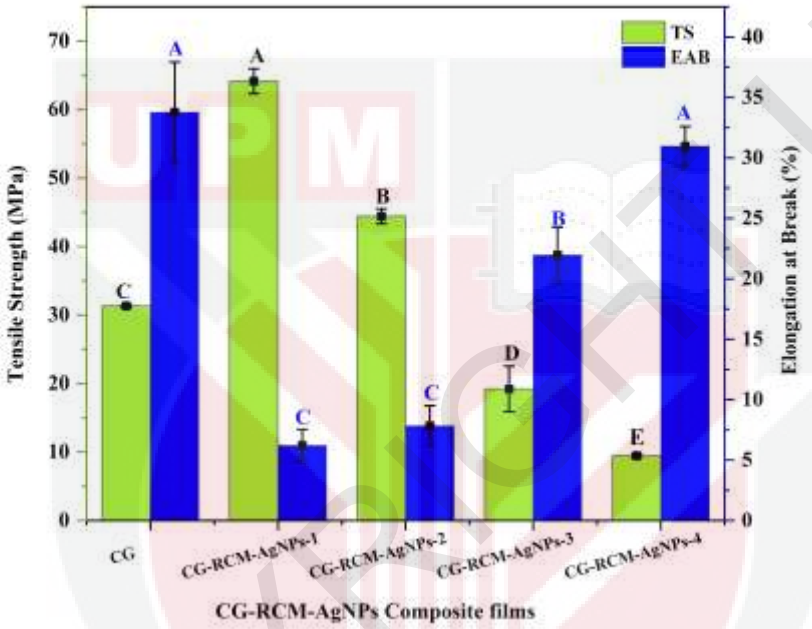

Figure 5.5: Mechanical properties of CG-RCM-AgNPs composite films
Note: Different letters $^{A, B, C.}$ indicated significant differences within each parameter ($P < 0.05$).

5.3.7 Scanning Electron Microscopy of CG-RCM composite films

As depicted in Figure 5.6, the gradual introduction of higher concentrations of RCM 80% ethanol extract into the film formulation resulted in a noticeable shift in the colour of the composite films, transitioning from a pale-yellow hue to a reddish- brown shade. The microstructure of a film's interior is influenced by the level of compatibility and miscibility among its components. This directly impacts the film's mechanical strength and ability to serve as a barrier (Haghighi et al., 2019). Therefore, understanding the

interactions between the various components is crucial for designing films with optimal properties. SEM images of surface and cross sections of CG, CG-RCM-1, CG-RCM-2, CG-RCM-3 and CG-RCM-4 are presented in Figure 5.6. Surface and cross-sectional analysis of the CG film revealed a uniform and dense structure devoid of cracks, wrinkles, or phase separation. This suggests excellent compatibility among the film's components, namely chitosan, gelatin and glycerol. The homogeneous microstructure of the CG film is likely due to the hydrophilic nature of its constituents, which allow them to interact through associative interaction. Overall, these findings highlight the successful blending of chitosan, gelatin and glycerol to form a cohesive and stable film (Kan et al., 2019). Numerous researchers have also reported observing similar occurrences in films made from blends of chitosan and gelatin (Jridi et al., 2014; Samsi et al., 2019).

When incorporating 0.1wt% of the extract into the blend, the composite film exhibited a smooth and uniform surface, with minor wrinkles and compaction the cross section of the composite film can be seen in Figure 5.6b. The addition of 0.2 and 0.4 wt % extract resulted in a more compact inner microstructure in the cross section of CG-RCM-2 and CG-RCM-3 films. This improvement in microstructure was beneficial for enhancing the mechanical properties of the films. This study supports previous research that showed how chitosan-gelatin blend films, when combined with gallic acid, exhibit a consistent and even microstructure. This observation suggests that the incorporation of gallic acid performed effectively, indicating good compatibility at the molecular level (Rezaee et al., 2018).

Nevertheless, as the RCM 80% ethanol extract content rose to 0.8 wt%, the surface of the CG-RCM-4 film became denser, more compact, and tighter, with the cross-section exhibiting agglomeration in the bottom layer. This phenomenon likely resulted from the constrained solubility of the RCM 80% ethanol extract in the film-forming solution, particularly at higher concentrations (Kan et al., 2019). These findings indicate a significant impact of the RCM 80% ethanol extract content on the microstructure of the composite films. Haghighi and colleagues also reported that adding cinnamon, citronella, pink clove, nutmeg, and thyme to chitosan-gelatin blend films led to notable features such as pores, irregular structures, air bubbles on the film surface. Similarly, Bonilla and collaborators found that incorporating eugenol and ginger essential oils into chitosan-gelatin blend films develop pores within the films. The occurrence was ascribed to the breakdown of oil droplets that repel water during the process of drying the film. The observations suggest that the characteristics of the additives had a significant impact on the microstructure of the composite films.

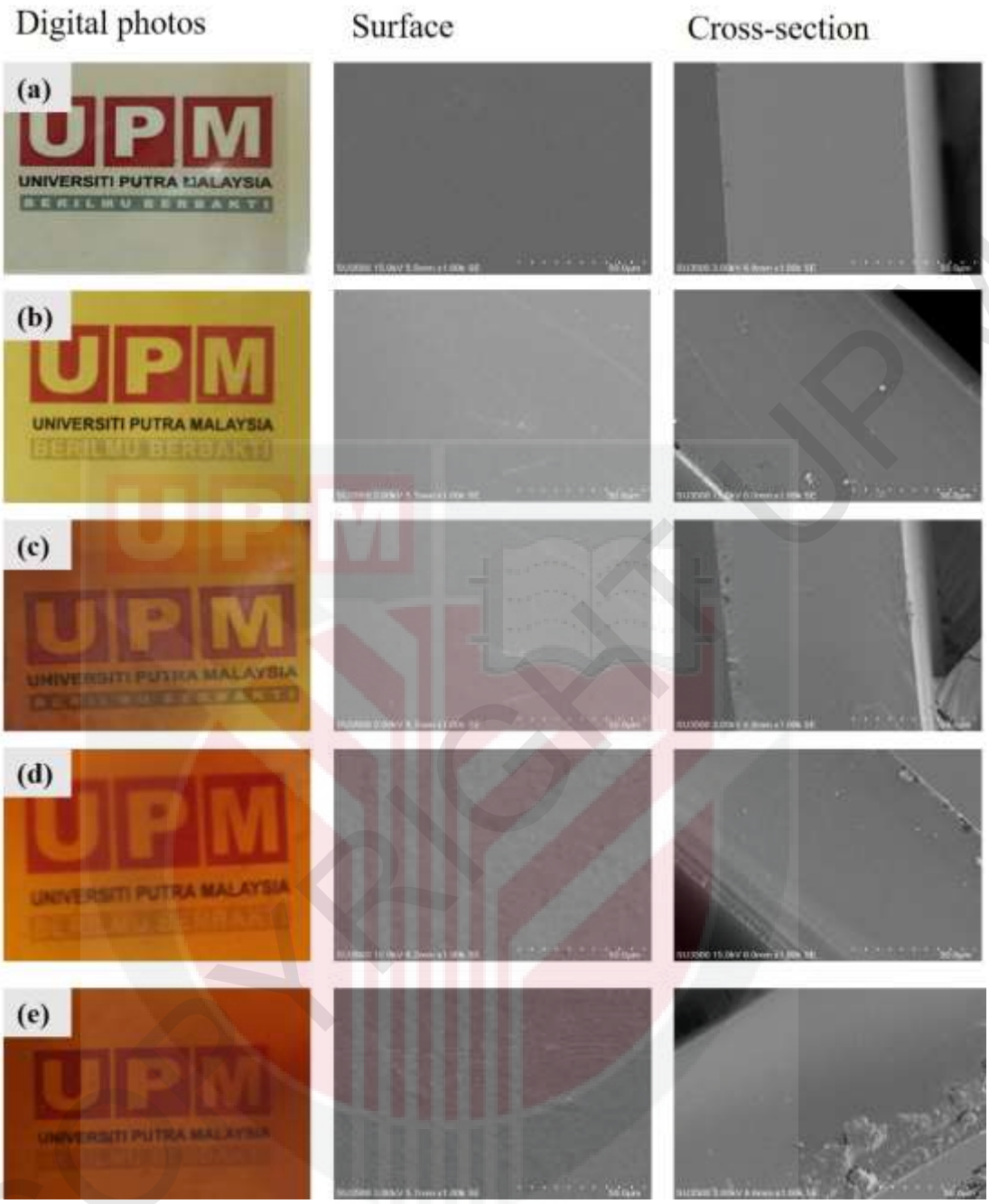

Figure 5.6: SEM of digital image, surface and cross section of CG (a) CG-RCM-1 (b) CG-RCM-2 (c) CG-RCM-3 (d) CG-RCM-4 (e) composite films

5.3.8 Scanning Electron Microscopy of CG-RCM-AgNPs composite films

As illustrated in Figure 5.7, the incremental incorporation of elevated concentrations of RCM-AgNPs into the film formulation led to a distinct change in the color of the composite films. The transition was evident as the films shifted from a light-yellow hue to a subtle light-brown shade. Upon the introduction of RCM-AgNPs, the CG-RCM-AgNPs-1 film displayed a uniformly even surface, and no discernible distinction was observed between the CG film and the CG-RCM-AgNPs-1 film. This similarity can be attributed to the low concentration (0.01%) of RCM-AgNPs, proving inadequate to induce changes in the microstructure of the film. Furthermore, the emergence of white spots on the surface of the CG-RCM-AgNPs composite films increased progressively with rising RCM-AgNPs content (0.02, 0.04 and 0.08%) signifying the aggregation of RCM-AgNPs within the CG matrix. Furthermore, the cross-section of the CG-RCM-AgNPs composite films displayed a dense and compact structure, even in the presence of particles agglomeration, especially at higher concentrations. These nanoparticles exhibited strong adherence to the CG matrix, potentially leading to modifications in the physical and chemical properties of the films. These observations align with findings reported in a previous study (Ediyilyam et al., 2021; Kumar et al., 2018).

Figure 5.7: SEM of digital image, surface and cross section of CG (a) CG-RCM-AgNPs-1 (b) CG-RCM-AgNPs-2 (c) CG-RCM-AgNPs-3 (d) CG-RCM-AgNPs-4 (e) composite films

5.3.9 Antimicrobial properties of composite films

The composite films were assessed for their antibacterial activity by measuring the diameter of the inhibition zone. Figure. 5.8 shows that composite films based on CG containing 0.8% RCM extract (CG-RCM-4) displayed an inhibition zone measuring against *S.aureus* at 15.32 ± 1.12 mm. On the other hand, the pure CG and CG-based composite films containing RCM 80% ethanol extract (0.1%, 0.2%, and 0.4%) did not show an inhibition zone. Instead, they demonstrated growth inhibition right below the discs. Similarly, composite films made with CG and doped with 0.08% RCM-AgNPs (CG- RCM-AgNPs-4) exhibited an inhibition zone against *E.coli* (10.15 ± 0.17 mm) and *S.aureus* (10.66 ± 0.32mm). On the other hand, composite films made with CG and RCM-AgNPs (0.01%, 0.02%, and 0.04%) showed no inhibition zone, only growth inhibition just below the disc. In addition, the film's low concentration of RCM-AgNPs and RCM extract may have hindered the formation of inhibition zones. It seems that only colonies in direct contact with these films were inhibited, suggesting that the active compounds had limited diffusion in the agar. The CG film showed effective inhibition against the tested bacteria, which can be attributed to the natural antimicrobial properties of chitosan. The amino groups in chitosan have a positive charge that interacts with the negatively charged bacterial cell membrane. This interaction causes proteins and intracellular components of the bacteria to be released (Bonilla & Sobral, 2016).

Moreover, the precise method by which RCM 80% ethanol extract inhibits bacterial growth was not entirely understood. A proposed hypothesis suggested that the hydroxyl groups present in the polyphenols within the RCM 80% ethanol extract

functioned as proton exchangers, causing destabilisation of the bacterial cell's cytoplasmic membrane. It was thought that these actions would reduce the pH gradient, disturb the permeability of the membrane to ions, and consequently disrupt the flow of electrons and proton motive forces. The release of ATPs and other necessary components for bacterial cell metabolism ultimately resulted in the bacteria's death (Tagrida et al., 2023) .

Figure 5.8 (A and B) shows that the films had less antibacterial effect on *E.coli* than on *S.aureus*, mainly because of differences in their cell wall structures. When it comes to bacteria like *E.coli*, their cell walls are made up of several layers including a thin peptidoglycan layer, a lipoprotein layer, and a phospholipid or lipopolysaccharide layer. On the other hand, bacteria that are classified as gram-positive, such as *S.aureus*, have cell walls made up of a single peptidoglycan layer (Wu et al., 2019) . As a result, RCM-AgNPs can more easily penetrate one type of bacteria compared to the other.

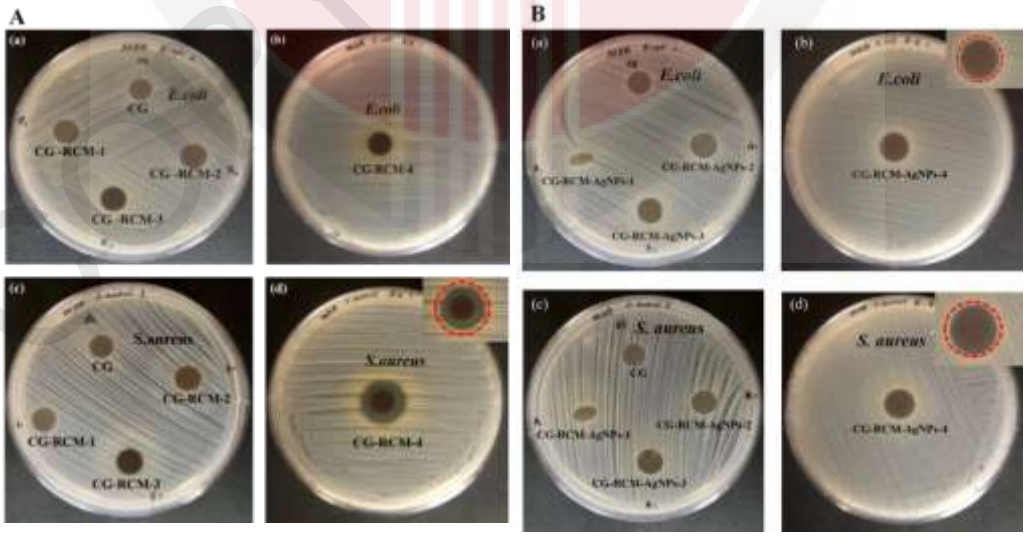

Figure. 5.8: A. antimicrobial activity of RCM composite film: *E. coli* (a & b) *S. aureus* (c & d) and B. antimicrobial activity of RCM-AgNPs composite film: *E. coli* (a & b) *S. aureus* (c & d)

5.4 Conclusion

In this study, two types of novel natural composite films were successfully developed using ultrasound treatment, incorporating varying ratios of RCM ethanol extract and RCM-AgNPs into chitosan-gelatin. The integration of RCM-E or RCM-AgNPs into composite films influenced their physicochemical, barrier, and mechanical characteristics. The incorporation of RCM-E or RCM-AgNPs may engage with the film matrix via hydrogen bonding and electrostatic interactions, leading to a denser inner microstructure within the films. Among the CG-RCM composite films, CG-RCM-4 (0.8%) has not only the lowest WVP value but also the highest thickness, the lowest Moisture content and Water Solubility ($P < 0.05$). The CG-RCM-2 (0.2%) exhibited better mechanical properties (TS = 49.58 ± 4.33, EAB = 25.48 ± 0.97) but the CG-RCM-4 (TS = 62.32 ± 2.33, EAB = 7.38 ± 0.19) exhibited effectiveness against *S.aureus* (15.32 ± 1.12 mm). Similarly, in CG-RCM-AgNPs composite films, CG-RCM-AgNPs-4 (0.08%) has significantly increased thickness, Moisture content, and Water Solubility, but the WVP value is unaffected, despite being the lowest value among the CG-RCM-AgNPs composite films. SEM revealed that the apparent structure of CG-RCM-4 and CG-RCM-AgNPs-4 composite films was dense and compact, even with particle agglomeration. The CG-RCM-AgNPs-1 of mechanical properties has the highest value (TS = 64.15 ± 1.82, EAB = 6.21 ± 1.33) but CG-RCM-AgNPs-4 (TS = 9.46 ± 0.27, EAB = 30.98 ± 1.62) has the highest inhabitation zone of *S.aureus* (10.66 ± 0.32 mm) and *E.coli* (10.15 ± 0.17 mm). In Chapter 6, CG-RCM-4 and CG-RCM-AgNPs-4 were chosen for additional characterisation due to their antimicrobial and barrier properties.

CHAPTER 6

CHARACTERISATION OF SELECTED BIOACTIVE COMPOSITE FILMS; CHEMICAL COMPOSITION, THERMAL, BIOLOGICAL PROPERTIES, AND THEIR APPLICATION IN CHICKEN PRESERVATION

6.1 Introduction

The optimised composition contains 0.8% of RCM 80% ethanol extract incorporated into the chitosan-gelatin film (CG-RCM-4) and 0.08% of RCM-AgNPs incorporated into the chitosan-gelatin film (CG-RCM-AgNPs-4) demonstrated the most satisfactory physical, barrier, and antimicrobial properties in previous chapter. Additional evaluations of these optimised bioactive composite films will include chemical composition, structure, thermal behaviour, and biological properties, as well as their use in chicken preservation. As a control experiment, a sample of chitosan and gelatin (CG) was tested. Figure 6.1 provides a detailed overview of the research approach described in this chapter.

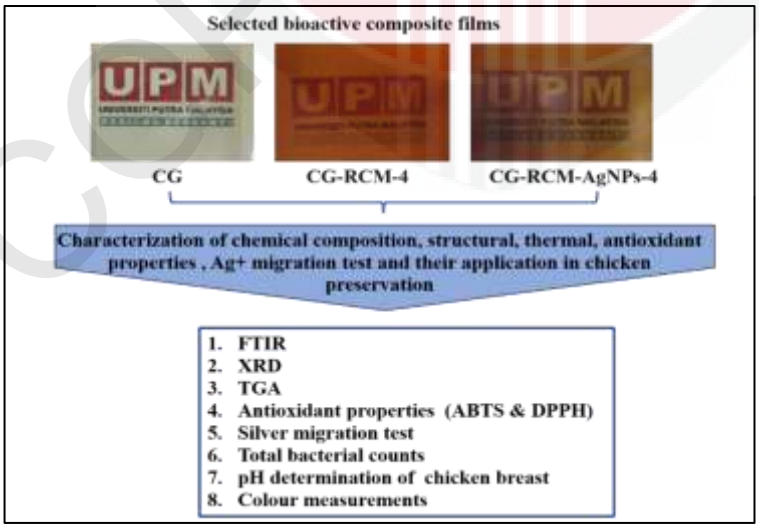

Figure 6.1: Overview of research approach outlined in this chapter

6.2 Materials and methods

6.2.1 Materials

Acetic acid (99.8%), gelatin and glycerol were purchased from R&M Chemicals UK. Chitosan (85% deacetylation degree) was purchased from thermoscientific, US.

6.2.2 Fabrication of chitosan-gelatin based bioactive composite films

The bioactive composite films made from Chitosan-Gelatin were prepared using a 20 kHz ultrasonic processor with a 12 mm probe diameter as described in Section 5.2.2.

6.2.3 Fourier Transformed Infrared (FTIR) Spectroscopy

Chitosan, gelatin, CG, CG-RCM-4, and CG-RCM-AgNPs-4 films were analysed using a Nicolet 380 Fourier Transform Infrared (FTIR) spectrometer (Thermo Corp., USA) equipped with attenuated total reflectance. In the wavenumber range of 4000-400 cm^{-1}, the spectra were acquired with a resolution of 4 cm^{-1}.

6.2.4 X-ray diffraction Analysis (XRD)

The crystalline nature of the selected composite films was examined using an X-ray diffraction meter (XRD-6000, Shimadzu, Japan) between 30° and 80° and at a scanning rate of 2°/min.

6.2.5 Thermogravimetric Analysis (TGA)

The thermal properties of CG, CG-RCM-4, and CG-RCM-AgNPs-4 composite films were determined using a thermogravimetric analyser (Hitachi STA7200RV, Japan). The samples (5-6 mg) were heated in a platinum pan from 40°C to 600°C in a nitrogen atmosphere at a rate of 10°C/min.

6.2.6 DPPH Radical Scavenging Assay

The method used to determine ABTS radicals scavenging activity of CG, CG-RCM-4 and CG-RCM-AgNPs-4 composite films is described in Chapter 3 (Section 3.2.6).

6.2.7 ABTS Radical Scavenging Assay

CG, CG-RCM-4 and CG-RCM-AgNPs-4 were tested for its ability to scavenge DPPH radicals in accordance Chapter 3 (Section 3.2.7).

6.2.8 Determination of silver migration

The measurement of silver migration in the CG-RCM-AgNPs-4 film was conducted using inductively coupled plasma-emission spectrometry (ICP-OES, PerkinElmer Optima 7300DV, USA) to determine the Ag^+ content. 100 mg of CG-RCM-AgNPs-4 film was submerged in 50 ml of deionised water. Every other day for a consecutive 7-day period, 5ml of the solution was withdrawn, and 5ml of deionised water was added to maintain a consistent volume (Y. Zhao, Yang, et al., 2022). A calibration curve was

created for concentrations of 2, 4, 6, 8, and 10 $\mu g \cdot L^{-1}$. All samples were analysed three times.

6.2.9 Sample preparation for chicken breast preservation

The uncooked chicken was acquired from Pasar Pagi, Seri Kembangan, Selangor. The chicken meat samples employed in this study were of the broiler variety and were maintained in a cooler box (2°C - 5°C) from the time of acquisition until the initiation of the experiments. Prior to treatment, the chicken meat was diced into small segments, each weighing approximately 10 g. Subsequently, the samples were wrapped the CG, CG-RCM-4, and CG-RCM-AgNPs-4 bioactive composite films and stored at 4 ± 1°C for 12 days. The unpackaged chilled chicken meat was served as the control. The samples were collected for total plate count, pH, and colour analyses after 0, 3, 6, 9, and 12 days.

6.2.10 Chicken breast Preservation

Aseptically transferring 10 grams of each chicken sample into stomacher bags containing 90 ml of Maximum Recovery Diluent composed of 0.1% w/V peptone and 0.85% w/v NaCl. The samples were homogenised for 2 minutes using a Stomacher (Wisemix WES-400, DAIHAN, Korea). A volume of 0.1 ml from the appropriate 10-fold serial dilutions was placed on plate count agar using the spread plate technique to enumerate the total plate counts. The agar was subsequently incubated at 35°C for 48-72 hours (Ekonomou et al., 2023). The results were expressed as log CFU/g, and a microbiological analysis was conducted every three days. Oxoid, UK, supplied all microbiological media.

6.2.11 Colour measurement

The colour of raw breast chicken meat was measured using a Japanese Colur Reader CR-10 (Minolta). The colour was expressed using the values L* (lightness), a* (redness), and b* (yellowness). Three measurement points were randomly chosen for each sample (L. Lin et al., 2023).

6.2.12 pH measurement

2 grams of meat samples were mixed with 20 millilitres of distilled water in a beaker using a homogeniser (Ultra Turrax T25, IKA, Germany) at a speed of 13,500 rpm for 30 seconds. Next, the pH of meat samples was measured at room temperature using the digital pH metre from Mettler-Toledo AG, Switzerland (Sani et al., 2021).

6.2.13 Statistical Analysis

The data was collected using IBM-SPSS version 25 with one-way analysis of variance (ANOVA). The mean differences were calculated using the Least Significance Difference (LSD) method.

6.3 Results and discussion

6.3.1 Fourier Transformed Infrared (FTIR) Spectroscopy

The interactions between the molecules of bioactive composite films were investigated using FT-IR measurements. Figure 6.2 shows the spectra of films made from pure chitosan, gelatin, and selected formulations. The FTIR spectrum of chitosan film shows distinct bands at 3357.60, 2871.85, 1655.17, 1591.53, and 1269.46 cm^{-1}, indicating O-H and amide-A band (N-H stretching) interactions (Hajji et al., 2021). Furthermore, these bands represent C-H stretching, amide-I (C=O stretching of the amide group), amide-II (N-H bending), and amide-III (C-N and N-H bonds), respectively. Furthermore, the absorption peak observed at 1154.23 cm^{-1} is attributed to the polysaccharide's structure (Ghaderi et al., 2019).The main absorbance presents in gelatin film at approximately 3293.06, 3071.69, 1629.62, 1529.33 and 1241.02 cm^{-1} are ascribed to amide-A (N-H stretching coupled with hydrogen bonding), amide-B (reflecting the asymmetric stretching vibration of C-H and NH_3^+), amide-I (related to C=O stretching), amide-II (stemming from the bending vibration of N-H groups and stretching vibrations of C-N groups), and amide-III (representing vibrations within the plane of C-N and N-H groups of bound amide or vibration of CH2 groups of glycine), respectively. This spectral pattern aligns with analogous findings by Jridi and colleagues concerning gelatin film (Jridi et al., 2014).

The distinctive bands mentioned earlier for both gelatin and chitosan were evident in the CG blend films, attributed to the presence of both constituents. This phenomenon was also observed in the study by Tessaro and co-authors (Tessaro et al., 2021). Incorporating gelatin into chitosan led to alterations in conformation, resulting in shifts

of chitosan peaks at 2871.85, 1655.17,1591.53 and 1027.91 cm^{-1} shifting to 2920,1643,1547 and 1036 cm^{-1} respectively in the CG film due to electrostatic interactions for the amino and carbonyl groups (Xu et al., 2020). The regions of amide I, amide II, and amide III bands in CG films exhibited significant alterations compared to pure films (C. Zhang et al., 2021). Prior research has established that the phenomenon resulted from intermolecular hydrogen bonds and electrostatic interactions between CS and GL.

The FT-IR spectra of the CG-RCM-AgNPs bioactive composite films exhibit resemblance to those of the CG bioactive composite film. Nevertheless, upon integrating RCM-AgNPs into the CG-based bioactive composite film, the distinctive absorption bands originally located at 3300, 1643, and 1549 cm^{-1} within the CG bioactive composite film experience a shift towards lower wavenumbers specifically, to 3297,1629, and 1536 cm^{-1} respectively. Remarkably, the addition of RCM-AgNPs does not induce structural alterations in the bioactive composite films, rather, it serves to fortify the interactions between the polymer components. A similar observation is reported in previous studies on the CS-GL-AgNPs hybrid film (Kumar et al., 2018) , the CSCT/G/AgNPs film (Cao et al., 2020) and P/CH/AgNPs film (Nguyen et al., 2023).

When incorporation of RCM ethanol extract into the CG bioactive composite film, noticeable variations in the relative intensity and band positions were discerned within the resulting RCM-CG bioactive composite film. Particularly, the amide-A band exhibited a slight broadening and shifted from 3300 to 3320 cm^{-1}. This alteration was ascribed to the establishment of hydrogen bonds between the hydroxyl groups of

polyphenols in the RCM ethanol extract and the amino/hydroxyl groups within the CG bioactive composite films (Kan et al., 2019). Moreover, the bands of CG film, encompassing amide-I, amide-II, and amide-III, underwent frequency shifts. They specifically transitioned from 1643 to 1630 cm^{-1}, 1547 to 1540 cm^{-1}, and 1248 to 1240 cm^{-1}, respectively. The alterations in the positions of the amide-I, amide-II, and amide-III bands were attributed to the electrostatic interactions between the amino and carbonyl groups present in the extract, chitosan, and gelatin (Tagrida et al., 2023; A. Zhang et al., 2023). Prior researchers similarly noted comparable findings in their investigations (Xu et al., 2020; S. Yadav et al., 2020).

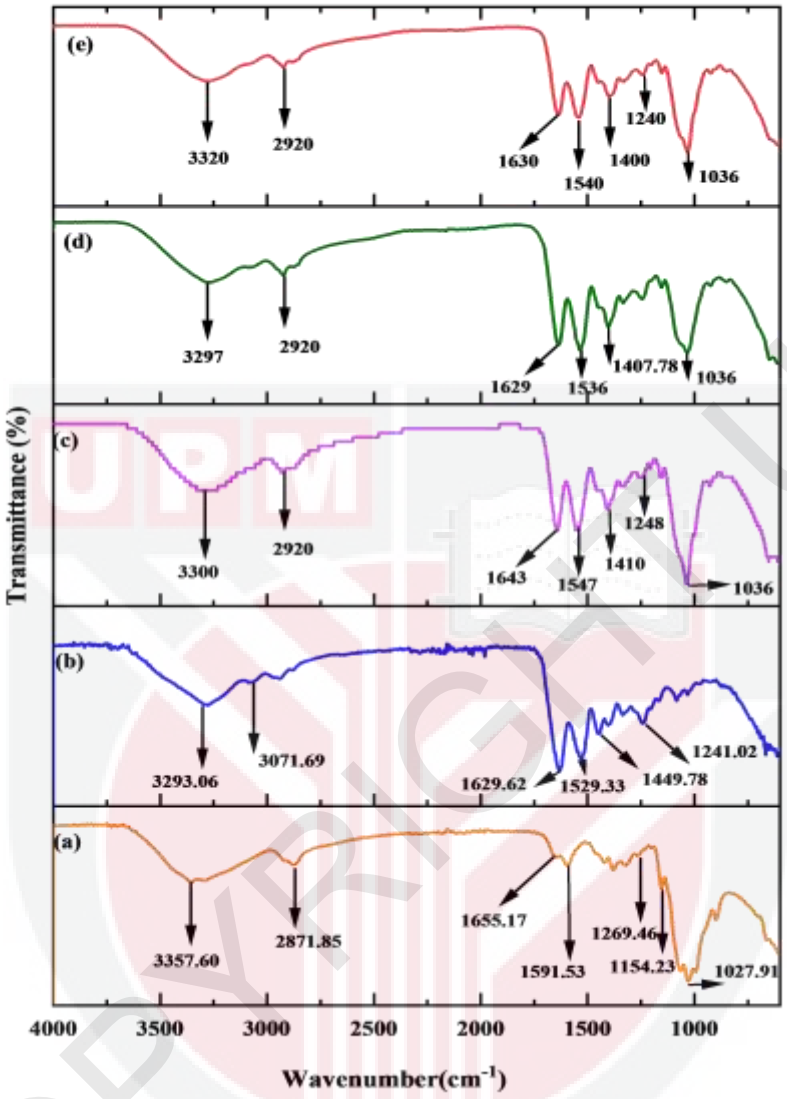

Figure 6.2: FTIR spectra of Chitosan (a), Gelatin (b), CG (c), CG-RCM-AgNPs-4 (d) and CG-RCM-4

6.3.2 X-ray diffraction Analysis (XRD)

Figure 6.3 displays the X-ray diffraction patterns of the fabricated films. From the given data, it is clear that there was a distinct peak at an angle of 20° (2θ). A semi-crystalline structure is present in all of the film samples, based on this observation. The XRD pattern of the CG bioactive composite film shows distinct diffraction peaks at

2θ = 9.47° and 21.78°. These peaks are associated with the triple-helix crystalline structure of gelatin and the regular crystal lattice of chitosan (Luis et al., 2018).

Additionally, there is evidence of an amorphous structure in chitosan and gelatin (A. Zhang et al., 2023). Numerous studies have reported that the characteristic peaks of chitosan and gelatin tend to diminish in intensity when they are combined to form blend films. This phenomenon can be attributed to the development of robust intermolecular interactions between chitosan and gelatin, disrupting their closely packed arrangement required for the formation of well-defined crystalline structure (Kan et al., 2019).

Furthermore, the inclusion of glycerol in the CG film can enhance the flexibility of polymer chains, but it can also reduce the internal cohesion of the matrix, consequently impeding the formation of extended chain arrangements over long distances (Pereda et al., 2011). After the addition of RCM-AgNPs to the film, the XRD peak signals of the CG-RCM-AgNPs bioactive composite film exhibit diffraction peaks at 2θ = 38.1°, 44.14°, 64.4° and 77.3°. These peaks closely align with the diffraction patterns of metallic silver in the face-centered cubic (111), (200), (220), and (311) orientations, as previously outline in our study (Qin et al., 2019). These findings collectively signify the successful incorporation and interactions of RCM-AgNPs into the CG-based bioactive composite films.

The incorporation of RCM 80% ethanol extract resulted in the emergence of small peaks at 2θ = 44.59° within the CG –RCM bioactive composite film. Despite this addition, the degree of crystallization exhibited only a marginal increase when

compared to the CG bioactive composite film. This elucidates the potential systematic alignment of polyphenolic chains resulting from the interactions, both physical and chemical, between the functional constituents and the CG based bioactive composite film. A comparable phenomenon was observed by Arshied Manzoor and colleagues, who introduced *Piper betle* extract into an edible film made of flaxseed gum (Manzoor et al., 2023).

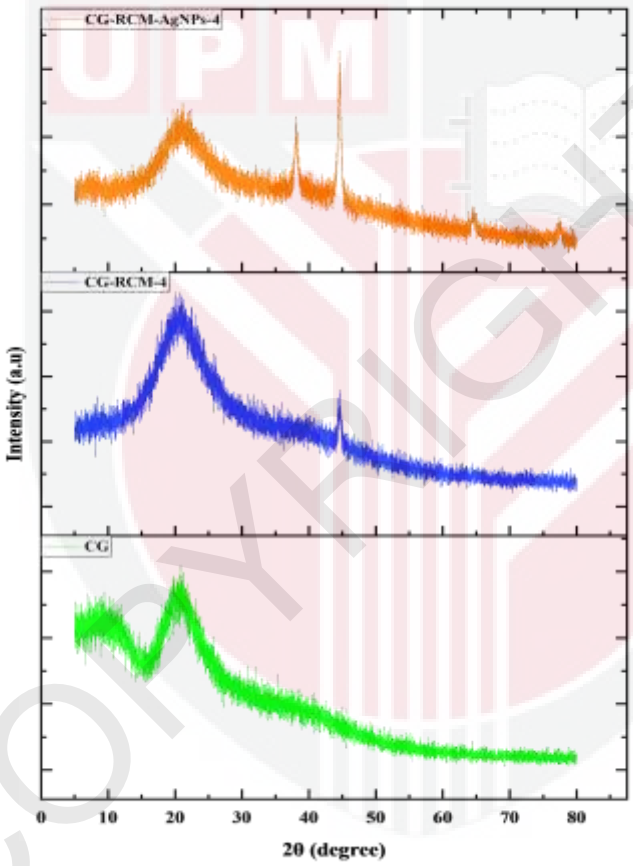

Figure 6.3: X-ray diffraction patterns of the CG, CG-RCM-AgNPs-4 and CG-RCM-4

6.3.3 Thermogravimetric Analysis

The thermal stability of three composite films, namely CG, CG-RCM-4, and CG-RCM-AgNPs-4, was examined through thermogravimetric analysis (TGA). The TGA and DTG thermograms can be found in Figure 6.4. CG-based films undergo thermal degradation in three major steps. In the temperature range of 40 to 140 °C, the initial stage involves the evaporation of water that is physically adsorbed on the film. This process is accompanied by the breaking of hydrogen bonds within and between molecules.

The second stage of weight loss, which happens at temperatures between 140 and 253 °C, is caused by the thermal decomposition of glycerol that is added as a plasticizer (Sul et al., 2023). The most significant decrease in mass occurred during the third stage, between 253 and 500 °C. This decrease was mainly caused by the breakdown and reduction of the biopolymers (chitosan and gelatin). At this stage, the weight loss of the CG-RCM-4 film was lower compared to the CG and CG-RCM-AgNPs-4 films. The decrease in strength can be attributed to the development of more robust hydrogen bonds between the phenolic compounds in RCM 80% ethanol extract and biopolymers or glycerol. Zhang and colleagues discovered that incorporating banana peel extract (BPE) enhances the thermal stability of films made from chitosan (W. Zhang et al., 2020).

The CG film had a maximum degradation temperature of 290°C, while for CG-RCM-AgNPs-4 and CG-RCM-4, the temperatures were 298 and 307°C, respectively. Our XRD results provide additional support for this observation. The internal crystalline

structure of macromolecules plays a crucial role in determining their thermal stability. Increased crystallinity results in enhanced thermal stability as it requires more energy to disrupt the stronger structure (Riaz et al., 2019) . It is worth noting that CG-RCM-AgNPs-4 exhibits slightly lower thermal stability the CG-RCM-4, which may be attributed to the relatively lower concentration of RCM-AgNPs in the CG-RCM-AgNPs-4. Additionally, previous reports have indicated that chitosan films incorporated with tea polyphenols-mediated green-synthesised silver nanoparticles (TP-AgNPs) show decreased thermal stability as the concentration of TP-AgNPs increases (W. Zhang & Jiang, 2020).

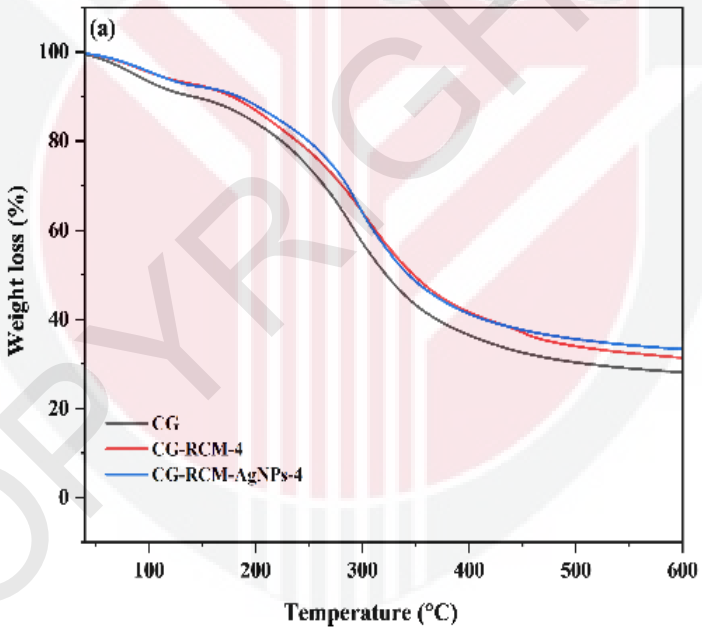

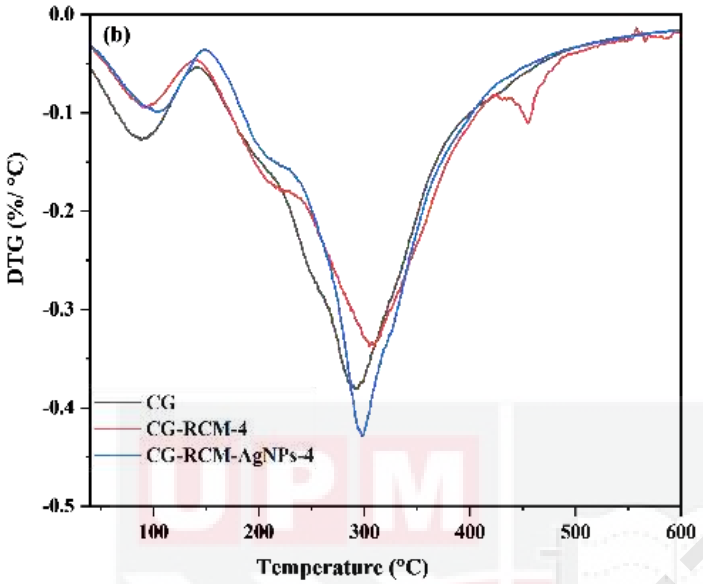

Figure 6.4: TGA (a) and DTG (b) thermograms of CG, CG-RCM-4 and CG-RCM-AgNPs-4 composite films

6.3.4 Antioxidant properties

The antioxidant efficacy of CG, CG-RCM-4, and CG-AgNPs-4 films was assessed using ABTS and DPPH free radical scavenging methods. Figure 6.5 depicts the radical scavenging percentage results. The CG film exhibited the lowest antioxidant properties, with the DPPH and ABTS free radical scavenging activities measuring 17.34 ± 0.36% and 6.05 ± 0.89%, respectively. According to Khan and co-authors, the hydroxyl, amide and carboxyl groups in biopolymers are responsible for the antioxidant capabilities of CG (A. Khan et al., 2023).

The incorporation of RCM-AgNPs increased antioxidant activity within the RCM-AgNPs-4 film when compared to the CG film. This enhancement can be attributed to the utilisation of a plant-mediated method for synthesis of AgNPs, employing RCM

fruit ethanol extract. This method retains polyphenolic compounds that interact with the particles, potentially contributing to the observed effect (Mouzahim et al., 2023). Additionally Yan and colleagues proposed that AgNPs might induce a subtle enhancement in the film's antioxidant activity by either accepting or donating electrons (Qin et al., 2019). After RCM 80% ethanol fruit extract was added to CG, the films' ability to scavenge DPPH and ABTS radicals was noticeably boosted. The polyphenols that released from CG-RCM-4 bioactive composite films were primarily responsible for the film's enhanced antioxidant capabilities. Polyphenols, known for their potent antioxidant properties, exert their effects by donating hydrogen atoms or electrons and effectively neutralizing free radicals, consequently halting lipid peroxidation reactions (Y. Zhang et al., 2023). Similarly, the addition of ethanol extract from Chinese hawthorn fruit to the chitosan and gelatin films led to an enhancement of their antioxidant properties (Kan et al., 2019).

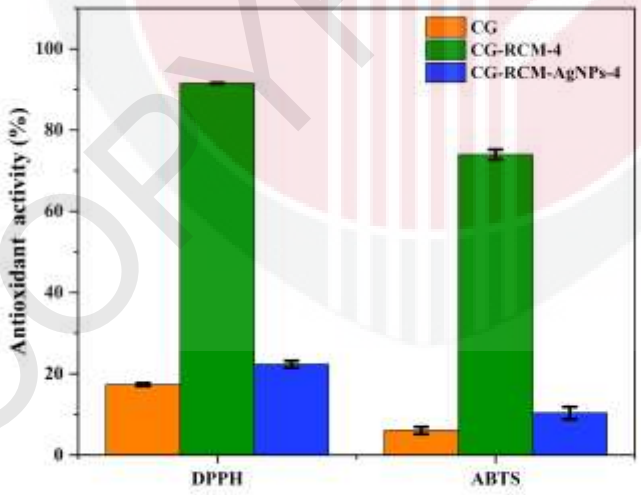

Figure 6.5: Antioxidant activity of the CG, CG-RCM-4 and CG-RCM-AgNPs-composite films determined by $ABTS^{+}$ and DPPH free radical scavenging methods

Note: Data are represented as mean ± standard deviation (n = 3). Letters $^{A, B, C}$ in the same group are statistically significant from each other ($P < 0.05$)

6.3.5 Determination of silver migration

Due to their strong antibacterial qualities, AgNPs inclusion composites have been widely used in many kinds of industries, including pharmaceutical, food, and the environmental (Azizi-Lalabadi et al., 2021). On the other hand, there are serious public health associated with the uncontrolled discharge of Ag from these composites into the ecosystem and food chain (Mouzahim et al., 2023). The European Food Safety Authority (EFSA) has put strict restrictions into place to address this issue, such as limiting the amount of Ag that can migrate from packaging to 0.05mg/kg for food and 0.05mg/L for water (Kumar et al., 2021).

Consequently, ICP-OES was used to quantify the silver migration form the CG-RCM-AgNPs-4 bioactive composite film into deionized water in Figure 6.6. The amount of liberated silver grew as the film soaked longer in the solution. RCM-AgNPs were rapidly released from composite film over the initial 120 hours of the first stage, which produced a concentration of 6 ± 0.2 µg/L in deionized water. The release of RCM-AgNPs from CG-RCM-AgNPs-4 films, however, showed a slower condition after 168 hours. This slowdown may be because RCM-AgNPs connect to the oxygen and nitrogen atoms with plentiful electrons in the ether and amine groups of CG, adding another cross-link to the chain networks.(Ediyilyam et al., 2021). This outcome aligns with the observed water barrier properties and water vapor permeability results. Furthermore, it is consistent with a previous study on Ag+ releases from AgNP/PVA/BNC films (W. Wang et al., 2020), CL2/LAP@AgNPs (Wu et al., 2018).

The final release total amount of silver migration within (336 hrs) 14 days was 7 ± 0.2 µg/L which is not only lower than the limit set by the EFSA but also below the maximum migration of non-approved substances through functional barriers, as stipulated by European Commission. The specified limit is 10 µg/kg (Cheng et al., 2021; H. Li, 2023). The migration of AgNPs depends on the amount incorporated into the bioactive composite film. It's important to note that the efficiency of the film's antimicrobial properties is governed by the concentration of AgNPs. Hence, the presence of RCM-AgNPs in the CG-RCM-AgNPs-4 bioactive composite film not only makes it well-suited for antimicrobial surface coating but also opens up promising opportunities for applications in areas such as food preservation and beyond.

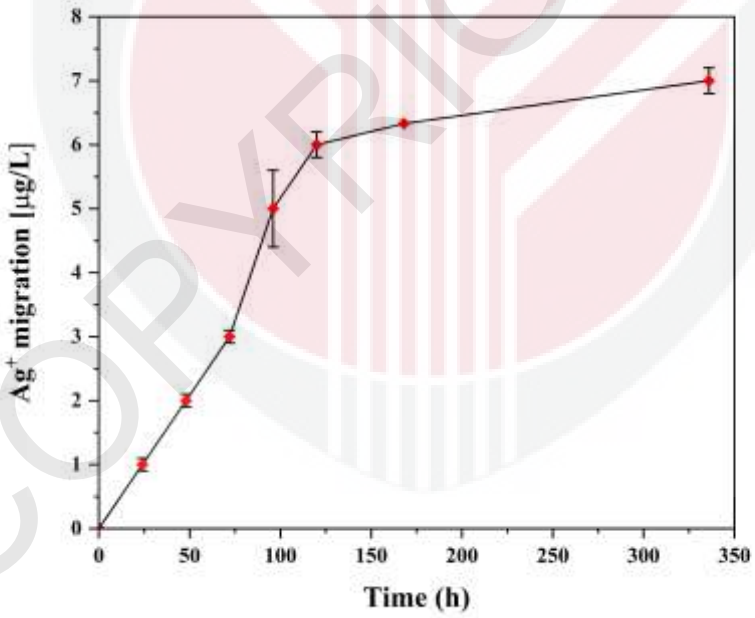

Figure 6.6: The release of Ag from the CG-RCM-AgNPs-4 composite film

6.3.6 Chicken breast Preservation

Figure 6.7 depicts the changes in plate count of chicken meat samples stored under various conditions over a 12-day refrigerated period at 4 ± 1°C. There was a significant increase in chicken meat plate counts from Day 0 to Day 12 ($P < 0.05$). On day 0, the control chicken meat had an average total plate count of 5.398 ± 0.3416 log CFU/g. Following storage in packages with the CG, CG-RCM-4 and CG-RCM-AgNPs-4 bioactive composite films, the total plate counts decreased to around 4.706 ± 0.0441, 4.435 ± 0.4374, and 4.369 ± 0.04067 log CFU/g on day 0, respectively. After 6 days of storage, the total plate counts in the control and CG bioactive composite film-treated chicken meat exceeded 6 log CFU/g, while those in the CG-RCM-4 and CG-RCM-AgNPs-4 treated samples were 5.487 ± 0.0738 and 5.261 ± 0.3159 log CFU/g, respectively. After 12 days of storage, the total plate counts in the treated samples was 6.913 ± 0.0673 and 6.306 ± 0.0415 log CFU/g for CG-RCM-4 and CG-RCM-AgNPs-4, respectively. This count was notably lower than that of the CG and control treated samples. This shows that the packaging of RCM 80% ethanol extract and RCM synthesis of silver nanoparticles in bioactive composite films had a notable antibacterial impact.

After storage, the total plate counts in the control and CG-treated samples were 8.970 ± 0.1341 and 7.213 ± 0.6754 log CFU/g, respectively. The International Commission on Microbiological Specification for Food (ICMSF) defines the acceptable limit for the total counts of good-quality poultry meat products as 7 log CFU/g (Rahnemoon et al., 2021). After 9 and 12 days, the total counts of the control and CG composite films exceeded the defined range. On the other hand, the samples wrapped in CG-RCM-4

and CG-RCM-AgNPs-4 met the microbiological standards after 12 days of storage. The bioactive composite films CG-RCM-4 and CG-RCM-AgNPs-4 have demonstrated an impressive capacity to inhibit bacterial colonisation on surfaces due to the antibacterial properties of RCM ethanol plant extract and RCM-AgNPs. Consequently, the total plate counts increase rate in fresh chicken meat covered with these films was notably lower in comparison to what was seen with the control and CG films.

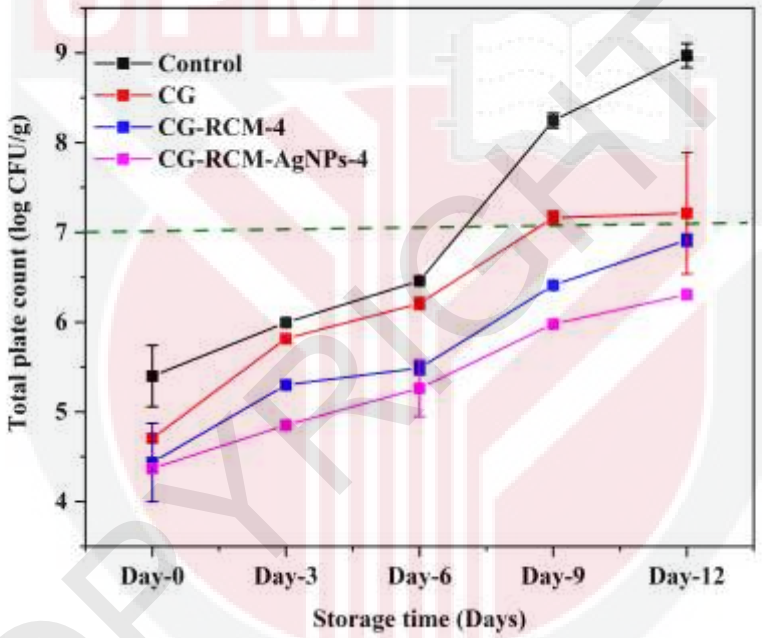

Figure 6.7: Total plate counts of chicken breast placed in control, CG, CG-RCM-4 and CG-RCM-AgNPs-4 bioactive composite films during refrigerated storage for 12 days

6.3.7 Colour measurement

The colour properties of food products significantly impact their overall look and consumer reception. The colour factors (L*, a*, and b*) of chicken meat treated with bioactive composite are presented in Table 6.1. The L* value of all samples exhibited a decline as the storage duration increased ($P < 0.05$). L* values of control, CG, CG-RCM-4 and CG-RCM-AgNPs-4 diminished from 52.133 ± 1.101 at day 0 to 36.033 ± 0.665, 38.36 ± 0.32, 39.7 ± 0.26 and 40.43 ± 0.75 at day 12 for the chicken meats packaged with these bioactive composite films, respectively. The reduction in lightness suggests that the meat of the chicken breast darkened while being stored. The findings on lightness were consistent with previous research that reported a decline in the lightness of chicken meat after storage, as mentioned by Takam and co-authors (Takma & Korel, 2019).

The a* values of chicken meat samples decreased significantly ($P < 0.05$) during storage. On day 12, the a* values of samples without wrap (2.46 ± 0.057) and CG films (2.733 ± 0.057) significantly decreased. CG-RCM-4 (3.1 ± 0.1) and CG-RCM-AgNPs-4 (3.533 ± 0.05) wrapped chicken meat retains a* values better than control and CG films-treated chicken meat colour. Protein breakdown within the muscle could explain the drop in L* and a* values observed in all chicken meats that had darkened on the twelfth day of storage. Furthermore, the darkening of the chicken meats may result from a decrease in the oxygen concentration in the surface tissue, which is induced by the proliferation of microorganisms (Aziman et al., 2021). According to Badee and co-authors, adding marjoram essential oil, a natural antibacterial, to raw chicken drumstick dipping treatments, resulted in a significant reduction in colour loss of the

meat during refrigerated storage for a period of 12 days (Badee et al., 2013). For the values of parameter b* showed the same trend.

Table 6.1: Color parameters of wrapped chicken meat samples with bioactive composite films during storage time at 4 ± 1°C

Storage time (Days)	Bioactive composite films	L*	a*	b*
0	Control	52.133± 1.101^{A}	7.766 ± 0.81^{A}	19.76 ± 0.81^{A}
	CG	52.133 ± 1.101^{A}	7.766 ± 0.81^{A}	19.76 ± 0.81^{A}
	CG-RCM-4	52.133 ± 1.101^{A}	7.766 ± 0.81^{A}	19.76 ± 0.81^{A}
	CG-AgNPs-4	52.133 ± 1.101^{A}	7.766 ± 0.81^{A}	19.76 ± 0.81^{A}
3	Control	44.33 ± 0.28^{D}	4.1 ± 0.1^{D}	15.566±0.23^{E}
	CG	45.3 ± 0.85^{D}	4.53 ± 0.57^{C}	16.66 ± 0.23^{D}
	CG-RCM-4	46.57 ± 1.19^{C}	5.2 ± 0.1^{C}	17.66 ± 0.11^{C}
	CG-AgNPs-4	48.2 ± 0.62^{B}	6.266 ± 0.45^{B}	18.733 ± 0.4^{B}
6	Control	41.867 ± 0.41^{F}	3.13 ± 0.057^{E}	13.63±0.208^{G}
	CG	42.567 ± 0.31^{E}	3.433± 0.577^{E}	14.6 ± 0.172^{F}
	CG-RCM-4	43.167 ± 0.288^{E}	3.733 ± 0.115^{D}	16.36 ± 0.115^{D}
	CG-AgNPs-4	43.7± 0.1^{E}	4.333 ± 0.49^{D}	17.56 ± 0.2^{C}
9	Control	39.133 ± 0.513^{H}	2.866 ± 0.057^{F}	12.533 ± 0.11^{H}
	CG	40.2 ± 0.62^{G}	3.1 ± 0.1^{E}	13.43 ± 0.4^{G}
	CG-RCM-4	41.6 ± 0.1^{F}	3.3 ^{E}	15.133 ± 0.2^{E}
	CG-AgNPs-4	41.4 ± 0.26^{F}	3.767 ± 0.057^{D}	16.5 ± 0.26^{D}
12	Control	36.033 ± 0.665^{I}	2.46 ± 0.057^{F}	11.43 ± 0.208^{I}
	CG	38.36 ± 0. 32^{H}	2.733 ± 0.057^{F}	12.4 ± 0.2^{H}
	CG-RCM-4	39.7 ± 0.26^{G}	3.1 ± 0.1^{E}	13 ± 0.26^{G}
	CG-AgNPs-4	40.43 ± 0.75^{G}	3.533 ± 0.05^{E}	14.73 ± 0.65^{F}

Note: All data are presented as mean ± standard deviation (n=3). Means with different letters ^{A,B,C,D} in the same column are significantly different at $p < 0.05$ according to LSD

6.3.8 pH measurement

Figure 6.8 displays the pH variations of fresh chicken meat samples during 4 ± 1°C storage with control, CG, CG-RCM-4, and CG-RCM-AgNPs-4 wrapping. The sample started with a pH of 5.85. After 12 days of storage, the control and CG composite film wrapped with chicken samples had significantly high values of 6.62 ± 0.005 and 6.45 ± 0.04, respectively ($P < 0.05$). The increase in pH of chicken samples can be attributed

to bacterial decomposition of proteins, amino acids, and other components, which results in the production of amine metabolites (Huang et al., 2020; Y. Liu et al., 2022). On the 12th day, the pH of CG-RCM-4 and CG-RCM-AgNPs-4 wrapped chicken ranged from 5.85 ± 0.08 to 6.20 ± 0.005. This shows a lower pH value compared to the control and CG significantly ($P < 0.05$). It is possible that RCM fruit ethanol extracts containing antibacterial and antioxidant properties, including phenolic compounds, gallic acid, and silver nanoparticles, inhibit microbial growth and delay protein oxidation, resulting in decreased pH values (Majumder et al., 2023). Past research by Nemkul and colleagues has documented the antioxidant and antibacterial properties of RCM fruit extract. The results indicate that the bioactive composite films show great potential in resisting oxidation and preserving chicken meat throughout storage (Nemkul et al., 2021).

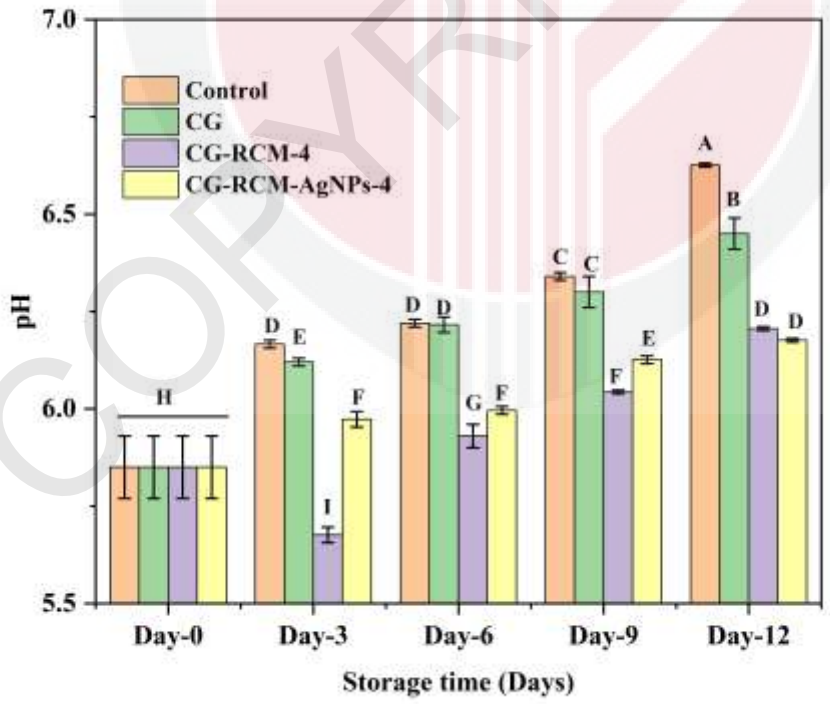

Figure 6.8: pH parameters of wrapped chicken meat samples with bioactive composite films during storage time at 4 ±1°C. Different letters $^{A, B, C, D}$ indicated significant differences between different group ($P < 0.05$) according to LSD

6.4 Conclusion

The CG, CG-RCM-4, and CG-RCM-AgNPs-4 bioactive composite films were characterised through FTIR, XRD, and SEM analysis. The study also included an evaluation of their antioxidant properties, thermal stability, and the assessment of silver migration from the RCM-AgNPs-4 film. The results indicate promising possibilities for enhancing the new CG-RCM-AgNPS-4 films, which demonstrated minimal silver release while still maintaining antimicrobial properties. Given the physicochemical and biological characteristics of CG-RCM-4 and CG-RCM-AgNPs-4, these composite films can be effectively used as antioxidant and antimicrobial active films. Furthermore, the study on chicken meat treated with these bioactive composite films demonstrated that CG-RCM-4 and CG-RCM-AgNPs-4 can improve the quality of chicken meat. This was achieved by reducing colour variation, slowing pH increase, and maintaining total plate counts below 7 log CFU/g at 4°C for 12 days. In summary, the bioactive composite films CG-RCM-4 and CG-RCM-AgNPs-4 not only improve the antibacterial effectiveness of the films but also decrease the potential silver nanoparticles release risk.

CHAPTER 7

CONCLUSION AND RECOMMENDATIONS

7.1 Summary and conclusion

In this study, researchers discovered that the extract of *Rhus chinensis* Mill. fruit, when using 80% methanol, 80% ethanol, and an aqueous solvent, exhibited greater potential as a bioactive agent than the extract of *Acacia concinna* (Willd) DC. pods. The fruit extract from RCM exhibited stronger antibacterial activity, with inhibition zones ranging from 8.46 ± 0.30 to 10.53 ± 0.25 mm against *E.coli* (Gram-negative) and from 6.51 ± 0.20 to 11.86 ± 0.72 mm for *S.aureus* (Gram-positive). Furthermore, 80% methanol and 80% ethanol RCM fruit extracts exhibited significantly greater antioxidant activities ($ABTS^{+}$ and DPPH) and TPC compared to RCM fruit aqueous extract, even with its lowest extraction yield percent (10.16%). The RCM fruit 80% ethanol extracts showed the highest antimicrobial efficacy, with MBC values of 0.391 mg/ml for *S.aureus* and 1.563 mg/ml for *E.coli*. Based on the GCMS analysis of the ethanol extract RCM, the primary phytochemical components include malic acid (32.96%), pyrogallol (15.39%), 2, 5-Furandione, 3-methyl (10.15%), palmitic acid (6.72%), and linoleic acid (5.40%). The RCM 80% ethanol extract was selected as the bioactive agent for creating silver nanoparticles via plant-mediated synthesis and embedding them into CG-based composite films.

The plant-mediated synthesis of silver nanoparticles utilised six different parameters related to temperature and pH, with RCM 80% ethanol extract serving as a reducing

and stabilising agent. Among the six parameters, RCM-AgNPs produced at pH7 and 80°C were chosen for their distinct shape peaks, strong intensity in UV-visible spectroscopy, small particle size, low PDI values, high stability, and antibacterial properties. The TEM results showed that the particle sizes ranged from 7 to 30 nm and were spherical. FTIR analysis showed that the biomolecules in the plant extract mainly functioned as reducing and stabilising agents in the synthesis of AgNPs. The XRD confirmed the crystalline nature of RCM-AgNPs, while the EDX revealed a dominant Ag peak at 3.0 kV, confirming the elemental composition of RCM-AgNPs. In addition, the MIC and MBC values against *E.coli* and *S.aureus* varied from 39 to 156 µg/ml. In the cytotoxicity assessment utilising the 3T3 cell line, RCM-AgNPs exhibited no toxic effects at a concentration of 20 µg/ml. Under specific conditions, the modulation of the quantity and release rate of RCM-AgNPs must be meticulously evaluated, particularly for food preservation purposes.

Two types of novel natural composite films were successfully developed using ultrasound treatment, incorporating varying ratios of RCM ethanol extract (0.1%, 0.2%, 0.4% and 0.8%) and RCM-AgNPs (0.01%, 0.02%, 0.04%, and 0.08%) into chitosan-gelatin. The presence of 80% ethanol RCM extracts or RCM-AgNPs may potentially interact with the film matrix via hydrogen bonding and electrostatic interactions, leading to a denser inner microstructure in the films. Among the CG-RCM composite films, CG-RCM-4 (0.8%) has not only the lowest WVP value but also the highest thickness, the lowest moisture content and WS ($P < 0.05$). The CG-RCM-2 (0.2%) exhibited better mechanical properties (TS = 49.58 ± 4.33, EAB = 25.48 ± 0.97) but the CG-RCM-4 (TS = 62.32 ± 2.33, EAB = 7.38 ± 0.19) exhibited effectiveness against *S.aureus* (15.32 ± 1.12 mm). In the CG-RCM-AgNPs composite

films, CG-RCM-AgNPs-4 (0.08%) shows notable improvements in thickness, moisture content, and water solubility. However, the WVP value remains unaffected, even though it is the lowest among the CG-RCM-AgNPs composite films. SEM analysis revealed that the composite films of CG-RCM-4 and CG-RCM-AgNPs-4 exhibited a dense and compact structure, despite the presence of particle agglomerations. The CG-RCM-AgNPs-1 of mechanical properties has the highest value (TS = 64.15 ± 1.82, EAB = 6.21 ± 1.33) but CG-RCM-AgNPs-4 (TS = 9.46 ± 0.27, EAB = 30.98 ± 1.62) has the highest inhabitation zone of *S.aureus* (10.66 ± 0.32 mm) and *E.coli* (10.15 ± 0.17 mm). Based on antimicrobial and barrier properties, CG-RCM-4 and CG-RCM-AgNPs-4 were selected for further characterisation and application.

The selected CG, CG-RCM-4, and CG-RCM-AgNPs-4 bioactive composite films were characterised by FTIR, XRD, and SEM analysis, as well as antioxidant properties, thermal stability, and silver migration from the RCM-AgNPs-4 film. Over 14 days, the cumulative silver migration was 7 ± 0.2 µg/L. This quantity is not only lower than the EFSA limit but also stays under the maximum migration threshold for non-approved substances set by the European Commission, which is 10 µg/kg. These findings suggest promising potential for optimising the novel CG-RCM-AgNPs-4 films, which displayed low silver release while retaining antimicrobial activity. Considering the physicochemical and biological properties of CG-RCM-4 and CG-RCM-AgNPs-4, these composite films can be effectively utilised as antioxidant and antimicrobial active films. Furthermore, the results of chicken meat treated with these bioactive composite films demonstrated that CG-RCM-4 and CG-RCM-AgNPs-4 can improve chicken meat quality by minimising colour variation, slowing pH increment,

and maintaining a total plate counts of less than 7 log CFU/g at 4 °C for 12 days. In conclusion, the CG-RCM-4 and CG-RCM-AgNPs-4 bioactive composite films may not only improve antibacterial efficiency but also reduce the risk of silver nanoparticle release.

Lastly, this investigation offers valuable insights into the selection of appropriate organic solvents and extraction techniques, as well as the optimisation of conditions for the synthesis of silver nanoparticles through plant-mediated methods using *Rhus chinensis* Mill. Furthermore, the proper proportions of RCM-AgNPs (0.08%) ensure that the antimicrobial effectiveness is maintained while minimising silver release. The findings indicate that RCM-AgNPs and RCM 80% ethanol extract could be effective antioxidants and antibacterial agents in food preservation. This step helps to reduce food waste and synthetic plastics.

7.2 Recommendations

Based on the findings of this study, a few recommendations are made as follows:

1. The response of chitosan-gelatin nanocomposites in the human body is anticipated to be significantly different from that of chitosan and gelatin. Cell viability and release from the composites can be influenced by the nanoparticles in the composites as time progresses. The covalent and non-covalent interactions between nanoparticles and chitosan-gelatin matrix must be understood to figure out the issues related to long term stability of nanoparticles within the matrix. Comprehensive research based upon biodistribution, biocompatibility and long-term cytotoxicity analysis of chitosan-gelatin nanocomposites are required to investigate their potential for biomedical application in depth.

2. The promising potential of chitosan gelatin nanocomposites can be enhanced by extensive research that concentrates on in-vivo studies, as the majority of the related work has been restricted to the in-vitro stage of development.

Additional clinical research is required to comprehend the intricate chemistry and biology of the chitosan-gelatin nanocomposite materials.

3. The economic feasibility of the production of chitosan-gelatin nanocomposites for their large-scale applications must also be taken into account.

4. Recommend conducting wettability and permeability studies for future research to enhance understanding and applicability.

REFERENCES

Abdollahzadeh, E., Nematollahi, A., & Hosseini, H. (2021). Composition of antimicrobial edible films and methods for assessing their antimicrobial activity : A review. *Trends in Food Science & Technology*, *110*(January), 291–303.

Ajesh, V., Pravitha, M., Yadav, A., & Pandiselvam, R. (2023). Influence of ultrasonic application on soybean aqueous extract based composite edible film : Characterization and their food application. *Food Hydrocolloids*, *135*(July 2022), 108210.

Al-maqtari, Q. A., Ali, A., Al-gheethi, S., Ghaleb, A. D. S., Ali, A., Al-ansi, W., Essam, A., Al-adeeb, A., Du, Y., Wei, M., & Yao, W. (2022). Fabrication and characterization of chitosan/gelatin films loaded with microcapsules of *Pulicaria jaubertii* extract. *Food Hydrocolloids*, *129*(March).

Alfian, G., Syafrudin, M., Farooq, U., Ma'arif, M. R., Syaekhoni, M. A., Fitriyani, N. L., Lee, J., & Rhee, J. (2020). Improving efficiency of RFID-based traceability system for perishable food by utilizing IoT sensors and machine learning model. *Food Control*, *110*(November 2019).

Alirezalu, K., Pateiro, M., Yaghoubi, M., Alirezalu, A., Hadi, S., & Lorenzo, J. M. (2020). Phytochemical constituents , advanced extraction technologies and techno- functional properties of selected Mediterranean plants for use in meat products . A comprehensive review. *Trends in Food Science & Technology*, *100*(March), 292–306.

Alkhulaifi, M. M., Alshehri, J. H., Alwehaibi, M. A., Awad, M. A., Al-enazi, N. M., Aldosari, N. S., Hatamleh, A. A., & Raouf, N. A.-. (2020). Green synthesis of silver nanoparticles using *Citrus limon* peels and evaluation of their antibacterial and cytotoxic properties. *Saudi Journal of Biological Sciences*, *27*, 3434–3441.

Alomar, T. S., Almasoud, N., Awad, M. A., & El-tohamy, M. F. (2020). An eco-friendly plant-mediated synthesis of silver nanoparticles : Characterization , pharmaceutical and biomedical applications. *Materials Chemistry and Physics*, *249*(April), 123007.

Amjadi, S., Emaminia, S., Davudian, S. H., Pourmohammad, S., Hamishehkar, H., & Roufegarinejad, L. (2019). Preparation and characterization of gelatin-based nanocomposite containing chitosan nanofiber and ZnO nanoparticles. *Carbohydrate Polymers*, *216*(March), 376–384.

Amooaghaie, R., Reza, M., & Azizi, M. (2015). Synthesis , characterization and biocompatibility of silver nanoparticles synthesized from *Nigella sativa* leaf extract in comparison with chemical silver nanoparticles. *Ecotoxicology and*

Environmental Safety, *120*(October 2021), 400–408.

An, J., Nie, Y., Shi, C., & Li, W. (2023). Treatment of colorectal , gastric , and pancreatic cancers by silver nanoparticles green-formulated using a medicinal plant. *Inorganic Chemistry Communications*, *158*(P1), 111416.

Anand, S. P., & Sati, N. (2013). Artificial Preservatives and Their Harmful Effects: Looking Toward Nature for Safer Alternatives. *International Journal of Pharmaceutical Sciences and Research IJPSR*, *4*(7), 2496–2501.

Arokiyaraj, S., Arasu, M. V., Vincent, S., Prakash, N. U., Choi, S. H., Oh, Y. K., Choi, K. C., & Kim, K. H. (2014). Rapid green synthesis of silver nanoparticles from chrysanthemum indicum land its antibacterial and cytotoxic effects: An in vitro study. *International Journal of Nanomedicine*, *9*(1), 379–388.

Arumai Selvan, D., Mahendiran, D., Senthil Kumar, R., & Kalilur Rahiman, A. (2018). Garlic, green tea and turmeric extracts-mediated green synthesis of silver nanoparticles: Phytochemical, antioxidant and in vitro cytotoxicity studies. *Journal of Photochemistry and Photobiology B: Biology*, *180*(October 2017), 243–252.

Aryan, Ruby, & Mehata, M. S. (2021). Green synthesis of silver nanoparticles using *Kalanchoe pinnata* leaves (life plant) and their antibacterial and photocatalytic activities. *Chemical Physicas Letters*, *778*(April).

Ashique, S., Upadhyay, A., Hussain, A., Bag, S., & Chaterjee, D. (2022). Green biogenic silver nanoparticles , therapeutic uses , recent advances , risk assessment , challenges , and future perspectives. *Journal of Drug Delivery Science and Technology*, *77*(September).

Avila-sosa, R., Palou, E., Teresa, M., Munguía, J., Nevárez-moorillón, G. V., Rhode, A., Cruz, N., & López-malo, A. (2012). Antifungal activity by vapor contact of essential oils added to amaranth , chitosan , or starch edible films. *International Journal of Food Microbiology*, *153*, 66–72.

Aziman, N., Jawaid, M., Mutalib, N. A. A., Yusof, N. L., Nadrah, A. H., Nazatul, U. K., Tverezovskiy, V. V., Tverezovskaya, O. A., Fouad, H., Braganca, R. M., Baker, P. W., Selbie, S., & Ali, A. (2021). Antimicrobial potential of plastic films incorporated with sage extract on chicken meat. *Foods*, *10*(11), 1–15.

Azizi-Lalabadi, M., Garavand, F., & Jafari, S. M. (2021). Incorporation of silver nanoparticles into active antimicrobial nanocomposites: Release behavior, analyzing techniques, applications and safety issues. *Advances in Colloid and Interface Science*, *293*.

Azmana, M., Mahmood, S., Hilles, A. R., Rahman, A., Arifin, M. A. Bin, & Ahmed,

S. (2021). A review on chitosan and chitosan-based bionanocomposites: Promising material for combatting global issues and its applications. *International Journal of Biological Macromolecules*, *185*(June), 832–848.

Badee, A. Z. ., Moawad, R. K., Elnoketi, M. M., & Gouda, M. M. (2013). Improving the Quality and Shelf-Life of Refrigerated Chicken Meat by Marjoram. *Journal of Applied Science Research*, *9*(11), 5718–5729.

Bao, Y., He, J., Song, K., Guo, J., Zhou, X., & Liu, S. (2021). Plant-Extract-Mediated Synthesis of Metal Nanoparticles. *Journal of Chemisry*, *2021*, 143–199.

Bathmanathan, V., Rajadurai, J., & Alahakone, R. (2023). What a waste ? An experience in a secondary school in Malaysia of a food waste management system (FWMS). *Heliyon*, *9*(10), e20327.

Bharath, B., Perinbam, K., & Devanesan, S. (2021). Evaluation of the anticancer potential of Hexadecanoic acid from brown algae Turbinaria ornata on HT – 29 colon cancer cells. *Journal of Molecular Structure*, *1235*, 130229.

Biswal, A. K., & Pramila, P. K. (2020). Biosynthesis and characterization of silver nanoparticles for prospective application in food packaging and biomedical fields. *Materials Chemistry and Physics*, *250*(March), 123014.

Bonilla, J., & Sobral, P. J. A. (2016). Investigation of the physicochemical, antimicrobial and antioxidant properties of gelatin-chitosan edible film mixed with plant ethanolic extracts. *Food Bioscience*, *16*, 17–25.

Bonilla, J., & Sobral, P. J. A. (2018). Original article Gelatin-chitosan edible film activated with Boldo extract for improving microbiological and antioxidant stability of sliced Prato cheese. *International Journal of Food Science and Technology*, *2017*, 1–8.

Cao, W., Yan, J., Liu, C., Zhang, J., Wang, H., Gao, X., Yan, H., Niu, B., & Li, W. (2020). Preparation and characterization of catechol-grafted chitosan/gelatin/modified chitosan-AgNP blend films. *Carbohydrate Polymers*, *247*(April), 116643.

Carbone, M., Tommasa, D., & Sabbatella, G. (2016). Silver nanoparticles in polymeric matrices for fresh food packaging. *Journal of King Saud University - Science*, *28*(4), 273–279.

Carson, L., Bandara, S., Joseph, M., Green, T., Grady, T., Osuji, G., Weerasooriya, A., Ampim, P., & Woldesenbet, S. (2020). Green Synthesis of Silver Nanoparticles with Antimicrobial Properties Using *Phyla dulcis* Plant Extract. *Foodborne*

Pathogens and Disease, *17*(7), 1–8.

Chemat, F., Vian, M. A., Ravi, H. K., Khadhraoui, B., Hilali, S., Perino, S., & Tixier, A. F. (2019). Review of Alternative Solvents for Green Extraction of Food and Natural Products : Panorama , Principles , Applications and Prospects. *Molecules*.

Cheng, J., Lin, X., Wu, X., Liu, Q., Wan, S., & Zhang, Y. (2021). Preparation of a multifunctional silver nanoparticles polylactic acid food packaging film using mango peel extract. *International Journal of Biological Macromolecules*, *188*(March), 678–688.

Chhetri, D. R., Mahanta, J., Chettri, A., & Pradhan, A. (2020). Phytochemical and antioxidant attributes of *Rhus chinensis* Mill., an edible wild fruit from Sikkim Himalaya. *Jour Pl Sci Res*, *36*, 163–172.

Chouhan, S., & Guleria, S. (2020). Green synthesis of AgNPs using *Cannabis sativa* leaf extract: Characterization, antibacterial, anti-yeast and α-amylase inhibitory activity. *Materials Science for Energy Technologies*, *3*, 536–544.

Dhaka, A., Chand Mali, S., Sharma, S., & Trivedi, R. (2023). A review on biological synthesis of silver nanoparticles and their potential applications. *Results in Chemistry*, *6*(March), 101108.

Djakpo, O., & Yao, W. (2010). Rhus chinensis and Galla Chinensis - Folklore to modern evidence: Review. *Phytotherapy Research*, *24*(12), 1739–1747.

Duan, C., Meng, X., Meng, J., Khan, M. I. H., Dai, L., Khan, A., An, X., Zhang, J., Huq, T., & Ni, Y. (2019). Chitosan as A Preservative for Fruits and Vegetables: A Review on Chemistry and Antimicrobial Properties. *Journal of Bioresources and Bioproducts*, *4*(1), 11–21.

Dudnyk, I., Janeček, E. R., Vaucher-Joset, J., & Stellacci, F. (2018). Edible sensors for meat and seafood freshness. *Sensors and Actuators, B: Chemical*, *259*, 1108–1112.

Ediyilyam, S., George, B., Shankar, S. S., Dennis, T. T., Waclawek, S., Cernik, M., & Padil, V. V. . (2021). Chitosan / Gelatin / Silver Nanoparticles Composites Films for Biodegradable Food Packaging Applications. *Polymers*.

Ettadili, F. E., Aghris, S., Laghrib, F., Farahi, A., Saqrane, S., Bakasse, M., Lahrich, S., & El Mhammedi, M. A. (2022). Recent advances in the nanoparticles synthesis using plant extract: Applications and future recommendations. *Journal of Molecular Structure*, *1248*, 131538.

Felter, S. P., Zhang, X., & Thompson, C. (2021). Butylated hydroxyanisole: Carcinogenic food additive to be avoided or harmless antioxidant important to protect food supply? *Regulatory Toxicology and Pharmacology*, *121*.

Gacem, M. A., Telli, A., Gacem, H., & Ould-El-Hadj-Khelil, A. (2019). Phytochemical screening, antifungal and antioxidant activities of three medicinal plants from *Algerian steppe* and *Sahara* (preliminary screening studies). *SN Applied Sciences*, *1*(12).

Ghaderi, J., Fakhreddin, S., Keyvani, N., & Gómez-guillén, M. C. (2019). Polymer blending effects on the physicochemical and structural features of the chitosan / poly (vinyl alcohol)/ fish gelatin ternary biodegradable films. *Food Hydrocolloids*, *95*(April), 122–132.

Gomez, A., Prokhorov, E., Luna-barcenas, G., Mendoza, S., Rojas-ch, H., Hern, J., & Rom, R. (2021). Chitosan-hydroxyapatite-MWCNTs nanocomposite patch for bone tissue engineering applications. *Materials Today Communications*, *28*(July).

Gu, B., Jiang, Q., Luo, B., Liu, C., Ren, J., Wang, X., & Wang, X. (2021). A sandwich-like chitosan-based antibacterial nanocomposite film with reduced graphene oxide immobilized silver nanoparticles. *Carbohydrate Polymers*, *260*(February), 117835.

Gudimalla, A., Jose, J., Jose, R., & Sabu, V. (2021). Green Synthesis of Silver Nanoparticles Using *Nymphae odorata* Extract Incorporated Films and Antimicrobial Activity. *Journal of Polymers and the Environment*, *May*.

Gupta, M., Thakur, S., Sharma, A., & Gupta, S. (2013). Qualitative and Quantitative Analysis of Phytochemicals and Pharmacological Value of Some Dye Yielding Medicinal Plants. *Oriental Journal of Chemistry*.

Haghighi, H., Biard, S., Bigi, F., De Leo, R., Bedin, E., Pfeifer, F., Siesler, H. W., Licciardello, F., & Pulvirenti, A. (2019). Comprehensive characterization of active chitosan-gelatin blend films enriched with different essential oils. *Food Hydrocolloids*, *95*(February), 33–42.

Hajji, S., Kchaou, H., Bkhairia, I., Ben, R., Salem, S., Boufi, S., & Nasri, M. (2021). Conception of active food packaging films based on crab chitosan and gelatin enriched with crustacean protein hydrolysates with improved functional and biological properties. *Food Hydrocolloids*, *116*(January).

Han, J. W., Ruiz-Garcia, L., Qian, J. P., & Yang, X. T. (2018). Food Packaging: A Comprehensive Review and Future Trends. *Comprehensive Reviews in Food Science and Food Safety*, *17*(4), 860–877.

Hanani, Z. A. N., Yee, F. C., & Nor-khaizura, M. A. R. (2019). Effect of pomegranate (*Punica granatum* L .) peel powder on the antioxidant and antimicrobial properties of fish gelatin films as active packaging. *Food Hydrocolloids*, *89*(June 2018), 253–259.

Hashemitabar, G., Aflakian, F., & Sabzevar, A. H. (2023). Assessment of antibacterial , antioxidant , and anticancer effects of biosynthesized silver nanoparticles using *Teucrium polium* extract. *Journal of Molecular Structure*, *1291*(June).

Hauser, C., Thielmann, J., & Muranyi, P. (2016). *Organic Acids : Usage and Potential in Antimicrobial Packaging*. *Ivv*.

Heirangkhongjam, D. M., & Iboyaima, S. N. (2021). *Rhus chinensis* Mill.: A medicinal plant with promising inhibition of calcium oxalate crystallization , an in-vitro study. *Journal of Herbal Medicine*, *29*(July), 100489.

Heirangkhongjam, M. D., & Ngaseppam, I. S. (2019). Nutritional evaluation of *rhus chinensis* Mill. (Heimang) and development of value added products. *Indian Journal of Traditional Knowledge*, *18*(1), 16–24.

Heymich, M., Friedlein, U., Trollmann, M., & Schwaiger, K. (2021). Generation of antimicrobial peptides Leg1 and Leg2 from chickpea storage protein , active against food spoilage bacteria and foodborne pathogens. *Food Chemistry*, *347*(December 2020).

Hinokidani, K., Aoki, R., Inoue, T., Irie, M., & Nakanishi, Y. (2022). Usability of mangrove plant leaves as tea materials : A comparison study on phenolic content and antioxidant capacities with commercial teas. *Biocatalysis and Agricultural Biotechnology*, *40*(January), 102307.

Hu, H., Yao, X., Qin, Y., Yong, H., & Liu, J. (2020). Development of multifunctional food packaging by incorporating betalains from vegetable amaranth (*Amaranthus tricolor L* .) into quaternary ammonium chitosan / fish gelatin blend films. *International Journal of Biological Macromolecules*, *159*, 675–684.

Huang, M., Wang, H., Xu, X., Lu, X., Song, X., & Zhou, G. (2020). Effects of nanoemulsion-based edible coatings with composite mixture of rosemary extract and ε -poly- L -lysine on the shelf life of ready-to-eat carbonado chicken. *Food Hydrocolloids*, *102*(September 2019), 105576.

Huie, C. W. (2002). A review of modern sample-preparation techniques for the extraction and analysis of medicinal plants. *Analytical and Bioanalytical Chemistry*, *373*(1–2), 23–30. https://doi.org/10.1007/s00216-002-1265-3

Jing, W., Xiaolan, C., Yu, C., Feng, Q., & Haifeng, Y. (2022). Pharmacological effects and mechanisms of tannic acid. *Biomedicine & Pharmacotherapy*, *154*(June), 113561.

Johnson, W. (2005). Final Report of the Safety Assessment of Acacia Catechu Gum , *Acacia Concinna* Fruit Extract , *Acacia Dealbata* Leaf Extract , *Acacia Dealbata* Leaf Wax , *Acacia Decurrens* Extract , *Acacia Farnesiana* Extract , *Acacia Farnesiana* Flower Wax , *Acacia Farnesiana*. *International Journal of Toxicology*, *24*, 75–118.

Jorge de Souza, T. A., Rosa Souza, L. R., & Franchi, L. P. (2019). Silver nanoparticles: An integrated view of green synthesis methods, transformation in the environment, and toxicity. *Ecotoxicology and Environmental Safety*, *171*(January), 691–700.

Jridi, M., Hajji, S., Ben, H., Lassoued, I., Mbarek, A., Kammoun, M., Souissi, N., & Nasri, M. (2014). Physical , structural , antioxidant and antimicrobial properties of gelatin – chitosan composite edible films. *International Journal of Biological Macromolecules*, *67*, 373–379.

Kadam, D., Momin, B., Palamthodi, S., & Lele, S. S. (2019). Physicochemical and functional properties of chitosan-based nano-composite films incorporated with biogenic silver nanoparticles. *Carbohydrate Polymers*, *211*(February), 124–132.

Kalpana, S., Priyadarshini, S. R., Maria Leena, M., Moses, J. A., & Anandharamakrishnan, C. (2019). Intelligent packaging: Trends and applications in food systems. *Trends in Food Science and Technology*, *93*(September), 145–157.

Kambale, E. K., Nkanga, C. I., Mutonkole, B. I., Bapolisi, A. M., Tassa, D. O., Liesse, J. I., Krause, R. W. M., & Memvanga, P. B. (2020). Green synthesis of antimicrobial silver nanoparticles using aqueous leaf extracts from three Congolese plant species (*Brillantaisia patula* , *Crossopteryx febrifuga* and *Senna siamea*). *Heliyon*, *6*(July).

Kan, J., Liu, J., Yong, H., Liu, Y., Qin, Y., & Liu, J. (2019). Development of active packaging based on chitosan-gelatin blend films functionalized with Chinese hawthorn (*Crataegus pinnati fida*) fruit extract. *International Journal of Biological Macromolecules*, *140*, 384–392.

Kanniah, P., Chelliah, P., Thangapandi, J. R., Gnanadhas, G., Mahendran, V., & Robert, M. (2021). Green synthesis of antibacterial and cytotoxic silver nanoparticles by *Piper nigrum* seed extract and development of antibacterial silver based chitosan nanocomposite. *International Journal of Biological*

Macromolecules, *189*(May), 18–33.

Kavak, D. D., Altıok, E., & Ülkü, S. (2010). *Pistacia terebinthus* extract: As a potential antioxidant, antimicrobial and possible □-glucuronidase inhibitor. *Journal of Molecular Catalysis B:Enzymatic*, *64*, 167–171.

Khalil, M. M. H., Ismail, E. H., EI-Baghdady, K., & Mohamed, D. (2013). Green synthesis of silver nanoparticles using olive leaf extract and its antibacterial activity. *Arabian Journal of Chemistry, February 2014*.

Khan, A., Ezati, P., & Rhim, J. (2023). Chitosan / gelatin-based multifunctional film integrated with green tea carbon dots to extend the shelf life of pork. *Food Packaging and Shelf Life*, *37*(December 2022), 101075.

Khan, R., Akter, M., Kamaraj, C., Malafaia, G., Ragavendran, C., & Rahman, M. (2023). Green synthesis of silver nanoparticles with its bioactivity , toxicity and environmental applications : A comprehensive literature review. *Environmental Nanotechnology, Monitoring & Management*, *20*(May), 100872.

Kilonzo, M., & Munisi, D. (2021). Antimicrobial activities and phytochemical analysis of *Harrisonia abyssinica* (Oliv) and *Vepris simplicifolia* (Verd) extracts used as traditional medicine in Tanzania. *Saudi Journal of Biological Sciences*.

Kothandaraman, G., Mohammed, M., & Azmi, A. A. (2023). Green synthesis of *Cicer arietinum* waste derived silver nanoparticle for antimicrobial and cytotoxicity properties. *Biocatalysis and Agricultural Biotechnology*, *47*(September 2022).

Krakowska-Sieprawska, A., Kiełbasa, A., Rafińska, K., Ligor, M., & Buszewski, B. (2022). Modern Methods of Pre-Treatment of Plant Material for the Extraction of Bioactive Compounds. *Molecules*, *27*(3).

Krishnan, K. R., James, F., & Mohan, A. (2016). Isolation and characterization of n-hexadecanoic acid from *Canthium parviflorum* leaves. *Journal of Chemical and Pharmaceutical Research*, *8*(8), 614–617.

Kumar, S., Basumatary, I. B., Sudhani, H. P. K., Bajpai, V. K., Chen, L., Shukla, S., & Mukherjee, A. (2021). Plant extract mediated silver nanoparticles and their applications as antimicrobials and in sustainable food packaging: A state-of-the-art review. *Trends in Food Science and Technology*, *112*(January), 651–666.

Kumar, S., Mukherjee, A., & Dutta, J. (2020). Chitosan based nanocomposite fi lms and coatings : Emerging antimicrobial food packaging alternatives. *Trends in*

Food Science & Technology, *97*(August 2019), 196–209.

Kumar, S., Shukla, A., Pratim, P., Mitra, A., & Halder, D. (2018). Biodegradable hybrid nanocomposites of chitosan / gelatin and silver nanoparticles for active food packaging applications. *Food Packaging and Shelf Life*, *16*(March), 178–184.

Lakkim, V., Reddy, M. C., Pallavali, R. R., Reddy, K. R., Reddy, C. V., Bilgrami, A. L., & Lomada, D. (2020). Green Synthesis of Silver Nanoparticles and Evaluation of Their Antibacterial Activity against Multidrug-Resistant Bacteria and Wound Healing Efficacy Using a Murine Model. *Antibiotics*.

Lee, K. J., Oh, Y. C., Cho, W. K., & Ma, J. Y. (2015). Antioxidant and Anti-Inflammatory Activity Determination of One Hundred Kinds of Pure Chemical Compounds Using Offline and Online Screening HPLC Assay. *Hindawi Publishing Corporation*, *2015*.

Lee, Y. H., Cheng, F. Y., Chiu, H. W., Tsai, J. C., Fang, C. Y., Chen, C. W., & Wang, Y. J. (2014). Cytotoxicity, oxidative stress, apoptosis and the autophagic effects of silver nanoparticles in mouse embryonic fibroblasts. *Biomaterials*, *35*(16), 4706–4715.

Li, H. (2023). Preparation of silver nanoparticles / polymethylmethacrylate / cellulose acetate film and its inhibitory effect on Cronobacter sakazakii in infant formula milk. *Journal of Dairy Science*, *106*(1), 84–95.

Li, M., Wang, A., Zhang, Y., Han, T., Guan, L., Fan, D., Liu, J., & Xu, Y. (2022). A comprehensive review on ethnobotanical , phytochemical and pharmacological aspects of *Rhus chinensis* Mill. *Journal of Ethnopharmacology*, *293*(March), 115288.

Li, S., Mu, B., Zhang, H., Kang, Y., & Wang, A. (2022). Incorporation of silver nanoparticles/curcumin/clay minerals into chitosan film for enhancing mechanical properties, antioxidant and antibacterial activity. *International Journal of Biological Macromolecules*, *223*(PA), 779–789.

Liang, Z., Veronica, V., Huang, J., Zhang, P., & Fang, Z. (2022). Combined effects of plant food processing by-products and high oxygen modified atmosphere packaging on the storage stability of beef patties. *Food Control*, *133*(PA), 108586.

Liao, C., Li, Y., & Tjong, S. C. (2019). Bactericidal and cytotoxic properties of silver

nanoparticles. *International Journal of Molecular Sciences*, *20*(2).

Lin, D., Yang, Y., Wang, J., Yan, W., Wu, Z., Chen, H., Zhang, Q., Wu, D., Qin, W., & Tu, Z. (2020). Preparation and characterization of TiO_2 -Ag loaded fish gelatin-chitosan antibacterial composite film for food packaging. *International Journal of Biological Macromolecules*, *154*, 123–133.

Liu, J., Meng, C., Liu, S., Kan, J., & Jin, C. (2017). Preparation and characterization of protocatechuic acid grafted chitosan fi lms with antioxidant activity. *Food Hydrocolloids*, *63*.

Liu, L., He, H. zhi, & Luo, S. (2015). Allelopathic potential of *Rhus chinensis* on seedling growth of radish , semen cassiae and black soyabean. *Springer International Publishing Switzerland*.

Liu, Y., Wang, R., Wang, D., Sun, Z., Liu, F., & Zhang, D. (2022). Development of a food packaging antibacterial hydrogel based on gelatin , chitosan , and 3-phenyllactic acid for the shelf-life extension of chilled chicken. *Food Hydrocolloids*, *127*(November 2021), 107546.

Lu, Y., Luo, Q., Chu, Y., Tao, N., Deng, S., Wang, L., & Li, L. (2022). Application of Gelatin in Food Packaging : A Review. *Polymers*.

Luangapai, F., & Iwamoto, S. (2023). Influence of blending and layer-by-layer assembly methods on chitosan – gelatin composite films enriched with curcumin nanoemulsion. *International Journal of Biological Macromolecules*, *249*(March), 126061.

Luis, J. P., Norton, I. T., Batchelor, H. K., Gkatzionis, K., Spyropoulos, F., & Sobral, P. J. A. (2018). Physico-chemical , antimicrobial and antioxidant properties of gelatin- chitosan based films loaded with nanoemulsions encapsulating active compounds. *Food Hydrocolloids*, *79*, 544–559.

Lyu, J. S., Choi, I., Hwang, K. S., Lee, J. Y., Seo, J., Kim, S. Y., & Han, J. (2019). Development of a BTB−/TBA+ ion-paired dye-based CO_2 indicator and its application in a multilayered intelligent packaging system. *Sensors and Actuators, B: Chemical*, *282*(July 2018), 359–365.

Majeed, S., Danish, M., Aini, N., Hashim, R., Tahir, M., & Patro, S. (2022). Tailored silver nanoparticles capped with gallic acid and its potential toxicity via ROS mediated pathway against osteosarcoma cells. *Materials Today Communications*, *32*(April), 1–11.

Majumder, S., Huang, S., Zhou, J., Wang, Y., & George, S. (2023). Tannic acid-loaded

halloysite clay grafted with silver nanoparticles enhanced the mechanical and antimicrobial properties of soy protein isolate films for food-packaging applications. *Food Packaging and Shelf Life*, *39*(December 2022), 101142.

Manzoor, A., Ahmad, S., & Yousuf, B. (2023). Development and characterization of edible films based on flaxseed gum incorporated with *Piper betle* extract. *International Journal of Biological Macromolecules*, *245*(June), 125562.

Mataragas, M., Bikouli, V. C., Korre, M., Sterioti, A., & Skandamis, P. N. (2019). Development of a microbial Time Temperature Indicator for monitoring the shelf life of meat. *Innovative Food Science and Emerging Technologies*, *52*(November 2018), 89–99.

Mingxing, W., Yue, W., & Shanshan, L. (2013). *Edible blend oil containing Rhus chinensis fruit oil and blending method thereof C.N. Patent CN 103070246 A,*.

Mir, M. A., Manzer, F., Andrews, K., Hasnain, S. M., Iqbal, A., Sehar, S., & Younis, A. (2023). Molecular dynamic , Hirshfeld surface , molecular docking and drug likeness studies of a potent anti-oxidant , anti-malaria and anti-Inflammatory medicine : Pyrogallol. *Results in Chemistry*, *5*(November 2022), 100763.

Mohammadalinejhad, S., Almasi, H., & Esmaiili, M. (2019). Simultaneous green synthesis and in-situ impregnation of silver nanoparticles into organic nano fi bers by *Lythrum salicaria* extract : Morphological , thermal , antimicrobial and release properties. *Materials Science & Engineering C*, *105*(May), 110115

.

Moteriya, P., & Chanda, S. (2017). Synthesis and characterization of silver nanoparticles using *Caesalpinia pulcherrima* flower extract and assessment of their in vitro antimicrobial , antioxidant , cytotoxic , and genotoxic activities. *Artificial Cells, Nanomedicine, and Biotechnology*, 1555–1566.

Mouzahim, M. El, Eddarai, E. M., Eladaoui, S., Guenbour, A., Bellaouchou, A., Zarrouk, A., & Boussen, R. (2023). Effect of Kaolin clay and Ficus carica mediated silver nanoparticles on chitosan food packaging film for fresh apple slice preservation. *Food Chemistry*, *410*(January), 135470.

Muthu, K., Rini, S., Nagasundari, S. M., & Akilandaeaswari, B. (2020). Photocatalytic reduction and antioxidant potential of green synthesized silver nanoparticles from *Catharanthus roseus* flower extract. *Inorganic and Nano-Metal Chemistry*, 1–11.

Nandhini, R. S., Nirmala Nithya, R., & Vidhya, K. (2021). GC-MS analysis of phytochemical compounds in different extracts of curculigo orchiodes. *Research Journal of Pharmacy and Technology*, *14*(8), 4355–4360.

Natarajan, V., & Natarajan, S. (2009). Antidermatophytic Activity of *Acacia concinna*. *Global Journal of Pharmacology*, *3*(1), 6–7.

Nemkul, C. M., Bajracharya, G. B., Maeda, H., & Shrestha, I. (2021). Ethnomedicinal Knowledge Verification for the Antidiarrheal and Antioxidant Effects of *Rhus chinensis* Mill. Fruits with Identification of Thirty Constituents. *Pharmacognosy Journal*, *13*(1), 37–43.

Nguyen, T. T. T., Tran, N. T. K., Le, T. Q., Nguyen, T. T. A., Nguyen, L. T. M., & Tran, T. Van. (2023). Passion fruit peel pectin/chitosan based antibacterial films incorporated with biosynthesized silver nanoparticles for wound healing application. *Alexandria Engineering Journal*, *69*, 419–430.

Nouri, A., Tavakkoli, M., Lajevardi, A., & Rezaei, Z. (2020). Ultrasonic-assisted green synthesis of silver nanoparticles using *Mentha aquatica* leaf extract for enhanced antibacterial properties and catalytic activity. *Colloid and Interface Science Communications*, *35*(March).

Odeniyi, M. A., Okumah, V. C., Adebayo-Tayo, B. C., & Odeniyi, O. A. (2020). Green synthesis and cream formulations of silver nanoparticles of *Nauclea latifolia* (African peach) fruit extracts and evaluation of antimicrobial and antioxidant activities. *Sustainable Chemistry and Pharmacy*, *15*(September 2019), 100197.

Ong, G., Kasi, R., & Subramaniam, R. (2021). A review on plant extracts as natural additives in coating applications. *Progress in Organic Coatings*, *151*(December 2020).

Orlo, E., Nerín, C., Lavorgna, M., Wrona, M., Russo, C., Stanzione, M., Nugnes, R., & Isidori, M. (2023). Antioxidant activity of coatings containing eugenol for flexible aluminium foils to preserve food shelf-life. *Food Packaging and Shelf Life*, *39*(August), 101145.

Oroian, M., & Escriche, I. (2015). Antioxidants : Characterization , natural sources , extraction and analysis. *Food Research International*, *74*, 10–36.

Pai, S., Hebbar, A., & Selvaraj, S. (2022). A critical look at challenges and future scopes of bioactive compounds and their incorporations in the food , energy , and pharmaceutical sector. *Environmental Science and Pollution Research*, 35518–35541.

Pampuinath, B., & Meitei, M. D. (2021). Astronomical explanation of the enigmatic sundial in Agra, India. *Reserach Communications*, *120*(5), 942–945.

Papuc, C., Goran, G. V, Predescu, C. N., Nicorescu, V., & Stefan, G. (2017). Plant Polyphenols as Antioxidant and Antibacterial Agents for Shelf-Life Extension of Meat and Meat Products : Classification , Structures , Sources , and Action Mechanisms. *Comprehensive Review in Food Science and Food Safety*, *00*, 1–26.

Patil, R. P. (2023). Medicinal Plants Are Used for Hair. *Tijer-International Research Journal*, *10*(2), 45–48.

Patle, T. K., Shrivas, K., Kurrey, R., Upadhyay, S., Jangde, R., & Chauhan, R. (2020). Phytochemical screening and determination of phenolics and flavonoids in *Dillenia pentagyna* using UV–vis and FTIR spectroscopy. *Spectrochimica Acta - Part A: Molecular and Biomolecular Spectroscopy*, *242*, 118717.

Pazhamalai, V. (2019). Molecular Docking Analysis of Bioactive Compounds of *Acacia Concinna* against Fungal Protein. *Journal of Pharmaceutical Sciences and Research*, *11*(4), 1216–1222.

Pereda, M., Ponce, A. G., Marcovich, N. E., Ruseckaite, R. A., & Martucci, J. F. (2011). Chitosan-gelatin composites and bi-layer films with potential antimicrobial activity. *Food Hydrocolloids*, *25*(5), 1372–1381.

Periasamy, S., Jegadeesan, U., Sundaramoorthi, K., Rajeswari, T., Naga, V., Tokala, B., Bhattacharya, S., Muthusamy, S., Sankoh, M., & Nellore, M. K. (2022). Comparative Analysis of Synthesis and Characterization of Silver Nanoparticles Extracted Using Leaf , Flower , and Bark of *Hibiscus rosasinensis* and Examine Its Antimicrobicidal Activity. *Journal of Nanomaterials*, *2022*.

Poomanee, W., Chaiyana, W., Intasai, N., & Leelapornpisid, P. (2015). Biological activities and characterization of the pod extracts from sompoi (*Acacia concinna linn*) grown in northern Thailand. *International Journal of Pharmacy and Pharmaceutical Sciences*, *7*(5), 237–241.

Poudyali, B., & Singh, B. (2020). Antibacterial and cell envelope damaging properties of different solvent extracts of *Rhus chinensis* mill against E. coli and staphylococcus aureus. *Indian Journal of Traditional Knowledge*, *19*(2), 428–434.

Preez-Bruwer, I. du, Mumbengegwi, D. R., & Louw, S. (2022). In vitro antimalarial properties and chemical composition of *Diospyros chamaethamnus* extracts. *South African Journal of Botany*, *149*, 290–296.

Prema, P., Veeramanikandan, V., Rameshkumar, K., Gatasheh, M. K., Hatamleh, A. A., Balasubramani, R., & Balaji, P. (2022). Statistical optimization of silver nanoparticle synthesis by green tea extract and its efficacy on colorimetric detection of mercury from industrial waste water. *Environmental Research*, *204*(June 2021).

Qadir, A., Khan, N., Arif, M., Husain, M., Nasar, S., Najib, M., & Yusuf, M. (2022). GC – MS analysis of phytoconstituents present in *Trigonella foenumgraecum L* .

seeds extract and its antioxidant activity. *Journal of the Indian Chemical Society*, *99*(6), 100503.

Qin, Y., Liu, Y., Yuan, L., Yong, H., & Liu, J. (2019). Preparation and characterization of antioxidant, antimicrobial and pH-sensitive films based on chitosan, silver nanoparticles and purple corn extract. *Food Hydrocolloids*, *96*(April), 102–111.

Rafique, M., Sadaf, I., Rafique, M. S., & Tahir, M. B. (2017). A review on green synthesis of silver nanoparticles and their applications. *Artificial Cells, Nanomedicine, and Biotechnology*, 1272–1291.

Rahnemoon, P., Sarabi-jamab, M., Bostan, A., & Mansouri, E. (2021). Nano-encapsulation of pomegranate (*Punica granatum L* .) peel extract and evaluation of its antimicrobial properties on coated chicken meat. *Food Bioscience*, *43*(July), 101331.

Raja, X. V., & Sivaraj, R. (2012). Antibacterial Activity Of Bark Extract Of *Acacia Concinna*. *International Journal of Pharma Sciences and Research*, *3*(10), 487–490.

Ramesh, A. V., Devi, D. R., Battu, G. R., & Basavaiah, K. (2018). A Facile plant mediated synthesis of silver nanoparticles using an aqueous leaf extract of *Ficus hispida Linn. f.* for catalytic, antioxidant and antibacterial applications. *South African Journal of Chemical Engineering*, *26*(June), 25–34.

Ramli, S. binti. (2018). *PhD thesis Antimicrobial activity, phytochemical and Toxicity analyses of SALAM [Syzygium pplyanthum (wight) Walp.] leaf extract and its application in food*.

Ramziia, S., Ma, H., Yao, Y., Wei, K., & Huang, Y. (2018). Enhanced antioxidant activity of fish gelatin–chitosan edible films incorporated with procyanidin. *Journal of Applied Polymer Science*, *135*(10), 1–10.

Rangaraj, V. M., Rambabu, K., Banat, F., & Mittal, V. (2021). Natural antioxidants-based edible active food packaging: An overview of current advancements. *Food Bioscience*, *43*(March), 101251.

Rani, N., Singh, P., Kumar, S., Kumar, P., Bhankar, V., & Kumar, K. (2023). Plant-mediated synthesis of nanoparticles and their applications: A review. *Materials Research Bulletin*, *163*(January).

Razali, N. S. M. (2019). *Antioxidant Activity of Plant-derived Extracts as Assessed through Dietary Supplementation of Chicken Diets and Via Active Packaging Applications Employing Commercial Chicken Packaging Formats*.

Rezaee, M., Askari, G., EmamDjomeh, Z., & Salami, M. (2018). Effect of organic additives on physiochemical properties and anti-oxidant release from chitosan-gelatin composite films to fatty food simulant. *International Journal of Biological Macromolecules*, *114*, 844–850.

Riaz, A., Lagnika, C., Abdin, M., Muhammad, M., & Waqar, H. (2019). Preparation and Characterization of Chitosan / Gelatin - Based Active Food Packaging Films Containing Apple Peel Nanoparticles. *Journal of Polymers and the Environment*, *0123456789*.

Rolim, W. R., Pelegrino, M. T., Araújo, B. De, Ferraz, L. S., Costa, F. N., Bernardes, J. S., Rodigues, T., & Brocchi, M. (2019). Green tea extract mediated biogenic synthesis of silver nanoparticles : Characterization , cytotoxicity evaluation and antibacterial activity. *Applied Surface Science*, *463*(August 2018), 66–74.

Romanelli, M., Bertolo, V., Danilo, L., Gonçalves, J., Filho, D. O., Alves, F., Aparecida, C., Conceiç, V., David, M., Salvador, V., Maria, A., Plepis, D. G., & Bogusz, S. (2022). Central composite design optimization of active and physical properties of food packaging films based on chitosan / gelatin / pomegranate peel extract. *Food Packaging and Shelf Life*, *34*(October).

Rónavári, A., Kovács, D., Igaz, N., Vágvölgyi, C., Boros, I. M., Kónya, Z., Pfeiffer, I., & Kiricsi, M. (2017). Biological activity of green-synthesized silver nanoparticles depends on the applied natural extracts: A comprehensive study. *International Journal of Nanomedicine*, *12*, 871–883.

Samsi, M. S., Kamari, A., Fatimah, I., Sunardi, & Yusoff, S. N. M. (2019). Synthesis, Characterization and application of Gelatin -Chitosan Blend Films for Fruit Preservation. *Fresnius Environmental Bulletin*, *January*.

Sana, S. S., & Dogiparthi, L. K. (2018). Green synthesis of silver nanoparticles using *Givotia moluccana* leaf extract and evaluation of their antimicrobial activity. *Materials Letters*, *226*, 47–51.

Sani, I. K., Geshlaghi, S. P., Pirsa, S., & Asdagh, A. (2021). Composite film based on potato starch/apple peel pectin/ZrO_2 nanoparticles/ microencapsulated *Zataria multiflora* essential oil; investigation of physicochemical properties and use in quail meat packaging. *Food Hydrocolloids*, *117*(October 2020).

Sankaranarayanan, A., Munivel, G., Karunakaran, G., Kadaikunnan, S., Alharbi, N. S., Khaled, J. M., & Kuznetsov, D. (2017). Green Synthesis of Silver Nanoparticles Using *Arachis hypogaea* (Ground Nut) Root Extract for Antibacterial and Clinical Applications. *Journal of Cluster Science*, *28*(3), 995–1008.

Saravanakumar, K., Sriram, B., Sathiyaseelan, A., Mariadoss, A. V. A., Hu, X., Han, K. S., Vishnupriya, V., MubarakAli, D., & Wang, M. H. (2021). Synthesis, characterization, and cytotoxicity of starch-encapsulated biogenic silver nanoparticle and its improved anti-bacterial activity. *International Journal of Biological Macromolecules*, *182*, 1409–1418.

Saravanan, A., Kumar, P. S., Karishma, S., Vo, D. N., Jeevanantham, S., Yaashikaa, P. R., & Susan, C. (2021). A review on biosynthesis of metal nanoparticles and its environmental applications. *Chemosphere*, *264*.

Sariozlu, N. Y., & Kivanc, M. (2011). Gallnuts (Quercus infectoria Oliv. and *Rhus chinensis* Mill.) and Their Usage in Health. In *Nuts and Seeds in Health and Disease Prevention*.

Seal, T., & Chaudhuri, K. (2014). Ethnobotanical importance and nutritional potential of wild edible fruits of Meghalaya state in India. *Journal of Chemical and Pharmaceutical Research*, *September*, 680–684.

Sethi, S., & Singh, B. (2022). A review on chitosan-gelatin nanocomposites : Synthesis , characterization and biomedical applications. *Reactive and Functional Polymers*, *179*(August).

Sharma, P. B., Handique, P. J., & Devi, H. S. (2015). Antioxidant properties, physico-chemical characteristics and proximate composition of five wild fruits of Manipur, India. *Journal of Food Science and Technology*, *52*(2), 894–902.

Shen, L., Pang, S., Zhong, M., Sun, Y., Qayum, A., Liu, Y., Rashid, A., Xu, B., Liang, Q., Ma, H., & Ren, X. (2023). A comprehensive review of ultrasonic assisted extraction (UAE) for bioactive components: Principles, advantages, equipment, and combined technologies. *Ultrasonics Sonochemistry*, *101*(August).

Shi, X., Huang, J., Wu, J., Cai, X., Tian, Y., & Rao, P. (2022). Fabrication , interaction mechanism , functional properties , and applications of fish gelatin-polysaccharide composites : a review. *Food Hydrocolloids*, *122*(March 2021), 107106.

Shinde, V., & Mahadik, K. (2019). Supercritical fluid extraction: A new technology to herbals. *Int J Herb Med*, *7*(January 2019), 27–34.

Sid, S., Mor, R. S., Kishore, A., & Sharanagat, V. S. (2021). Bio-sourced polymers as alternatives to conventional food packaging materials : A review. *Trends in Food Science & Technology*, *115*(May), 87–104.

Siddiquee, A., Hassan, S., Ahmed, K., Ali, A., Ahmad, M., & Patel, R. (2020). Green synthesis of silver nanoparticles from *Delonix regia* leaf extracts : In-vitro cytotoxicity and interaction studies with bovine serum albumin. *Materials Chemisty and Physics*, *242*(November 2019).

Silva, A. O., Cunha, R. S., Hotza, D., & Machado, R. A. F. (2021). Chitosan as a matrix of nanocomposites: A review on nanostructures, processes, properties, and applications. *Carbohydrate Polymers*, *272*(May).

Simbine, E. O., Rodrigues, L. da C., Lapa-Guimarães, J., Kamimura, E. S., Corassin, C. H., & de OLIVEIRA, C. A. F. (2019). Application of silver nanoparticles in food packages: A review. *Food Science and Technology*, *39*(4), 793–802.

Soltani Firouz, M., Mohi-Alden, K., & Omid, M. (2021). A critical review on intelligent and active packaging in the food industry: Research and development. *Food Research International*, *141*(January), 110113.

Sombatsiri, P., & Chairote, G. (2005). *Volatile Compounds from " Som Poy " (Acacia concinna DC .)*. *5*, 189–194.

Sportelli, M. C., Izzi, M., Id, A. V., Clemente, M., Anna, R., Id, P., Ancona, A., Mario, P., Palazzo, G., & Cioffi, N. (2018). The Pros and Cons of the Use of Laser Ablation Synthesis for the Production of Silver Nano-Antimicrobials. *Antibiotics*, 1–28.

Strupiechonski, E., Moreno-r, M., Erika, O. Á., Prokhorov, E., Kovalenko, Y., Diana, G. Z., Medina, D. I., & Luna-barcenas, G. (2021). Relaxation Phenomena in Chitosan-Au Nanoparticle Thin Films. *Polymers*, 1–18.

Sukweenadhi, J., Irianti, K., Avanti, C., Kartini, K., Jahan, E., & Yang, D. (2021). Scale-up of green synthesis and characterization of silver nanoparticles using ethanol extract of *Plantago major L* . leaf and its antibacterial potential. *South African Journal of Chemical Engineering*, *38*(April), 1–8.

Sul, Y., Ezati, P., & Rhim, J. (2023). Preparation of chitosan / gelatin-based functional films integrated with carbon dots from banana peel for active packaging application. *International Journal of Biological Macromolecules*, *246*(June), 125600.

Suo, C., Sun, Z., Wang, Y., Dong, S., Lv, C., Wang, T., Yan, S., & Wang, C. (2020). Active components on leaves of *Rhus Chinensis* Mill. *Thermal Science*, *24*(3), 1729–1735.

Susanna, D., Balakrishnan, R. M., & Ponnan Ettiyappan, J. (2022). Comprehensive

insight into the extract optimization, phytochemical profiling, and biological evaluation of the medicinal plant *Nothapodytes foetida*. *Biocatalysis and Agricultural Biotechnology*, *42*(February).

Tagrida, M., Nilsuwan, K., Gulzar, S., Prodpran, T., & Benjakul, S. (2023). Fish gelatin/chitosan blend films incorporated with betel (*Piper betle L.*) leaf ethanolic extracts: Characteristics, antioxidant and antimicrobial properties. *Food Hydrocolloids*, *137*(March 2022), 108316.

Takma, D. K., & Korel, F. (2019). Active packaging films as a carrier of *black cumin* essential oil : Development and eff ect on quality and shelf-life of chicken breast meat. *Food Packaging and Shelf Life*, *19*(November 2017), 210–217.

Taylor, P., Bahar, B., & Altug, T. (2009). Flavour Characterization of Sumach (*Rhus Coriaria L* .) by Means of GC / MS and Sensory Flavour Profile Analysis Techniques. *International Journal of Food Properties*, *August 2014*, 37–41.

Tessaro, L., Luciano, C. G., Quinta Barbosa Bittante, A. M., Lourenço, R. V., Martelli-Tosi, M., & José do Amaral Sobral, P. (2021). Gelatin and/or chitosan-based films activated with "Pitanga" (*Eugenia uniflora L.*) leaf hydroethanolic extract encapsulated in double emulsion. *Food Hydrocolloids*, *113*(August 2020).

Tiwari, B. K. (2015). Ultrasound: A clean, green extraction technology. *TrAC - Trends in Analytical Chemistry*, *71*, 100–109.

Todkar, S., Chavan, V. ., & Kulkarni, A. . (2010). Screening of secondary Metabolites and antibacterial Activity of *Acacia concinna*. *Research Journal of Microbiology*, *5*(June 2010), 974–979.

Todkar, S., Todkar, R., & Kavathekar, V. (2011). *Secondary Metabolite Profiling of Acacia concinna*. *8*(December), 653–660.

Triterpenes, D., Ee, I. S. L., Hn, K. A., & Ee, H. L. (2001). Semialactone , Isofouquierone Peroxide and Fouquierone , Three New Dammarane Triterpenes from *Rhus javanica*. *Chem.Pharm.Bull.*, *September*, 11–14.

Vieira, I. R. S., Carvalho, A. P. A. de de, & Counte-Jounior, C. A. (2022). Recent advances in biobased and biodegradable polymer nanocomposites , nanoparticles , and natural antioxidants for antibacterial and antioxidant food packaging applications. *Comprehensive Review in Food Science and Food Safety*, *June*.

Vilela, C., Kurek, M., Hayouka, Z., Röcker, B., Yildirim, S., Dulce, M., Antunes, C., Nilsen-nygaard, J., Kvalvåg, M., & Freire, C. S. R. (2018). A concise guide to active agents for active food packaging. *Trends in Food Science & Technology*,

80(July), 212–222.

Wadia, A., Owais, M., Altaf, I., & Farheen, S. (2022). *Rumex nervosus* mediated green synthesis of silver nanoparticles and evaluation of its in vitro antibacterial , and cytotoxic activity. *OpenNano*, *8*(September).

Wang, H., Ding, F., Ma, L., & Zhang, Y. (2021). Edible films from chitosan-gelatin : Physical properties and food packaging application. *Food Bioscience*, *40*(January), 100871.

Wang, R.-R., Gu, Q., Yang, L., Chen, J., Li, S., & Zheng, Y. (2006). Anti-HIV-1 activities of extracts from the medicinal plant *Rhus chinensis*. *Jouranal of Ethnopharmacology*, *105*, 269–273.

Wang, W., Yu, Z., Alsammarraie, F. K., Kong, F., Lin, M., & Mustapha, A. (2020). Properties and antimicrobial activity of polyvinyl alcohol-modified bacterial nanocellulose packaging films incorporated with silver nanoparticles. *Food Hydrocolloids*, *100*(June 2019), 105411.

Wang, X., Yong, H., Gao, L., Li, L., Jin, M., & Liu, J. (2019). Preparation and characterization of antioxidant and pH-sensitive films based on chitosan and black soybean seed coat extract. *Food Hydrocolloids*, *89*(October 2018), 56–66.

Witkowska, A. M., Hickey, D. K., Alonso-gomez, M., & Wilkinson, M. (2013). Evaluation of Antimicrobial Activities of Commercial Herb and Spice Extracts Against Selected Food-Borne Bacteria. *Journal of Food Research*, *June*.

Wong, S. X. E., Kiew, S. F., Lau, S. Y., & Pottas, P. W. (2023). Procedures to investigate potential of plants as natural food preservatives: Extraction technology, phytochemical characterisation, and antimicrobial bioassays. *Food Chemistry Advances*, *3*(January), 100435.

Wu, Z., Deng, W., Luo, J., & Deng, D. (2019). Multifunctional nano-cellulose composite films with grape seed extracts and immobilized silver nanoparticles. *Carbohydrate Polymers*, *205*(October 2018), 447–455.

Wu, Z., Huang, X., Li, Y., Xiao, H., & Wang, X. (2018). Novel chitosan films with laponite immobilized Ag nanoparticles for active food packaging. *Carbohydrate Polymers*, *199*(March), 210–218.

Wuthi-udomlert, M., & Vallisuta, O. (2011). In vitro Effectiveness of *Acacia concinna* Extract against Dermatomycotic Pathogens. *Pharmacognosy Journal*, *3*(19), 69–73.

Xu, J., Wei, R., Jia, Z., & Song, R. (2020). Characteristics and bioactive functions of chitosan/gelatin-based film incorporated with ε-polylysine and astaxanthin extracts derived from by-products of shrimp (Litopenaeus vannamei). *Food Hydrocolloids*, *100*(October 2019).

Yadav, R., & Agarwala, M. (2011). Phytochemical Analysis of Some Medicinal Plants. *Liaquat Medical Research Journal*, *3*(8), 1–5.

Yadav, S., Mehrotra, G. K., Bhartiya, P., Singh, A., & Dutta, P. K. (2020). Preparation , physicochemical and biological evaluation of quercetin based chitosan-gelatin film for food packaging. *Carbohydrate Polymers*, *227*(August 2019), 115348.

Yan, X., He, B., Liu, L., Qu, G., Shi, J., Hu, L., & Jiang, G. (2018). Antibacterial mechanism of silver nanoparticles in Pseudomonas aeruginosa: proteomics approach. *Metallomics*, *10*(4), 557–564.

Yang, D., Liu, Q., Gao, Y., Wan, S., Meng, F., Weng, W., & Zhang, Y. (2023). Characterization of silver nanoparticles loaded chitosan/polyvinyl alcohol antibacterial films for food packaging. *Food Hydrocolloids*, *136*(PB), 108305.

You, S., Zhang, X., Wang, Y., Jin, Y., Wei, M., & Wang, X. (2022). Development of highly stable color indicator films based on κ -carrageenan , silver nanoparticle and red grape skin anthocyanin for marine fish freshness assessment. *International Journal of Biological Macromolecules*, *216*(June), 655–669.

Yuan, D., Meng, H., Huang, Q., Li, C., & Fu, X. (2021). Preparation and characterization of chitosan-based edible active films incorporated with Sargassum pallidum polysaccharides by ultrasound treatment. *International Journal of Biological Macromolecules*, *183*, 473–480.

Zhang, A., Han, Y., & Zhou, Z. (2023). Characterization of citric acid crosslinked chitosan/gelatin composite film with enterocin CHQS and red cabbage pigment. *Food Hydrocolloids*, *135*(September 2022), 108144.

Zhang, C., Ma, Y., Zhao, Y., Hong, Y., Cai, S., & Pang, M. (2018). Phenolic composition, antioxidant and pancreatic lipase inhibitory activities of Chinese sumac (*Rhus chinensis* Mill.) fruits extracted by different solvents and interaction between myricetin-3-O-rhamnoside and quercetin-3-O-rhamnoside. *International Journal of Food Science and Technology*, *53*(4), 1045–1053.

Zhang, C., Yang, Z., Shi, J., Zou, X., Zhai, X., Huang, X., Li, Z., Holmes, M., Daglia, M., & Xiao, J. (2021). Physical properties and bioactivities of chitosan / gelatin-based films loaded with tannic acid and its application on the preservation of fresh-cut apples. *Food Science and Technology*, *144*(November 2020), 111223.

Zhang, W., & Jiang, W. (2020). Antioxidant and antibacterial chitosan fi lm with tea polyphenols- mediated green synthesis silver nanoparticle via a novel one-pot method. *International Journal of Biological Macromolecules*, *155*, 1252–1261.

Zhang, W., Li, X., & Jiang, W. (2020). Development of antioxidant chitosan film with banana peels extract and its application as coating in maintaining the storage quality of apple. *International Journal of Biological Macromolecules*, *154*, 1205–1214.

Zhang, X., Liu, Y., Yong, H., Qin, Y., Liu, J., & Liu, J. (2019). Development of multifunctional food packaging films based on chitosan , TiO_2 nanoparticles and anthocyanin-rich black plum peel extract. *Food Hydrocolloids*, *94*(March), 80–92.

Zhang, Y., Zhang, Y., Yi, J., & Cai, S. (2023). Phytochemical characteristics and biological activities of *Rhus chinensis* Mill .: a review. *Current Opinion in Food Science*, *48*, 100925.

Zhao, W., Liang, X., Wang, X., Wang, S., Wang, L., & Jiang, Y. (2022). Chitosan based film reinforced with EGCG loaded melanin-like nanocomposite (EGCG@MNPs) for active food packaging. *Carbohydrate Polymers*, *290*(April), 119471.

Zhao, Y., An, J., Su, H., Li, B., Liang, D., & Huang, C. (2022). Antimicrobial food packaging integrating polysaccharide-based substrates with green antimicrobial agents : A sustainable path. *Food Research International*, *155*(January).

Zhao, Y., Yang, L., Xu, M., Wang, H., Gao, X., Niu, B., & Li, W. (2022). Gallic acid functionalized chitosan immobilized nanosilver for modified chitosan / Poly (vinyl alcohol) composite film. *International Journal of Biological Macromolecules*, *222*(PB), 2987–3000.

Zhu, S., Jiao, W., Xu, Y., Hou, L., Li, H., Shao, J., Zhang, X., Wang, R., & Kong, D. (2021). Palmitic acid inhibits prostate cancer cell proliferation and metastasis by suppressing the PI3K / Akt pathway. *Life Sciences*, *286*(April), 120046.

BIODATA OF STUDENT

Lu Lu Taung Mai was born on July, 1994, in Myitkyina, Kachin State, in the northern part of Myanmar. She began her primary education at Alam Middle School and completed her secondary and matriculation studies at N0 (3) Basic Education High School in Myitkyina. In 2014, she earned her BSC (Hons) degree from Myitkyina University. Subsequently, she pursued her Master of Science in the Chemistry Department of Myitkyina University. Upon the completion of her MSC degree, she worked as a demonstrator for undergraduate courses in the department of Chemistry of Myitkyina University. In September 2019, she embarked on her Ph.D program in the field of materials science under the Institute of Tropical Forestry and Forest Products (INTROP). During her research journery, she had the opportunity to present a poster at the Wood Biofibre International Conference (WOBIC 2019) and deliver an oral presentation at the Symposium on Multidisciplinary Science (SMS-2021).

LIST OF PUBLICATIONS

Mai, L. L. T., Aung, M. M., Saidi, S. A. M., H'ng, P. S., Rayung, M., & Jaafar, A. M. (2021). Non edible oil-based epoxy resins from jatropha oil and their shape memory behaviors. *Polymers*, *13*(13), 1–12.

Mai, L. L. T., San, H. P. S., Aung, M. M., Uyama, H., Mohammed, A. Z., Bahrin, E. K., Masarudin, M. J., Zulkifli, A. A. binti, & Chew, T. W. (2024). Antimicrobial Effect of Waterborne Polyurethane-Based Cellulose Nanofibril/Silver Nanoparticles Composites and Acacia concinna (Willd.) DC Extract (Shikakai). *Polymers*, *16*, 1–13.

Aung, M. M., Uyama, H., Rayung, M., **Mai, L. L. T**., Khaing, M. T., Sapuan, S. M., & Ilyas, R. A. (2021). Manufacturing of Biobased Packaging Materials. In *Bio-based packaging: Material, Environmental and Economic Aspects*.